DESIGN AND DEVELOPMENT OF COMPACT MIMO ANTENNA SYSTEM FOR 5G SMARTPHONE APPLICATIONS

Thesis submitted in fulfillment of the requirements for the Degree of

DOCTOR OF PHILOSOPHY

By

VISHAKHA THAKUR

Department of Electronics and Communication Engineering

JAYPEE UNIVERSITY OF INFORMATION TECHNOLOGY

WAKNAGHAT, SOLAN-173234, HIMACHAL PRADESH, INDIA

MAY, 2025

TABLE OF CONTENTS

CONTENTS

DECLARATION BY THE SCHOLAR

I hereby declare that the work reported in the Ph.D. thesis entitled **"Design and Development of Compact MIMO Antenna System for 5G Smartphone Applications"** submitted at **Jaypee University of Information Technology, Waknaghat, India,** is an authentic record of my work carried out under the supervision of **Dr. Naveen Jaglan**. I have not submitted this work elsewhere for any other degree or diploma. I am fully responsible for the contents of my Ph.D. thesis.

Vishakha Thakur
Department of Electronics and Communication Engineering
Jaypee University of Information Technology,
Waknaghat, Solan-173234, Himachal Pradesh, India
Date: 26-5-24

JAYPEE UNIVERSITY OF INFORMATION TECHNOLOGY
(Established by H.P. State Legislative vide Act No. 14 of 2002)
P.O. Waknaghat, Teh. Kandaghat, Distt. Solan - 173234 (H.P.) INDIA
Website: www.juit.ac.in
Phone No. (91) 01792-257999
Fax: +91-01792-245362

SUPERVISOR'S CERTIFICATE

This is to certify that the work reported in the Ph.D. thesis entitled **"Design and Development of Compact MIMO Antenna System for 5G Smartphone Applications",** submitted by **Vishakha Thakur** at **Jaypee University of Information Technology, Waknaghat, India,** is a bonafide record of her original work carried out under our supervision. This work has not been submitted elsewhere for any other degree or diploma.

Dr. Naveen Jaglan
Associate Professor
Department of ECE
Jaypee University of Information Technology,
Waknaghat, H.P, India

ACKNOWLEDGEMENT

*My first and foremost thanks to **Almighty God** for providing me the strength and bestowing his endless blessings upon me throughout this endeavor. All this could never be possible without his persistence and wisdom. The successful completion of this research work has been possible by the contribution of number of people in different aspects. I would like to extend by sincere gratitude to all of then who stood by me during the entire course of my Ph.D. work.*

*I would like to extend my foremost gratitude and special appreciations to my Ph.D. supervisor **Dr. Naveen Jaglan** for his tremendous encouragement, unconditional support and guidance through their enlightening views on several issues related to my research topic. He has always inspired me with his intelligence, perseverance and constructive criticism that have kept me going in the positive path of success throughout the entire course of my Ph.D. I would like to thank him for the undying support, endurance and motivation during tough times. It's my privilege to work under his supervision as his advices on both research as well as on my career has been priceless. I have been blessed with his continuous moral support, invaluable inputs and suggestions when I needed the most.*

*I gratefully acknowledge Jaypee University of Information Technology for offering me the platform for this research and providing the necessary facilities and support. I owe my gratitude to the Vice-chancellor **Prof. (Dr.) Rajendra Kumar Sharma** for his optimism and humble nature that has always been an inspiration for me and also to the Dean Academic Head **Prof. (Dr.) Ashok Kumar Gupta and** Dean Research **Prof. (Dr.) Sudhir Siyal** for his co-operation and support. A special thanks to the Ex Director & Academic Head **Prof. (Dr.) Samir Dev Gupta** for imparting quality education with ethics and values as its bedrock.*

*My heartfelt appreciation to **Prof. (Dr.) Rajiv Kumar** Head of Department of Electronics and Communication, for his co-operation, support and constant encouragement. I wish to convey my sincere thanks to all the faculty members of Department of Electronics and Communication Engineering, for their help and guidance*

at the various stages of this study. I am also thankful to ***Prof. (Dr.) Sunil Kumar Khah, Dr. Shweta Pandit,*** *and* ***Dr. Vikas Bhagel*** *for their guidance and valuable suggestions throughout my research work. It is my pleasure to acknowledge the timely help of the members of technical staff of the department, special thanks to* ***Mr. Pramod Kumar, Mr. Dhirendra and Mr. Mohan Lal*** *for always providing the technical support whenever needed.*

I would like to extend my thanks to Prof. Kumud Ranjan Jha of Mata vaishno Devi Institute of Jammu and all the electronics department faculty of Jaypee Institute of information technology for providing the lab facilities for measurement of radiation patterns.

I cannot forget the serenity of my parents throughout my research work. It is only because of their support, love and blessings that I could overcome all frustrations and failures. I would like to thank ***my parents, my husband, both Sisters Narita Thakur and Kritika Negi, and also my brother Kartik Thakur and all other family members and relatives*** *for their unconditional moral support, extraordinary belief and care throughout my Ph.D. They always stood by me and provided all the resources to help me achieve my goals and realize my dreams.*

Besides, I am also very thankful to my colleagues and friends ***Charu Bhardwaj, Priya, Garima Thakur, Diksha Thakur, Nikita, Anjana, Vipasha Rishi*** *and others for helping me in numerous ways and creating a healthy atmosphere for work. Their optimism, support and encouraging opinions kept me focused and positive in the pathway of my research work. I cherish the years spent in the Department of Electronics and Communication Engineering, JUIT, Waknaghat.*

I am indebted to all those people who have made this Ph.D. work possible and because of whom this research experience and wonderful journey shall remain everlasting and memorable forever.

All may not be mentioned, but no one is forgotten.

Thanks to all of you!
Vishakha

LIST OF ABBREVIATIONS AND ACRONYMS

5G	5^{th} Generation
ECC	Envelope Correlation Coefficient
CC	Channel Capacity
PCB	Printed Circuit Board
MIMO	Multiple Input Multiple Output
GHz	Giga Hertz
FR4	Flame retardant 4
1G	1^{st} Generation
2G	2^{nd} Generation
3G	3^{rd} Generation
4G	4^{th} Generation
mm	Millimetre
LTE	Long Term Evolution
dB	Decibel
iid	independent identically distributed
SNR	Signal to noise ratio
AMC	Artificial Magnetic Conductor
HFSS	High Frequency Structure Simulator
IFA	Inverted F Antenna
PIFA	Planar Inverted F Antenna
E-Field	Electric Field

TM	Transverse Magnetic
CTIA	Cellular Telecommunication Industry Association
SHM	Single Hand Mode
VNA	Vector Network Analyzer
Ant	Antenna

LIST OF FIGURES

LIST OF TABLES

ABSTRACT

In the era of fifth generation (5G) mobile communication, higher data rates are expected, along with better link reliability and lower latency than the previous generations. The utilization of multiple-input multiple-output (MIMO) technology is vital in meeting the increasing demands of higher data rates. This is the most popular approach adopted in 5G mobile communications. However it is a daunting job to install multiple antennas into the confined spaces of mobile phones as doing so can lead to performance degradation of MIMO antenna system. Hence, it is crucial to take this point into consideration while designing any MIMO system for 5G smartphones.

In this work, MIMO antenna systems resonating at single band as well as multi bands are presented for 5G smartphone applications. Firstly, a 12-Element compact dualband MIMO antenna system is presented as a possible solution for 5G mobile applications. In this approach adding multiple antennas in the confined space of mobile-phone is used to increase the data-rate. Exciting T-shaped slots that are etched on the ground plane with a special U-shaped arrangement were two main design aspects that were used to design and realize this dual-band compact, 12-element MIMO antenna system. Experimental validation of the antenna element asserted its suitability to be used as 12×12 Massive MIMO antenna for future 5G smartphones. Another design is developed for full screen ultra-thin smartphone by exploring a new space to install antenna. Ultra-thin smartphones are the new trend now a day which can lead to a lot of problems for antenna designs as the space needed to install antenna reduces. This research work also deals with designing of a small loop based MIMO system to fit into the ultrathin smartphone. The novelty of this proposed design lies in the size of the side-frame that is required to install elements of antenna. It has a small footprint of 9.5×3 mm^2. Which means it can fit in the 3 mm high side frame and it is the minimum size achieved so far when compare to the design presented in open literature. The structure resonates at 3.5 GHz covering the LTE-42 band with decent isolation of 14.8 dB. Another characteristic that is highly desirable for MIMO performance is ECC and it is less than 0.1 achieved through this design. To determine the data rate that can be achieved through these designs, channel capacity is calculated and it comes out to be 41 b/s/Hz. This method utilizes side-frame area optimally. Now to extract the capability of operating at multiple bands from a single resonant antenna, that also provides high isolation, a T-shaped MIMO antenna system has

been proposed. Finally to compete with the recent trend of using mobile-phones with metal body, a metal-rim compact MIMO antenna system has been designed. Combination of inverted F-antenna (IFA mode) and slot antenna is used for the composition of single antenna element. Total eight such antennas have been arranged on the single printed circuit board (PCB). This design was able to cover three 5G bands assigned in the sub-6Hz range. By this approach a compact, high efficiency antenna solution for 5G smartphone applications was obtained. It is essential to check the behaviour of this MIMO system in the hand of user to fully understand its performance in the real life scenario. Therefore this study also includes effect of hand on the individual antenna performance.

The fabrication had been done for all the proposed designs and validation of the S-parameters is done using vector network analyzer and radiation pattern was done using anechoic chamber.

CHAPTER 1
INTRODUCTION

CHAPTER 1

INTRODUCTION

1.1 EVOLUTION OF MOBILE COMMUNICATION

The first generation (1G) of cell phones was analog in nature introduced in 1980. It is also worth mentioning that the 1G cell-phone had electrically small antenna because of which they had poor radiation efficiency. Second generation was 2G and it was deployed with digital ecosystem. Figure 1.1 provides the progression of different generations in mobile communication. Since the introduction of there was a constant growth in the next generation after every decade. Due to the lack of signal processing system for analog data the data rates in 1G were very limited. Front-end transmission has always been analog, even in the 2G era, even while back-end devices enabled digital signal processing [1-2]

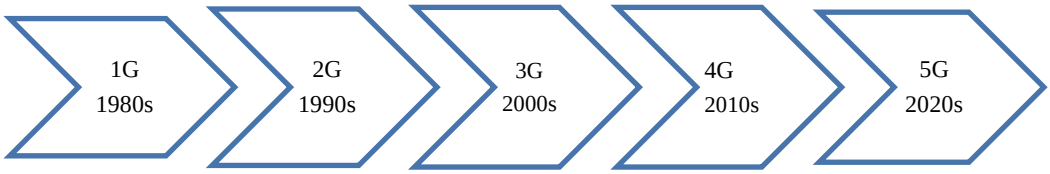

Figure 1.1 Evolution of mobile communication

Front end transmission included antenna which was not able to transmit digital signal per se and therefore there was a need to convert digital to analog signal so that antenna can transmit this signal. Since mobile phones were not as tiny in size during the 2G period, the requirements for antenna designs were also less crucial. In actuality, they were 30% bigger than smartphones from this decade. The monopole and helical antennas used in the first cellphones with internal antennae had to fit within the phones, but in order to achieve the necessary operating frequency, their length had to be double that of the mobile phone. When the user called someone else, these antennas needed to be extended. Smartphones were evolving into multi-featured, multifunctional devices that could fit many wireless chipsets in addition to traditional cellular chipsets into a very small mobile terminal. Along with conventional cellular standards, chipsets for WiFi, Bluetooth, and GPS were developed [3].

The development in the mobile communication field has led to the growth of antenna designs research this is covered in the following chapter. Antenna design analysis attains the changes in the design that occurred for different generations for effective data rate enhancement which cannot be done effectively using traditional design used in previous generation. Printed circuit antennas were used in the 2G mobile phone era and were commercially feasible. Typically, a system ground coupled to various printed lines that meandered and had parasitic structures leading to enable dual band operation. The majority of these antennas, which are a trend even in commercial devices that are already on the market, exhibited nearly omni-directional patterns and low radiation efficiency in 2G devices.

When data rates requirement increased that manufacturers and service providers needed to support as wireless standards, the transition from 2G to 3G happened (around year 2000). As there is a geographic dependence of carrier operating frequencies, it was customary to support numerous bands. The main factor behind 4G's remarkable data growth and commercial success was the introduction of video streaming services. Mobile phones with 4G capabilities included several printed multiband antennas, or multiple input multiple output (MIMO) technology.

Mobile users are continually rising throughout the world and mobile applications are becoming more and more data-intensive, the usage of mobile devices has been expanding quickly over the past several decades and is expected to do so in the near future.

1.2 CLASSIFICATION OF 5G BANDS

A significant advancement has been made in Third Generation Partnership Project (3GPP), in both network and device technology as there isn't a single solution or technology that can perfectly fit all the many possible 5G applications. The two main technologies of 5G are thought to be MIMO technology and millimeter wave (mm-Wave) communication [4]. Current research and design of 5G smartphone antenna relies on MIMO technology for efficient data-rate enhancement. There are mainly two different bands assigned to 5G communication: Sub-6 GHz band and Millimeter wave band. In Millimeter wave band frequency ranges from 10 to 300 GHz. For early deployment of 5G communication sub-6 GHz band is very crucial. In sub-6 GHz 3.3-

3.6 GHz, 3.6-3.8 GHz, are the two main bands assigned for 5G. Other than these bands an unlicensed band ranges from 5.15-5.925 GHz. These three bands are popularly known as Long term evolution (LTE) 42, 43 and 46 bands respectively. In this work the antennas that are designed are working in sub-6 GHz range.

1.3 PERFORMANCE INDICES

Quantitative evaluation of antenna after designing an antenna is important to judge the performance and suitability of antenna. The reflection coefficient, total efficiency, ECC (envelop correlation coefficient), radiation pattern, channel capacity, and bandwidth are often used metrics in cellular antenna designs. The contents of this section are only a brief review of frequently used parameters [5-8].

- **Total Efficiency**: The total simulated efficiency is an efficiency which take accounts of the losses and may be estimated using equation 1.

$$\text{Total Efficiency} = \eta_{\text{rad}} * (1 - |\text{r}|^2) \tag{1.1}$$

where, r = is the reflection coefficient and, η_{rad} denote the radiation efficiency.

- **Envelop Correlation Coefficient (ECC):** ECC value is an indicator of the correlation between MIMO antenna radiation patterns. The most important factor in determining the diversity gain of MIMO antennas is thought to be the ECC. For 5G MIMO, ECC values less than 0.5 indicate strong diversity performance. Higher ECC value (i.e > 0.5) degrades MIMO performance because there is a substantial correlation between the antenna elements and the channel routes. Since MIMO systems execute finest when there is independence between the signals they receive. Using far field radiation patterns, the ECC between antenna i and j is computed using the formulas provided below [6].

$$ECC = \left| \frac{\int_0^{2\pi}\int_0^{\pi}\left(XPR.E_{\theta i}.E_{\theta j}^{*}.P_{\theta} + XPR.E_{\phi i}.E_{\phi j}^{*}.P_{\phi}\right)\sin(\theta)d\theta d\phi}{\sqrt{\prod_{k=i,j}\int_0^{2\pi}\int_0^{\pi}\left(XRPE_{\theta k}.E_{\theta k}^{*}.P_{\theta} + XRPE_{\phi k}.E_{\phi k.}^{*}P_{\phi}\right)\sin(\theta)d\theta d\phi}} \right|^2 \tag{1.2}$$

Here,$E_{\theta i}$, $E_{\theta i}$, $E_{\phi i}$, and $E_{\phi j}$, are the far-field radiation components. i and j are two antenna element , while θ and ϕ indicate the vertical and horizontal polarizations.

The cross polarization ratio in between the horizontal and vertically polarized components is known as XPR. The propagation environment's angular power spectrum that satisfies the subsequent conditions is represented by P_{θ}, and P_{φ}.

$$\int_0^{2\pi}\int_0^{\pi}\left(P_{\phi}\right)d\Omega = 1 \tag{1.3}$$

$$\int_0^{2\pi}\int_0^{\pi}\left(P_{\theta}\right)d\Omega = 1 \tag{1.4}$$

Since most works use the assumption that the environment has a uniform distribution (i.e., an isotropic environment), this scenario can be compared under the same assumptions. When MIMO systems are operating in rich multipath settings, this environment is frequently employed.

$$ECC = \frac{\left|\iint_{4\pi} E_i(\theta,\phi) * E_j(\theta,\phi)^{*}\partial\Omega\right|^2}{\iint_{4\pi}|E_i(\theta,\phi)|^2\partial\Omega \iint_{4\pi}\left|E_j(\theta,\phi)\right|^2\partial\Omega} \tag{1.5}$$

where $E_i(\theta,\phi)$ and $E_j(\theta,\phi)$are two radiation field, θ and ϕ are direction coordinates and i and j are the two ports being excited.

Equation 1.6 is based on S-parameters

$$ECC = \left|\frac{\left|S_{ii}^{*}\ S_{ij} + S_{ji}^{*}\ S_{jj}\right|}{\left(\sqrt{1-|S_{ii}|^2-\left|S_{ji}\right|^2}\right)\left(\sqrt{1-\left|S_{jj}\right|^2-\left|S_{ij}\right|^2}\right)\eta_{radi}\,\eta_{radj}}\right|^2 \tag{1.6}$$

Where two elements under observation are represented by symbol i and j and η_{radi} and η_{radj} are the radiation efficiency of element i and j.

Channel Capacity: It find its use in assessing the performance of multiplexing for any MIMO system. Instantaneous channel capacity C_o assuming that the assigned power of each antenna is the same is stated as

$$C_o = log_2\left(I_N + \frac{\rho}{Nn_T} HH^H\right) \tag{1.7}$$

The channel (H) used for rayleigh fading environment is independent identically distributed (iid)

$$H = R^{1/2} H_w \tag{1.8}$$

Where R signifies the the receive correlation matrix which completely characterizes correlation among the receive antennas, as well as the impacts of the antennas on the channel.

MIMO performance can be estimated using equation (1.9) that is obtained by averaging large number of channel realization.

$$C = E\left\{log_2\left[det\left(I_N + \frac{\rho}{Nn_T} HH^H\right)\right]\right\} \tag{1.9}$$

Where E stands for expectation, channel matrix is H, (N×N), and average SNR is ρ/N, identity matrix is I_N, and transmitting antennas is n_T. and SNR of 20 dB in the receiver is considered.

1.4 SOFTWARE AND HARDWARE PLATFORM

The HFSS (HFSS 2015b) environment is used for all of the experimentation completed for this thesis. To evaluate how the user's hand influences antenna performance, simulations were carried out in CST Microwave Studio. To test the S-parameters vector a Rohde and Schwarz ZVL vector network analyzer (VNA) is used. It is suitable for all constructed antennas and operates between 9 KHz and 13.6 GHz.

Figure 1.2 Image of the VNA used for testing

For radiation pattern testing anechoic chamber was used.

1.5 PRACTICAL CONSIDERATION

1.5.1 User Hand Effect

The dielectric properties of human hand are presented in table 1.1. It includes the relative permittivity and conductivity values at different frequencies (0.3 GHz to 6 GHz).

..

Table 1.1 Dielectric properties of hand phantom

Frequency (MHz)	Conductivity (σ ,S/m)	Relative Permittivity (ε_r)
300	0.36	37.1
450	0.43	33.9
835	0.59	30.3
900	0.62	30.0
1450	0.85	27.9

1575	**0.90**	**27.5**
1800	**0.99**	**27.0**
1900	**1.04**	**26.7**
1950	**1.07**	**26.6**
2000	**1.09**	**26.5**
2100	**1.14**	**26.3**
2450	**1.32**	**25.7**
3000	**1.61**	**24.8**
4000	**2.18**	**23.5**
5000	**2.84**	**22.2**
5200	**2.98**	**22.0**
5400	**3.11**	**21.7**
5600	**3.25**	**21.4**
5800	**3.38**	**21.2**
6000	**3.52**	**20.9**

1.5.2 Environmental effect

The impact of temperature fluctuations and moisture on antenna performance can lead to changes in material properties, such as shifts in the dielectric constant or conductivity. In order to mitigate these effects, the following strategies should be considered:

- **Material Selection**: Choosing materials with stable dielectric properties across a range of environmental conditions is crucial. Engineers can conduct simulations and experimental measurements to determine the ideal material for specific conditions, ensuring that the antenna maintains optimal performance.
- **Hydrophobic Coatings**: Moisture can degrade antenna performance by altering the conductivity and dielectric properties of the materials used. Applying hydrophobic coatings to antennas can reduce moisture absorption, thus minimizing the impact of environmental moisture.

- **Robust Mounting Structures**: A well-designed mounting structure ensures that antennas maintain their optimal position and minimize exposure to stresses caused by environmental factors. This can be achieved by using durable materials and providing sufficient protection from physical and environmental wear.
- **Sophisticated Signal Processing Techniques**: To neutralize the degradation caused by environmental factors, advanced signal processing algorithms can be employed. These techniques can help compensate for performance loss due to changes in the antenna's characteristics, improving the overall system reliability in variable conditions.

  The negative effects of different environmental factors on antennas can be minimized with these methods.

1.6 MOTIVATION

Mobile communications have advanced dramatically in recent years. This progress led to advancements in the design of base station and smartphone antennas. Although various researches have been done on mobile-phone antenna design, new antenna solutions are constantly needed to keep up with the current and upcoming generations of wireless technology.

In addition, there is a desire for providing simultaneous high-quality mobile communication services (5G) in compact sizes and with fewer aerial platforms. Despite the fact that several work have already been done, on the design of MIMO mobile-phone antennas, still, designing compact, inexpensive, multi-element, multi-standard (wideband or multi-band), antennas for smartphones is still a difficult problem.

MIMO can meet several additional 5G requirements in addition to satisfying user’s needs for high data speeds. By adding more antennas to the mobile phone, the wireless communication system's channel capacity may be efficiently expanded. Nevertheless, because mobile phones have a limited amount of space, it is challenging to install more antennas there while still preserving effective isolation with low envelope correlation coefficient (ECC).

Each design has been validated by fabricating and measuring its prototype. The performances of MIMO system with various mobile-phone components (antenna performance with battery, side frame and with user's hand) have been considered. The inadequacies of the current antenna designs is addressed by the suggested designs

1.6.1 Challenges in antenna design

MIMO system can enhance the channel capacity so ideally it would be better to install more number of antennas in the printed circuit board of mobile phone. However, practically it is not possible as increasing the antenna elements can lead to bad performing MIMO system with high mutual coupling [9-10]. Hence, it is important to install only that number of antennas element such that it should not severely affect the working of the other antenna elements. Additionally, researchers are looking for new locations to attach antennas due to the growing need for thin mobile phones. Decoupling techniques need to be installed [11-12].

The side-frame of the smartphone is being considered as a new space where antenna can be installed [13]. But this could result in a bulky smartphones if not designed properly. Hence the size of the side-frame must be reduced so that it would not impact the appearance of the device and also must work properly despite such space constraints. Another aspect is to miniaturize and add multiband antenna in the mobile phone so as to cater the two or more bands simultaneously. Various literature are providing dual band but they are only focused on improving one or two components of 5G smartphones. To compete with the recent trend of using mobile-phones with metal body a metal-rim compact MIMO antenna system has been proposed

Some research gaps have been identified and are addressed in the section that follows. These were formed in light of this motivation and the extensive literature survey that was given in Chapter 2.

1.7 RESEARCH GAPS

Several research gaps are identified based on a thorough analysis of several 5G antenna design methodologies. These gaps serve as the basis for the objective structuring of this research project.

Research Gap 1: Data rate enhancement

One key challenge in densely packed MIMO antenna systems is the interference caused by mutual coupling between antennas. One way to remove this is to use any decoupling structure. But it will need extra space and increase the design complexity hence, a multiband structure is requires that avoid mutual coupling among the antennas that are tightly arranged.

Research Gap 2: Space Restriction

The printed circuit board is cluttered with tons of electronic circuitry. This makes it difficult to install any further antennas in it and now with the demand of slim mobile phones. It is important to achieve an ultrathin smartphone with decent MIMO performance.

Research Gap 3: Focusing on one parameter at a time

Another challenge is to extract multibands from single resonant antenna element. To achieve this T-shaped resonating structure is used.

Research Gap 4: Performance degradation due to the presence of metal-rim

The new trend of metal body smartphone is imposing new design challenge on antenna designers. Metal bezel smartphone will improve the durability of the mobilephones. But antenna radiation is affected with the presence of metal element in the side-frame. Some of these limitations are have been workedon in this research work.

1.8 OBJECTIVES

This research focuses on designing antenna solutions tailored for modern 5G smartphones. The design of compact MIMO systems with robust MIMO performance for 5G devices, which this research endeavors to achieve, is guided by the following objectives

Objective I

To design a compact, 12-element dual-band MIMO antenna with high isolation for 5G mobile applications.

Objective II

To design a compact side edge printed eight-element MIMO system for 5G smartphone applications.

Objective III

To design a t-shaped, multi-band MIMO antenna system for 5G smartphone applications.

Objective IV

To design a tri-band MIMO antenna system for 5G metal frame smartphone applications.

1.9 MAJOR CONTRIBUTION OF THE THESIS

This work is novel and highly beneficial to the scientific community, particularly in the field of 5G communication. As discussed, MIMO antenna systems are the key solution for the sub-6 GHz range. To maximize the performance of any MIMO system, the antennas must provide uncorrelated communication paths with optimal signal orthogonality.

Table 1.2 :Contributions of Proposed Work

S. No	Contributions
Design 1	A novel compact twelve-element MIMO antenna system using a slot antenna is presented. Optimal placement of MIMO antenna elements to minimize mutual coupling. A unique feeding system is designed to take up less space on the PCB.
Design 2	A compact-sized MIMO antenna system for ultra-thin smartphones based on a loop antenna is proposed. The MIMO system is installed on a 3 mm high side frame, the smallest size in current literature. Despite the low-profile design, the system maintains a high isolation of 14.8 dB, which is rare for such compact designs in the

	literature.
Design 3	A T-shaped structure installed on a 3.6 mm high side frame is proposed. An 8x8 MIMO antenna system is developed using this antenna unit. This design provides a unique combination of compactness, multiband coverage, and high isolation, features not offered simultaneously by any current state-of-the-art designs.
Design 4	A novel octal-element MIMO antenna for metal-rim smartphones is introduced. The design excites IFA and slot modes from the metal rim and ground plane slot, respectively. A feeding technique with a stub and meandered structure is presented for fine-tuning the two modes. This design improves antenna efficiency, addressing a major drawback in metal-rim-based antenna designs.

However, smartphones have practical limitations, such as limited space for antenna installation, as many other components are placed close to the antenna. These components can negatively affect antenna performance. Therefore, the primary focus of the designs presented in this thesis is achieving better isolation between antenna elements.

- **Impact of Physical Components:** The physical components around the antenna, such as the human hand, battery, and frame, can affect electromagnetic (EM) interactions if they are in close proximity to the antenna. These factors must be incorporated into MIMO antenna designs to ensure realistic and practical MIMO system performance. This thesis addresses the effects of the human hand, battery, and frame on the MIMO system's performance.
- **Compact Antenna Design for Ultra-thin Smartphones:** With antennas increasingly placed in the side frames of smartphones to optimize space without compromising functionality, there is a risk of making the device bulky. This thesis proposes a compact MIMO antenna for ultra-thin smartphones, overcoming the bulkiness that is typically associated with side-frame-based antenna structures. The proposed loop antenna-based MIMO system is installed on a 3mm-high side frame, which is the smallest side-frame size reported in current literature.
- **Multiband Coverage:** To reduce the number of required antennas, this work introduces a compact MIMO antenna system with multiband coverage, offering efficient functionality while minimizing antenna size.

- **Mitigating Mutual Coupling:** Mutual coupling remains a significant challenge in MIMO systems, especially within the confined space of smartphones. Since space is already limited, adding decoupling structures would further reduce available space for other circuitry. Each proposed design in this thesis provides adequate isolation between adjacent antennas without any extra decoupling structures, leading to a cost-effective solution.
- **Aesthetic Considerations:** Keeping in mind the aesthetic preferences of consumers for metal-rim structures, this thesis also presents a metal-rim-based MIMO system.

In summary, this thesis highlights how to effectively utilize the available space in smartphones to install antennas, achieving substantial MIMO performance while maintaining the device's compact size and modern aesthetics.

1.10 OUTLINE OF THE THESIS

There are seven chapters in this thesis, starting with chapter 1. **Chapter 1** contains the basic introduction along the preliminaries related to this research work. The remaining thesis is arranged in the chapters that follow.

Chapter 2 discusses a brief assessment of the past work in the field of 5G antenna design for smart phones. It also provides specifics on the research gaps found after reading the recent literature as well as the objectives that established for this investigation.

Chapter 3 deals with the design simulation, fabrication and experimental measured carried out for compact twelve antenna element system using slot antenna. This design was proposed to improve channel capacity while maintaining a decent isolation between antenna elements.

Chapter 4 addresses the issue of bulky designs while exploring the side-edge for the installation of antenna elements. An effective solution is presented for ultrathin smartphones with full screen. The comparisons between the theoretical and experimental results on these MIMO antenna configurations are also presented.

Chapter 5 presents dual-band T-Shaped compact MIMO antenna system. The simulated S-parameters have been presented along with different performance measures of MIMO system. The validation of the simulated results is done after fabricating the design and testing it under anechoic chamber.

Chapter 6 deals with the implementation of antenna design for the metal-rim smartphones. The designing of structure is done using combination of slot and inverted F-antenna (IFA) based antenna element. Design is supported by presenting all the design steps followed. Comparison between simulated and measured results is illustrated.

Chapter 7 summarizes the key outcomes of this thesis. The conclusion derived from the theoretical and experimental studies are described. Salient features of the proposed antenna systems and the scope of further extension of this research work is also outlined.

CHAPTER 2
LITERATURE REVIEW

CHAPTER 2

LITERATURE REVIEW

Fifth generation (5G) has become the research hotspot after the announcement of the bands assigned for 5G communication. From design point of view, investigation of different antenna solutions is getting more and more important nowadays. This chapter provides a broad review of the several antenna design techniques that have been developed recently to address the difficulty of placing a number of antennas in tight locations. Even though many academics have tackled this difficult task in a variety of ways, it remains a daunting task that needs more effort to establish a reliable strategy for effective antenna design.

This chapter comprises of a brief findings of the present state of research in the subject of 5G antenna design for smartphones, which motivated the authors to develop compact antenna solutions for the different challenges faced by antenna designers. The main advantages of 5G will include high data rates than previous generations, shorter time latency and increased channel capacity. Two new spectrum bands in the millimeter-wave (mm-wave) and sub-6 GHz ranges have been allocated for 5G. The two bands assigned to 5G are LTE 42/43 (3400-3800 MHz) [4].

MIMO technology was very popular technology for providing higher data rate and hence it was adopted in the antenna design field. It has been extensively being used in vehicle communication applications [14], wearable antennas [15]. In latest designs also existence of mutual coupling was inevitable with the MIMO system if used in confined spaces. Various techniques are presented in the latest researches to improve isolation. In vehicle communication a cross-shaped substrate is used instead of a square one. The purpose of changing the substrate was to enhance isolation [14]. In another design, a frequency-selective surface (FSS) based superstrate is used to improve isolation [16]. Another methods to improve isolation includes designing of an array of metamaterial unit cells to improves isolation[17], or surround a cavity wall made up of copper [18] with antenna elements, use defective ground structure [19] and Band-Gap (EBG) [20].

2.1 MIMO ANTENNA SYSTEMS

For 5G smartphone application this MIMO technology played very important role in initial deployment of 5G communication in sub-6 GHz range.

2.1.1 MIMO system based on slot antennas

Slot antennas are already popular in designing for WLAN/WiMAX applications. In one design a defective ground plane and F-shaped slot radiators are used to design an antenna for WLAN/Wimax applications. Three separate bands are covered by the antenna these are: band one if from 2.0 to 2.76, second is from 3.04 to 4.0, and third is from 5.2 to 6.0 GHz [20]. The first antenna types preferred for 5G cellphone applications is the slot antenna. This is due to the fact that the quarter-wavelength-long open slot resonance mode is readily excited, enabling a significant decrease in the slot antenna's real size [21-27]. These designs can improve bandwidth.

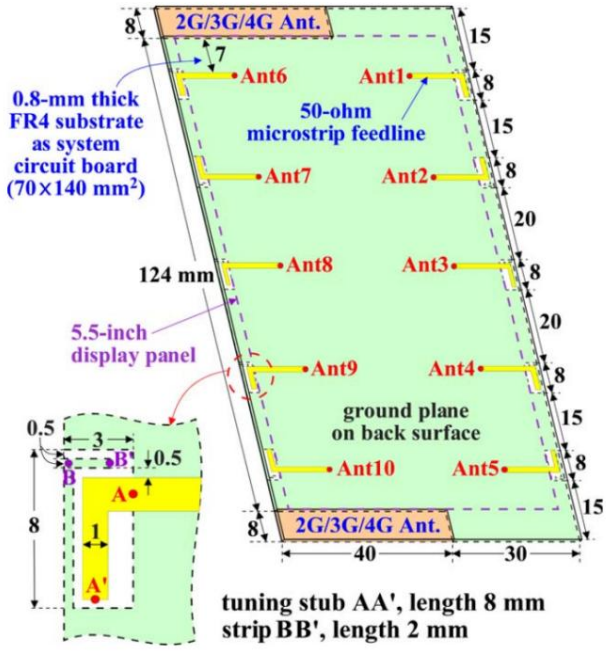

Figure 2.1: Geometry of 10-element MIMO system based on slot antenna [21]

As can be seen from Figure 2.1 that slot antennas are present on system ground that are fed by feeding line of L-shaped [22]. The drawback of using a slot design is that it must be embedded or integrated into the smartphone system ground, which requires reserving a large portion of the ground plane to place antennas.

2.1.2 MIMO system based on Inverted-F antenna

Inverted F-antenna is also an antenna that is of quarter wavelength. For designing MIMO system for 5G smartphone applications various researchers have used this antenna [28-33]. In one design the planar inverted-F antenna (PIFA) is constructed by attaching a vertical metallic patch to it, and then adjusting a different PIFA to excite the antenna. MIMO system of eight elements is then created using this structure (see Figure 2.2).

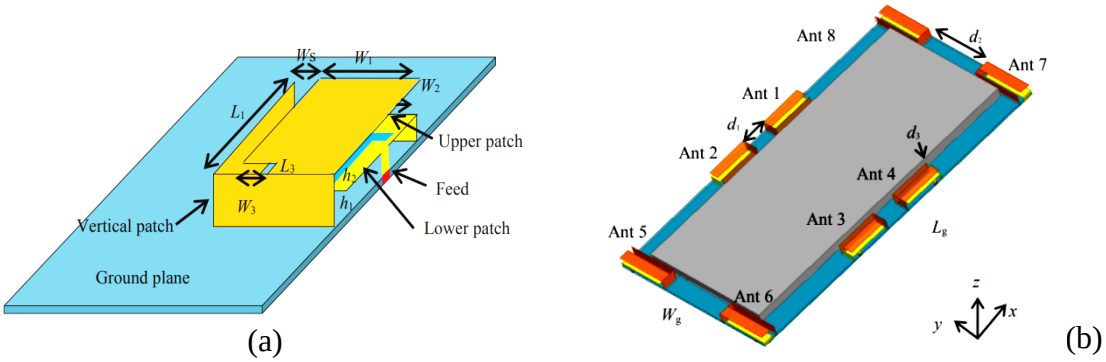

Figure 2.2: (a) Geometry of single antenna element (b) MIMO system [28]

This type of antenna is compatible with various platforms as it effectively suppress ground current effect [28]. In the next approach several inverted-F antennas (IFAs) are positioned on an artificial magnetic conductor (AMC) ground to create the antenna design. The local resonant mode and the TM_0 surface-wave mode are the two different modes that the IFAs excite on the AMC [31]. Another design for 5G phone provides controllable electric field (E-field) null. A basic feeding network and inverted-F antenna (IFA) make up the suggested antenna pair [32]. Wider impedance bandwidths may be achieved by the stub-loaded IFA. Excellent isolation performance may be achieved by this approach.

2.1.3 MIMO system based on monopole antenna

In addition to using the slot and IFA antennas, the monopole antenna design is another simple way to achieve a single resonance mode (with quarter-wavelength) [34-40]. The mutual coupling is reduced by exciting two separate bands [34]. In another design as well antenna pairs are made up of a monopole and a loop antenna

that co-locate and have a small combined size [37]. There is a technique of couple feeding the monopole antenna element instead of using direct feeding. By this couple feeding monopole resonates at half wavelength instead of quarter wavelength [39]. In another design monopole antenna is used to excite higher order modes [40]

2.1.4 MIMO system based on loop antenna

Any form of traditional loop antenna, including square, circular, and folded-dipole loops, resonates at full wavelength resonance mode with its current null (Inull) or voltage maximum point situated on the two sides, and its maximum current (Imax) position usually dispersed at the top section and bottom part (feeding point) as revealed in Figure 2.3 [41].

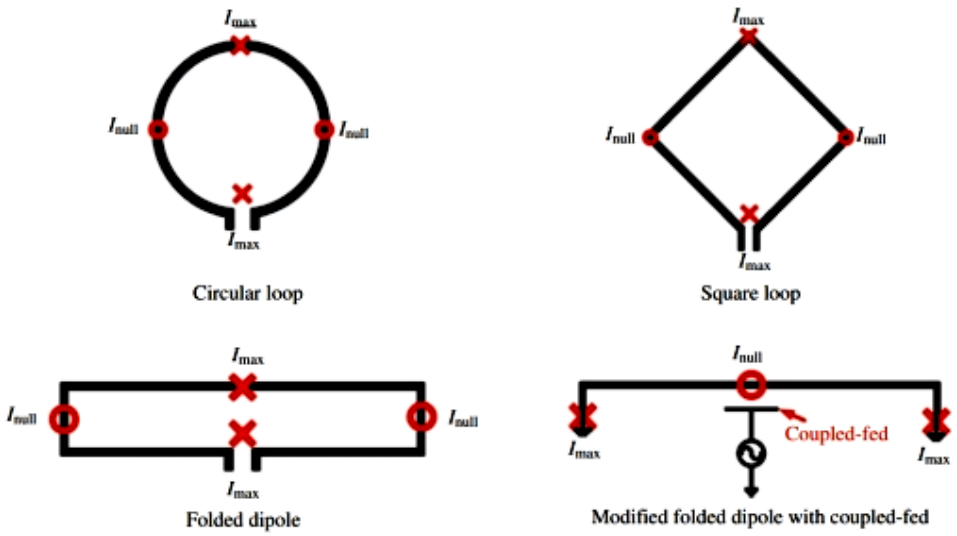

Figure 2.3: Fundamental loop antenna structures [40]

There are various MIMO antenna designs in 5G communication that are based on loop structure [42-52]. A slot mode and double coupled-fed loop modes are effectively stimulated with the help of connection of feed line with tuning strip [34]. Folded monopoles and gap-coupled loop branches make up an antenna unit and used to create a MIMO system [48]. In another design it is suggested to use a building block made up of a loop and a slot antenna. Interestingly single antenna element compactness is successfully enhanced by the rectangular clearance shared by the slot and loop antennas. The suggested construction block shows better isolation (> 19 dB) [49].

2.1.5 Multiband and wideband MIMO antenna system

This section discusses antenna with dual band or wide band coverage. To provide the seamless connectivity globally multiband and wideband antenna were proposed [53-73]. A MIMO antenna system is created by using metal rims of a mobile phone [56]. In the next design it is suggested to use a unique design strategy to excite many useful modes beneath an inverted-L antenna (ILA) for bandwidth augmentation. Using an analogous transmission line model as a basis, the operating idea of exciting numerous modes with the same order/electrical-length is first studied theoretically. The antenna theoretically overcomes the restrictions on the number of suitable resonances and available operating bands using this manner. In order to attain expanded bandwidth in different working bands, the second step involves investigating how to load a parallel capacitor in order to shift resonant modes to the appropriate band [53].

2.2 RESEARCH PROBLEM FORMULATION

Various researchers have utilized MIMO technology in 5G mobile communication [74-82]. By including more antennas in the mobile handset, the data-rate can be improved [76]. However, due to the limited space inside the cell phone, it is challenging to add more antennas while still maintaining good isolation [77]. An eight element antenna system is created with slot and monopole with 12 dB isolation [78]. In another design [79], a tri-band 12 element MIMO is revealed, of which 2 components operate at both bands while the remaining 6 elements operate at 3.6 GHz as well as LTE band 46 (5.15–5.925 GHz). Therefore, to enhance the channel capacity, this design does not completely utilize all the 12 elements. In one of the designs parasitic structure [81] is used as a method to achieve 15 dB isolation. In [61], balanced antenna elements are utilized to achieve improved isolation.

It is important to focus on the compactness of the smartphone also as, ultra-slim phones are in high demand. Recently antenna researchers are searching for different locations to install antenna on smartphones. The main circuit board of the smartphone is full of electronic circuitry and as already discussed that in 5G multiple antennas need to be installed. Hence recently many literatures are exploring side-frame of the smartphones to install antennas [83-89]. One of the effects of using side-frame is that it

can make the overall design of smartphone bulky if not designed properly and it might not be suitable for ultrathin smartphones. The height of the side frame is important to take into consideration while designing the antenna that will be installed on the side-frame. Although the designs mentioned in [83-89] are proving to provide reasonable MIMO performance, however, side-frames height is 6 mm or more in these designs and after installation of smartphone's actual frame (outer body of the smartphone) this height will increase further. This might limit their use in the ultra-thin smartphones. Hence there was a need to design a MIMO system wherein if the side-frame was being used to install antenna than overall design must be miniaturized such that the smartphone does not become bulky. Taking these points in consideration in reference [13] a MIMO system was presented where the antennas were mounted on the side-frame of height 3 mm. This was the lowest height achieved till now and is appropriate for thin smartphones. The isolation achieved was 10 dB. But still there is a need to design an MIMO system that is suitable for ultrathin smartphones and also provide decent isolation.

Another aspect of designing MIMO systems for 5G communication is that the there must be seamless internet access globally. Hence to achieve this MIMO systems should be designed to operate on multiple bands simultaneously. Many researchers were also interested in working in this direction as well therefore designs in [90-98] realized to work on dual or multiband. In one of the design [90] use of multiple branch based monopole antenna was done to construct the eight element complete MIMO system. Another design [60] used loop antenna and monopole antenna to work on two different bands. To reduce mutual coupling, decoupling stubs and neutralized lines are employed between parts in these systems. The isolation offered by the aforementioned MIMO antenna designs is 11.5 dB and 10 dB, respectively, and may be enhanced. However, LTE 46 band was not taken into account by the design. An array of self-decoupled antenna elements is formed [91], using two radiating branches of varying lengths are combined to produce two resonances. An identical antenna is also positioned close to this one, sharing a single shared ground between both. Using this method, isolation has increased to 17.5 dB.

Additionally, wide band antennas covering all 5G channels in the sub-6 GHz range are being built, according to recent research [95-100]. Their ability to operate across all sub-6 GHz 5G band frequencies is a benefit. Nonetheless, in these designs, the

antenna components are mounted using side frames that are 5 mm in diameter or larger. The use of these structures in incredibly thin cellphones may be restricted as a result. Every design that was previously discussed is geared more toward enhancing one of the MIMO array's properties; for example, some designs prioritize enhancing isolation, others offer dual band coverage, while yet others are more concerned with downsizing. However, very few solutions take into account simultaneous improvements in isolation, compactness, and working on LTE 42/46 bands.

For meal rim antennas, researchers have developed a number of intriguing designs. Creating an antenna radiator out of the metal rim is a common move towards getting adequate bandwidth and efficiency. Based on the usage of metal frames as a radiator, it can be separated into two categories: those that exploit the full metal rim as a radiator [101–106] and those that only use a section of metal rim [107–116] as radiator. Metal rims with no gaps between them typically have greater mechanical stability. Though, each of the aforementioned concepts has its own drawbacks. Every antenna design exhibits -6 dB impedance bandwidth, which impact the efficiency. Design has 7.49 dB isolation in [105]. In the most recent studies [117–120], various designs for the 5G smart phone antenna arrays were put forth. A capacitive-decoupler based MIMO system is suggested [117]. It is compatible with both the frequency ranges of 3.3-3.69 GHz and the 3.42-3.73 GHz. A high level of 24 dB isolation between antenna elements is provided by the design. The design in [118] is centered on supporting the wide bandwidth. Additionally, the designs in [121-123] are not appropriate for smart phones with metal rims. In the most recent literatures [124–126], numerous efficient decoupling techniques are suggested. Antenna interference cancelation utilizing LTCC technology [125], ceramic superstrate-based [126], and meta-surface-based [123] have all been suggested. However, because these methods of decoupling are multi-layer based, fabrication challenges are increased. In order to include these technologies into the metal-rim smart phone, it is also necessary to notice their decoupling capabilities in such environment. Another design [127] is able to e attain the high isolation of 18 dB. The design combination does not, however, cover LTE 42/43.

2.3 RESEARCH GAPS

There exist many attempts by the researchers towards devising loop antenna based techniques for designing 5G smartphones. The exhaustive literature survey of various antenna systems for 5G Smartphone carried out in this work leads to the formulation of the following research gaps. Mutual coupling between densely integrated antennas used in MIMO setup is the primary drawback. One way to remove this is to use any decoupling structure. But it will need extra space and increase the design complexity hence, a multiband structure is requires that avoid mutual coupling among the antennas that are positioned in near vicinity with each other.

1. There is a need to install multiple antennas in the smartphones in order to achieve the user's demand of higher data rates. The main set back in achieving higher data rate was low isolation between antenna elements. There is a need of a MIMO system that can enhance the data rate without getting much affected by mutual coupling.

2. The printed circuit board (PCB) of a smartphone is filled with many electronic components. Hence it is challenging to find space for installing multiple antennas in it, because of the space restrictions. As the demand of ultra-thin smartphone is increasing it made it even more challenging for an antenna designer to find space to install antennas. This problem can be resolved by utilizing a different place to install antenna, other than the main PCB of smartphone. But doing so can make the overall design of smartphone bulky. Hence the size of the side-frame must be reduced so that it would not impact the appearance of the device and also must work properly despite such space constraints. Keeping in mind the user demands there is a need to design a MIMO system that is compact, and also provide decent isolation.
3. Another challenge is to extract multiple performance parameters simultaneously from a single resonant antenna structure such as multiband coverage, good isolation and compact size. Hence, there is a need to design a structure that is compact, operates on multiple bands and provide high isolation as well.

4. The new trend of metal body smartphone is imposing new design challenge on antenna designers. Metal bezel smartphone will improve the durability of the mobilephones. But antenna radiation is affected with the presence of metal element in the side-frame. Some of these limitations are being addressed in this work.

Based on the research gaps following research objective have been framed.

Objective I

To design a compact 12-element dual-band MIMO antenna with high isolation for 5G mobile applications

Objective II

To design a compact side edge printed eight-element MIMO system for 5G smartphone Applications

Objective III

To design a T-Shaped multi-band MIMO antenna system for 5G smartphone applications

Objective IV

To design a tri-band MIMO antenna system for 5G metal frame smartphone applications

The four objectives outlined for this study have led to the division of the research approach into four stages for this thesis that are presented in the following chapters The suggested MIMO antenna system employs a strategic placement of antenna elements that ensure optimum isolation, contributing to improved performance.

CHAPTER 3

DESIGN AND DEVELOPMENT OF A COMPACT 12-ELEMENT DUAL-BAND MIMO ANTENNA WITH HIGH ISOLATION FOR 5G MOBILE APPLICATIONS

CHAPTER 3

DESIGN AND DEVELOPMENT OF A COMPACT 12-ELEMENT DUAL-BAND MIMO ANTENNA WITH HIGH ISOLATION FOR 5G MOBILE APPLICATIONS

3.1 INTRODUCTION

The fifth generation (5G) of mobile communication is now seeing very great interest from the researches as it is on the horizon in today's technologically dynamic world of communication. The mobile communication standard is moving into its next phase, which will offer numerous enticing improvements over earlier iterations. The main advantages of 5G will include high data rates than previous generations, shorter time latency and increased channel capacity [74]. Two new spectrum bands in the millimeter-wave (mm-wave) and sub-6 GHz ranges have been allocated for 5G. The researchers have utilized multiple-input multiple-output (MIMO) technology in 5G mobile communication. By including more antennas in the mobile handset, the data-rate can be improved [76]. However, due to the limited space inside the cell phone, it is challenging to add more antennas while still maintaining good isolation [77]. Recent research [78-152] is based on MIMO antenna arrays.

In the literature review, although various MIMO system for 5G smartphones are reported, but these methods do possess certain limitations in improving data-rate along with decent isolation. Hence a twelve-element MIMO system is designed for the forthcoming 5G smartphone in sub-6 GHz applications

This research aims to address the inadequacies of the current methodologies by offering potential resolutions for each problem. This chapter's goal is to maintain a trade-off between isolation and datarate improvement.

3.2 ANTENNA DESIGN

Figure 3.1 demonstrates the construction of the suggested slot antenna based MIMO system. The circuit board of the design has dimensions of 150×80×0.8 mm^3, which is appropriate for most 6-inch mobile phones.

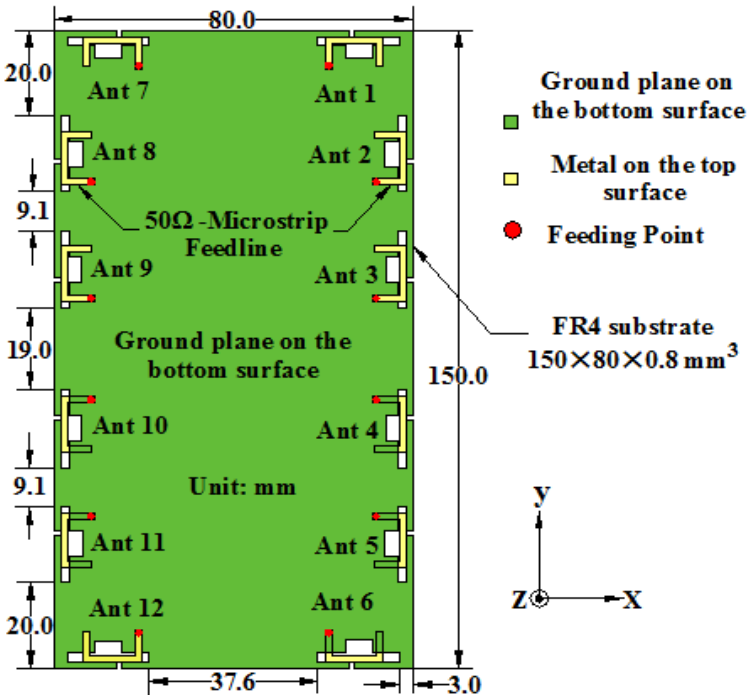

(a)

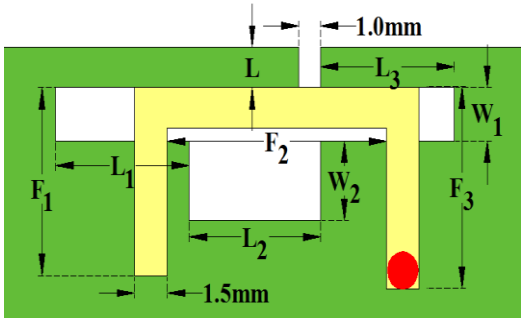

(b)

Figure 3.1 (a) Overall view of the geometry (b) single antenna

The substrate is made of FR4 and has a thickness of 0.8 mm (loss tangent is 0.02 and dielectric constant is 4.4). Antenna structure is composed of slot antenna along with the feeding strip. We take advantage of two orthogonal slot sites to lessen mutual

coupling. Four antenna components (antenna 1, 6, 7 and 12) are positioned along the ground plane's shorter edges, and eight antennas (antenna 2, 5, and antenna 8 to antenna 11) are mounted along the ground plane's longer edges.

3.2.1 Antenna Unit

Single antenna elements complete structure is exhibited in Figure 3.1 (b). The defect at the bottom (slit antenna) can be divided into different parts, first is the three horizontal slots of length L_1=6.1 mm, L_2 =6 mm, L_3=6.1 mm, and one Slit antenna of length L=1.5 mm. Width W_1 is 2 mm. The slot L_2 exhibits extra width of W_2. It is included in order to shorten the slot, just as it was in the reference [89]. This slot is fed by a feeding strip. This feed line's C-type design helps to minimize the size of the single antenna element overall. Thus feeding strip has three sections of length F_1=7 mm, F_2 =10 mm, and F_3=7.5 mm with a width of 1.5 mm. The width W_2 for different antennas is varied to precisely tune the antennas regarding their locations. Therefore antenna-1, 2, 5, 6, 8, L_1, and L_2 have width W_2=3 mm. The rest of the antennas (3, 4, 9, and 10) have width W_2=2.5 mm.

3.3 PARAMETRIC ANALYSIS

To study the overall performance of this MIMO system it is significant to know the effect of each parameter on the antenna performance. Hence, few of the important parameters that severely effect antenna performance have been discussed in this section. After altering the width W_2 and length L_2, the antenna's S_{11} characteristic is examined in Figures 3.2(a) and 3.2(b), respectively.

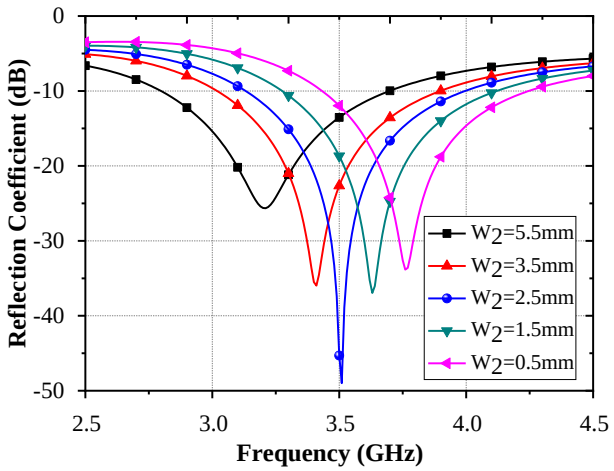

(a)

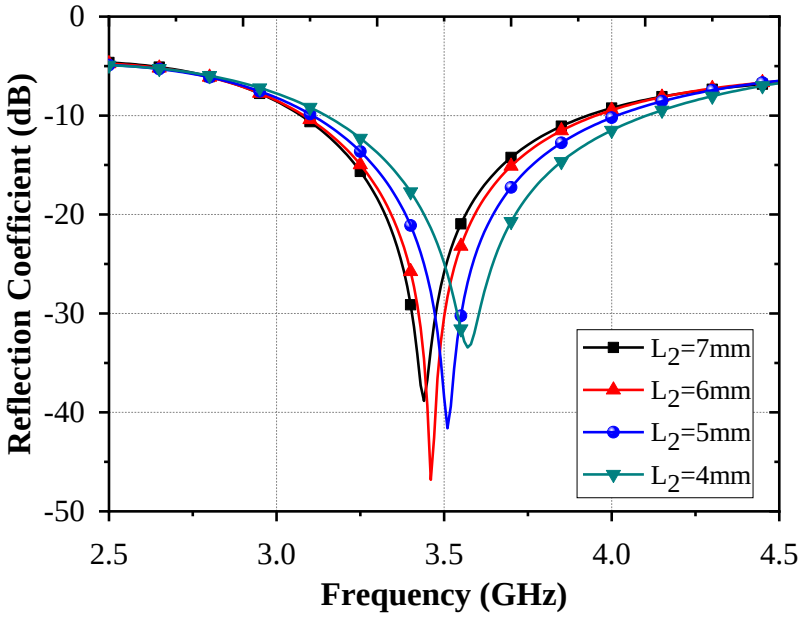

(b)

Figure 3.2 Reflection coefficient of varying (a) width W_2 (b) length L_2 when W_2=2.5 mm

The effect of changing the width W_2 on frequency is indicated in Figure 3.2 (a). As the width increases frequency decreases. The length L_2 also change the resonant frequency as revealed in Figure 3.2 (b). The raise in frequency can be seen when length L_2 is reduced.

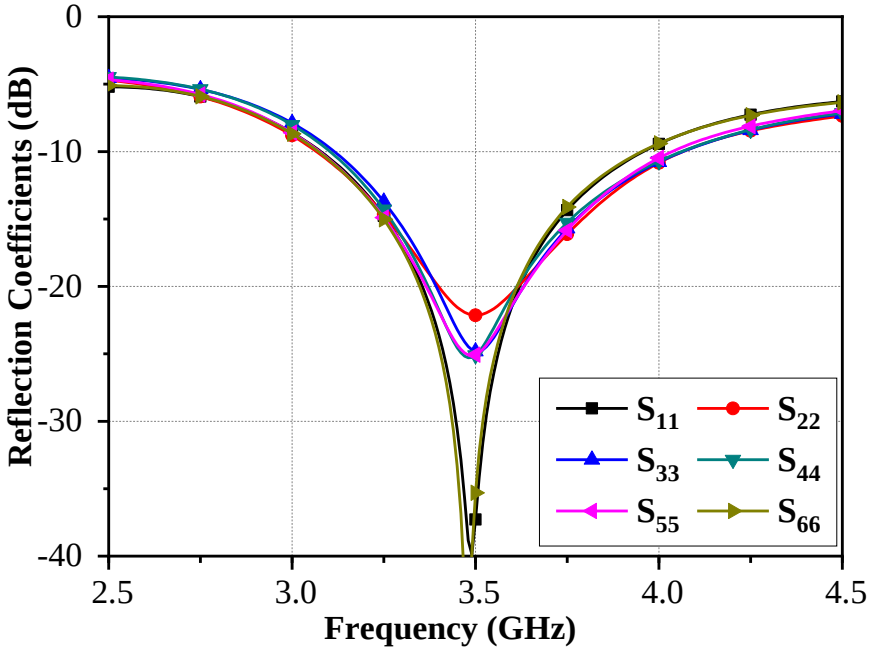

(a)

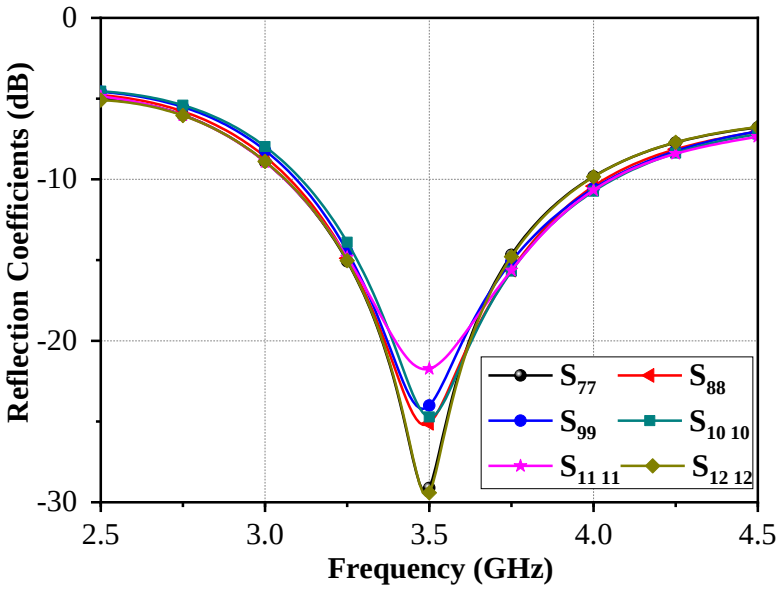

(b)

Figure 3.3 Simulated reflection coefficient of the proposed array

Hence, to get desired resonant frequency W_2 and length L_2 can be adjusted. As shown in Figure 3.3(a) and 3.3(b), LTE bands 42/43 (10 dB impedance bandwidth) can be supported by the suggested antenna system. Isolation of nearby antennas is shown in Figure 3.4. The design offers greater than 15 dB isolation among any two antennas. The two major cause for obtained isolation are orthogonal antenna placements and spatial variety (feeding points of adjacent elements are not facing each other; therefore spacing between the two ports is greater). With these fair reflection and isolation performance, MIMO can achieve better diversity and multiplexing performance.

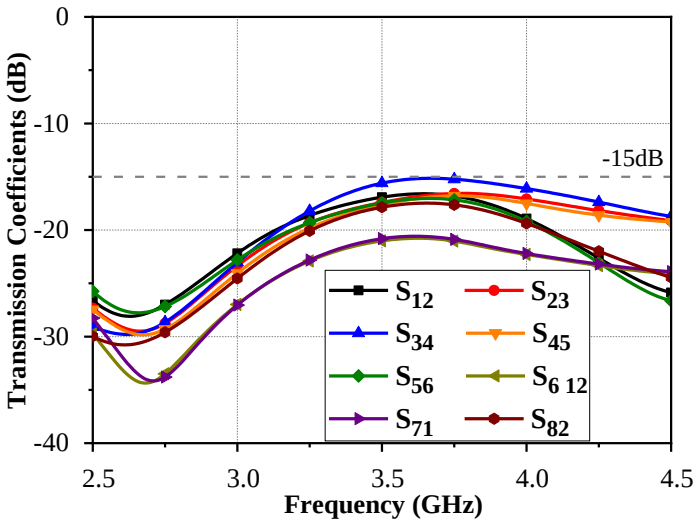

Figure 3.4 Simulated isolation of the proposed MIMO

3.4 RESULTS AND DISCUSSION

A prototype was fabricated as revealed in Figure 3.5. With the help of this prototype the simulated results can be verified. A vector network analyzer (VNA) had been used to determine the S-parameters as shown in Figure 3.6 and 3.7.

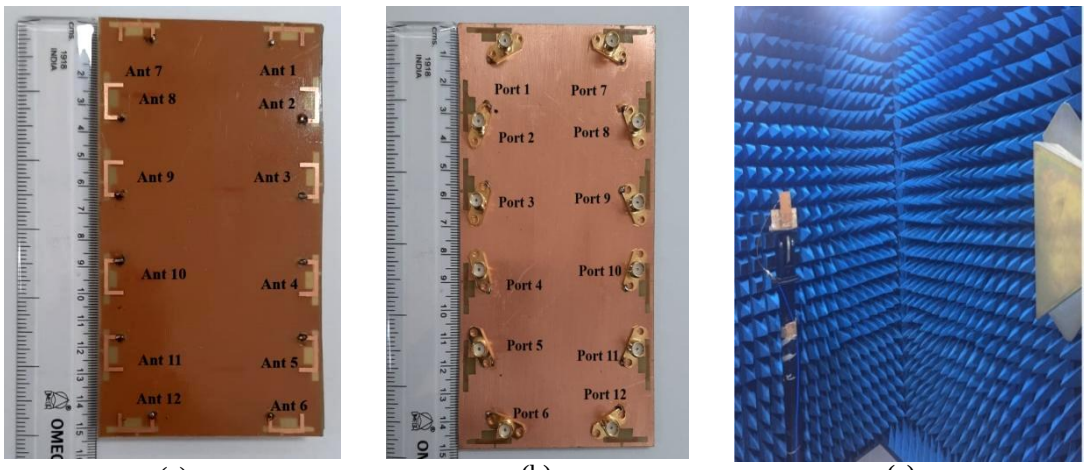

(a) (b) (c)

Figure 3.5 Fabricated prototype of proposed antenna (a) Front view (b) Back view (c) MIMO Antenna placement in anechoic chamber for radiation pattern testing*

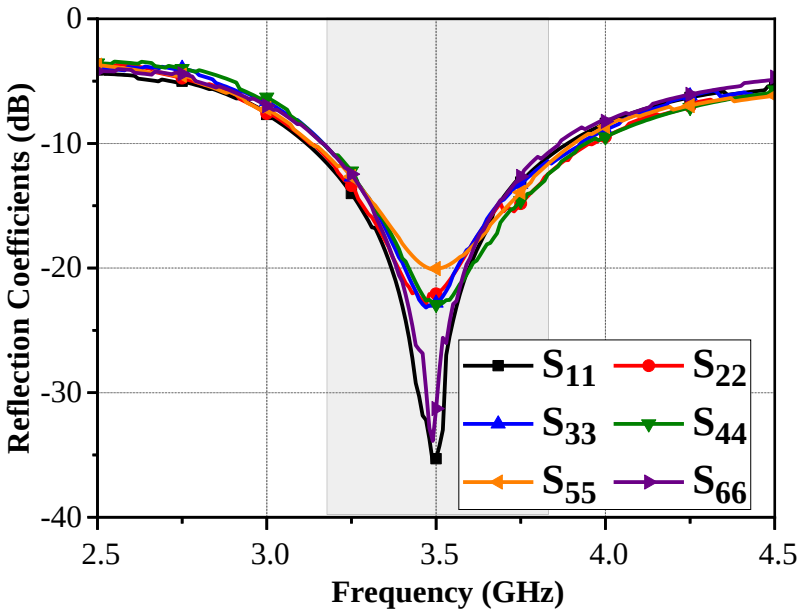

(a)

* The fabrication has been performed in School of Computational and Integrative Sciences, JNU, Delhi, India
Measurement has been performed in Electronics and Communication Engineering Department, Shri Mata Vaishno Devi University, Katra, J&K, India and Jaypee Institute of Information Technology, Noida, India

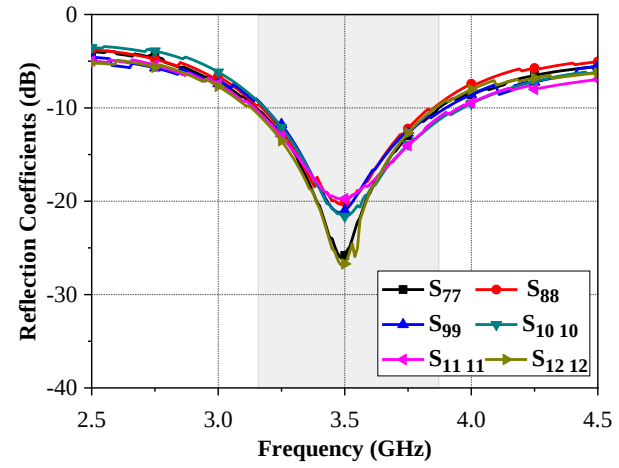

(b)

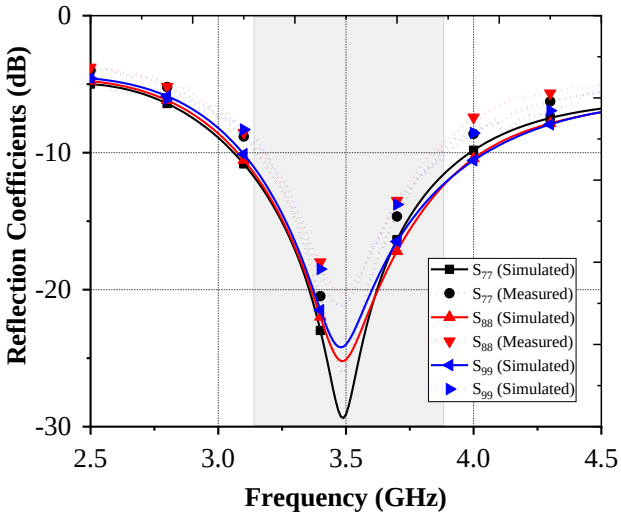

(c)

Figure 3.6 Measured (a) Reflection coefficient of Ant 1 to Ant 6 (b) Reflection coefficient of Ant 7 to Ant 9 (c) Comparison of few measured and simulated results

The measurement results are revealed in Figure 3.7. Measured reflection coefficients are represented in Figure 3.6 (a) and 3.6 (b). Antennas still cover the complete LTE 42/43 (3.4 GHz-3.8 GHz) bands. Figure 3.7 represent the Mutual coupling of antennas where S_{12}, S_{23}, S_{45}, S_{56}, S_{612}, S_{82}, and S_{71} are better than 17 dB and S_{34} is superior than 14.8 dB. The results are consistent with the simulated results; connection and manufacturing loss may be the cause of the discrepancy in the results.

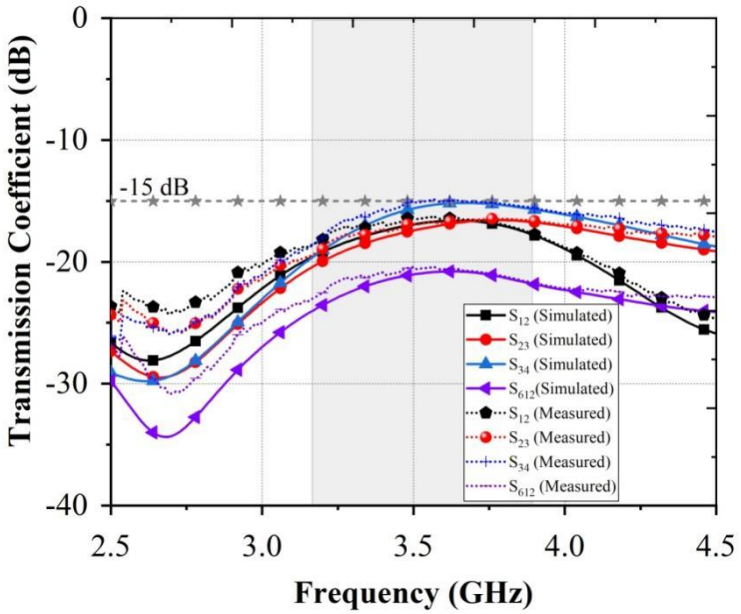

Figure 3.7 Measured isolation of proposed array.

3.4.1 Radiation Performance

Given that every antenna is symmetrically positioned and has the same size, for that reason results of the only Ant1 to Ant 3 and ant 6 are shown for brevity. The acceptable total efficiency of the suggested array is obtained as given in Figure 3.8. Efficiency varies between 74-89%. In order to save space, only the radiation performance of antenna 1 to 3 and antenna 6 is displayed in Figure 3.9. The radiation pattern resembles Omni-directional radiation pattern. Peak gain of antenna elements ranges

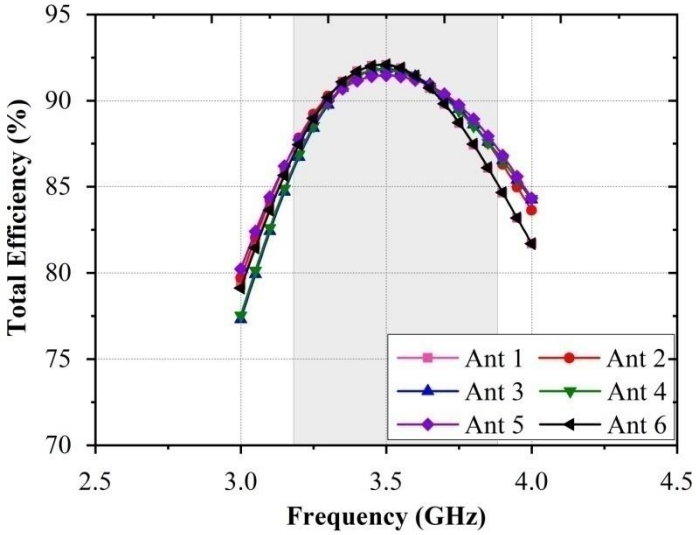

Figure 3.8 Simulated total efficiencies Ant1-Ant6

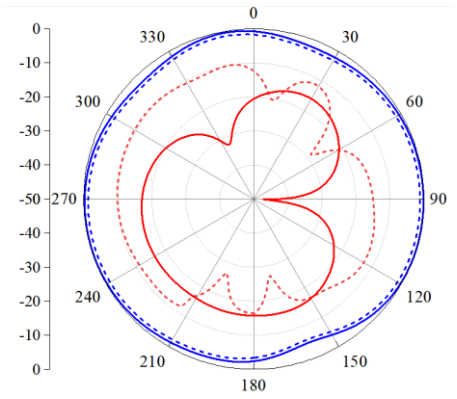
0
30
60
90
120
150
180
210
240
270
300
330
0
-10
-20
-30
-40
-50

(a)

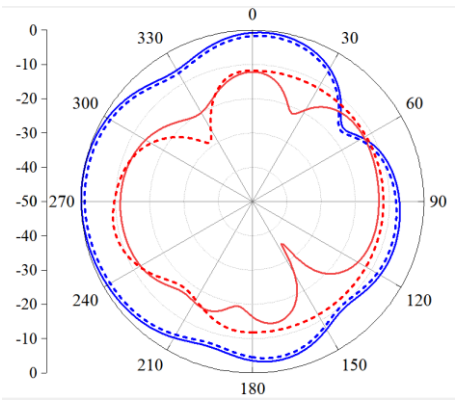
0
30
60
90
120
150
180
210
240
270
300
330
0
-10
-20
-30
-40
-50

(b)

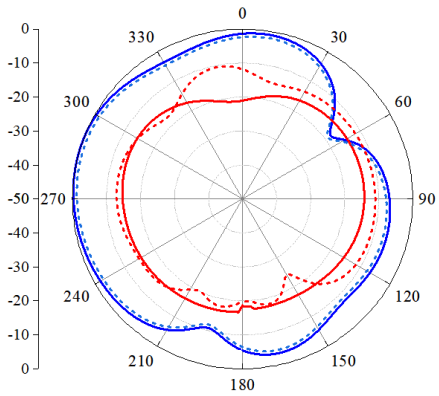
0
30
60
90
120
150
180
210
240
270
300
330
0
-10
-20
-30
-40
-50

(c)

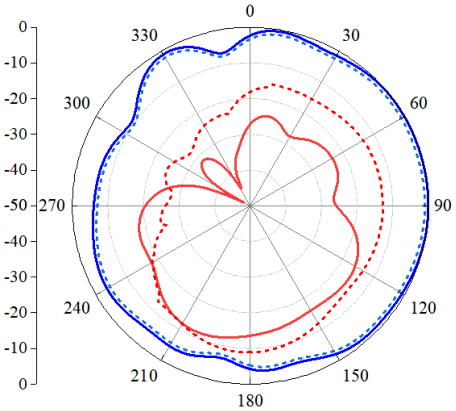
0
30
60
90
120
150
180
210
240
270
300
330
0
-10
-20
-30
-40
-50

(d)

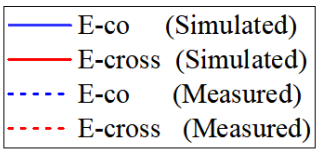
E-co (Simulated)
E-cross (Simulated)
E-co (Measured)
E-cross (Measured)

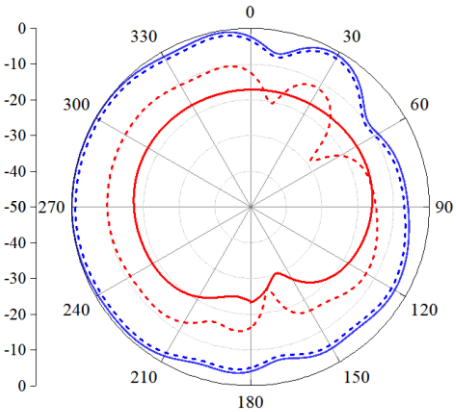
0
30
60
90
120
150
180
210
240
270
300
330
0
-10
-20
-30
-40
-50

(e)

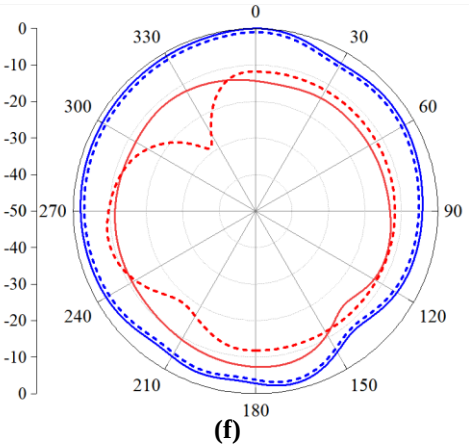
0
30
60
90
120
150
180
210
240
270
300
330
0
-10
-20
-30
-40
-50

(f)

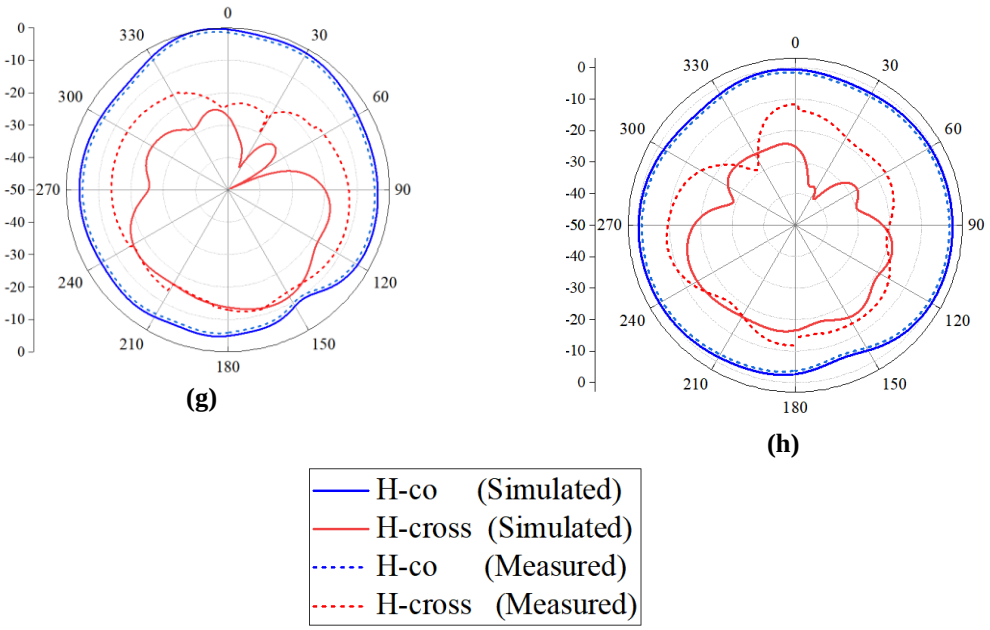

Figure 3.9 Simulated and Measured radiation pattern of (a) Ant 1 E-plane (b) Ant 2 E-plane (c) Ant 3 E-plane (d) Ant 6 E-plane (e) Ant1 H-plane (f) Ant 2 H-plane (g) Ant 3 H-plane (h) Ant 6 H-plane

between 0.8 to 2.5 dBi. As the antenna element exhibit omnidirectional radiation pattern it is focused on coverage rather than the directional properties hence lower gain can be expected

3.4.2 MIMO Parameters

A MIMO system's diversity and multiplexing performance will be determined by two different performance characteristics that must be studied. The diversity performance of MIMO can be depicted from its ECC curve, which is revealed in Figure 3.10. Using equation 3.1.

$$ECC = \frac{\left|\iint_{4\pi} E_i(\theta,\phi) * E_j(\theta,\phi)^* \partial\Omega\right|^2}{\iint_{4\pi}|E_i(\theta,\phi)|^2 \partial\Omega \iint_{4\pi}\left|E_j(\theta,\phi)\right|^2 \partial\Omega} \quad (3.1)$$

ECC value is 0.05 which is well below than the desired ECC value of 0.5. The proposed MIMO array shows decent diversity performance.

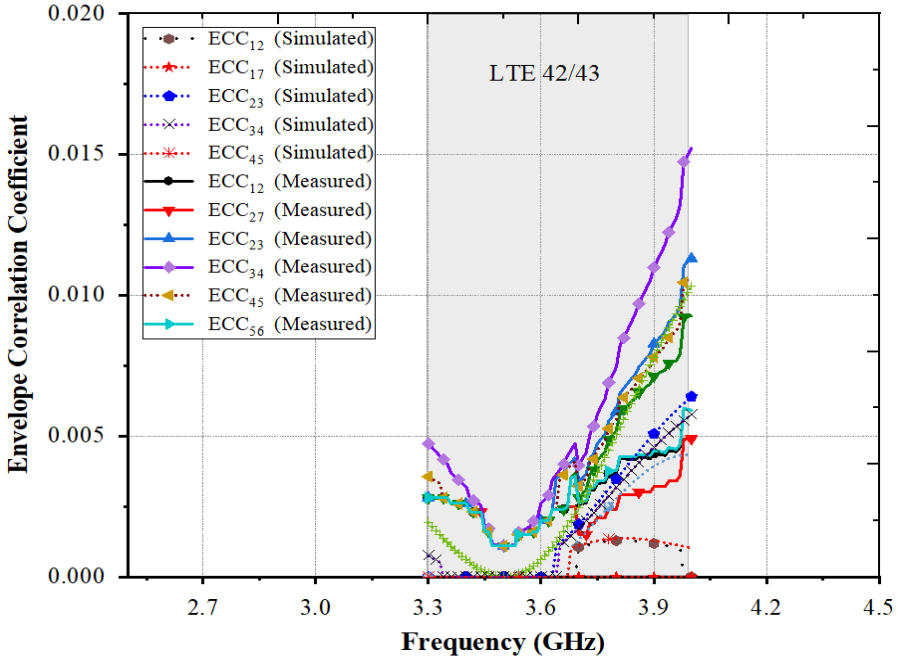

(a)

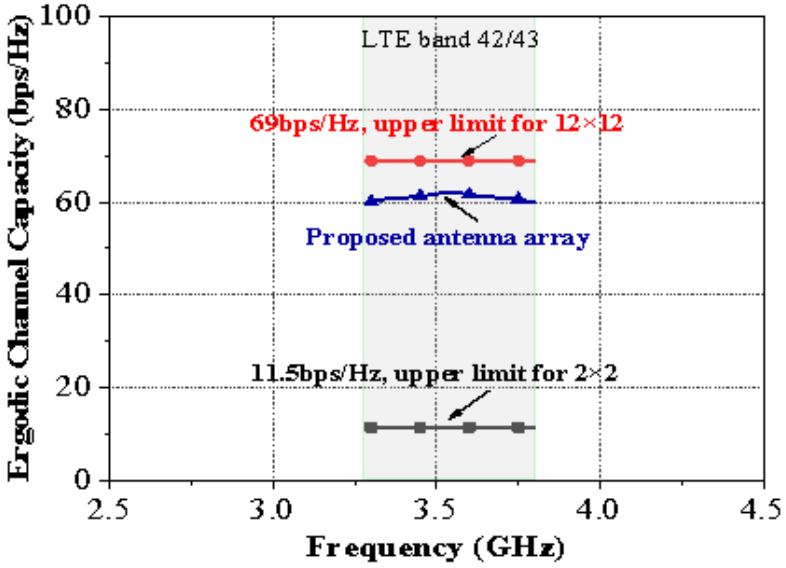

(b)

Figure 3.10 (a) ECC (b) Channel capacity of proposed 12 element MIMO system

The ideal channel capacity of 12 elements MIMO and the proposed array are 69 b/s/Hz and 61.9 b/s/Hz respectively as shown in Figure 3.10. It provides higher channel capacity compared to 2×2 MIMO.

3.5 USER HAND EFFECT FOR PRACTICAL APPLICATION OF PROPOSED MIMO SYSTEM

Since the human body is a lossy dielectric medium, the user's hand may have an impact on a MIMO system. Living tissues have a higher relative permittivity than the air. The human hand's relatively high permittivity (while holding a cell phone) may result in an impedance change in the near field zone of the antenna. The tissues of human are also relatively conductive due to their high water content. Microwave frequencies cause losses because of the electrical properties of the human hand. Consequently, antenna performance is significantly affected by the inclusion of the hand model. The user hand impact on the proposed MIMO system (see Figure 3.11). Although user can hold the mobile phone in variety of ways but single hand mode (SHM) case is considered here. The simulation for this was done in CST software. This hand phantom considered is in compliance with the Cellular telecommunication industry association (CTIA) standard [153], which resemble real hand of the user.

Figure 3.12(a) makes it clear how negatively SHM affects the reflection coefficients of antennas 2 and 3. This occurred as a result of the thumb coming into contact with these two antennas. All of the other antennas are functioning effectively. The isolation is better than 13 dB, as Figure 3.12(c) shows.

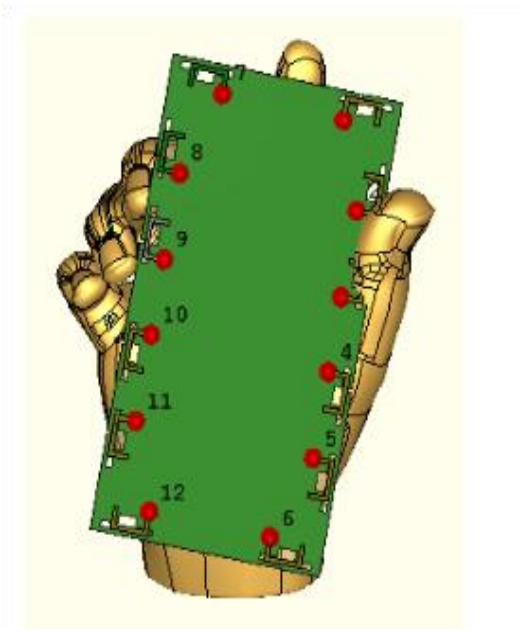

Figure 3.11 Proposed design in Single Hand Mode

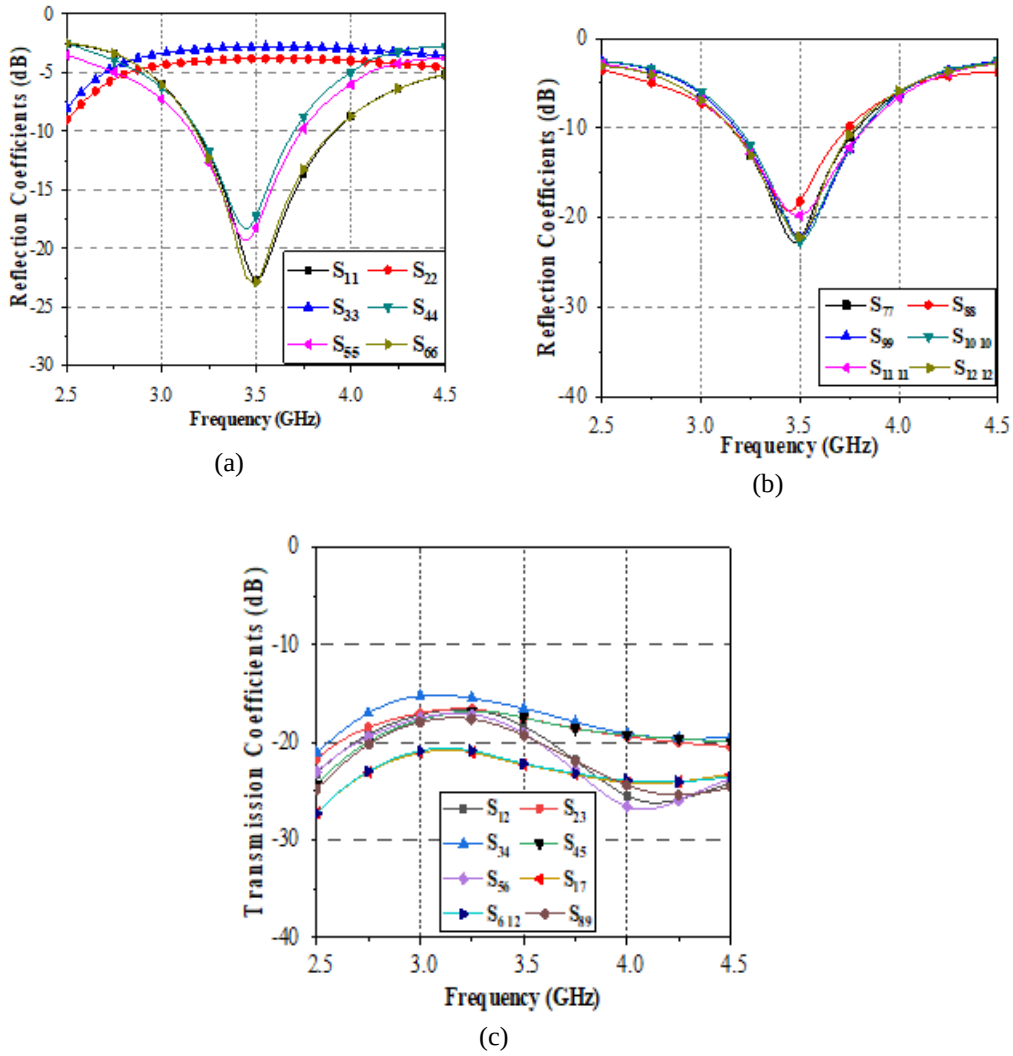

Figure 3.12 SHM, (a) Reflection coefficients of An 1 to Ant 6 (b) Reflection coefficient Ant 7 to Ant 12 (c) Transmission coefficient

3.6 COMPARATIVE ANALYSIS OF PROPOSED MIMO SYSTEM

Table 3.1 presents a comparison between the recommended array and the reported literature to evaluate the performance of the suggested MIMO antenna system. Important factors including frequency bands, element count, efficiency, ECC, and isolation are examined. Table 3.1 shows that it is doing quite well in terms of isolation and efficiency.

Table 3.1: Comparison of proposed design and state of the art designs

Ref.	**Number of Element**	**Frequency band (GHz)**	**Efficiency (%)**	**Channel capacity (b/s/Hz)**	**Isolation (dB)**	**ECC**
[75]	12 (8 (LB), 6 (HB))	3.4-3.8, 5.15-5.92	41-82(LB) 47-79(HB)	37 (LB) 29.5(HB)	>12	<0.15(LB), <0.1(HB)
[13]	8	3.4-3.6, 4.8-5.1	41-72(LB) 40-85(HB)	38.5(LB) 38(HB)	>11.5	<0.08(LB),<0.05(HB)
[61]	10	3.4-3.8, 5.15-5.925	42-65(LB) 62-82(HB)	40(LB) 51.4(HB)	>11	<0.15(LB) <0.05(HB)
[82]	8	3.4-3.6	62	40.8	>17.5	<0.05
[89]	8	3.3-3.8, 4.8-5,5.15-5.925	55-72 50-6543-73	37.6	>10.5	<0.12
[152]	8	3.26-4.48	>60	40	>14.5	<0.03
Proposed Antenna	**12**	**3.3-3.8**	**74-89**	**61.9**	**>14.8**	**<0.05**

3.7 CONCLUSION

For the LTE 42/43 bands, proposed MIMO antenna system (twelve element) with a slot antenna as a building block has been successfully studied. The isolation of the proposed antenna array is 14.8 dB. This is accomplished by using spatial diversity and placing the antenna elements orthogonally. Good MIMO performance is obtained at high channel capacity (61.9 b/s/Hz) with ECC < 0.05. Even when the user is nearby, the proposed MIMO system exhibits acceptable isolation of greater than 13 dB. Its decent performance, high channel capacity, and reliable isolation pave the way for enhanced user experiences and improved connectivity. Thus, the suggested antenna system satisfies the demanding requirements of 5G cellphones. This work is focused on improving the channel capacity of the 5G smartphone by installing antennas on the four sides of the PCB. However the antennas were installed on the ground plane, and hence utilized space that can be used to install other electronic circuitry. Therefore different locations can be explored to utilize the smartphone's PCB space efficiently. The next chapter utilizes side-frames of the smartphone to install antennas. This small change can help in utilizing the ground plane to mount some other smartphone components.

CHAPTER 4

COMPACT SIDE EDGE PRINTED MIMO SYSTEM 5G SMARTPHONE APPLICATIONS

CHAPTER 4

COMPACT SIDE EDGE PRINTED MIMO SYSTEM 5G SMARTPHONE APPLICATIONS

4.1 INTRODUCTION

The researches have witnessed a sharp inclination towards 5G of mobile communication, as it is one of the most recent technologies [129-137]. An 8×8 MIMO array balanced slot antenna is employed and thereby a good isolation (>17.5 dB) is achieve. Method of orthogonal mode are used to avoid mutual coupling [131].

Now that compact phones are in demand, antenna researchers are looking into alternative locations besides the mobile main circuit board to mount antenna. As a result, many studies [86-89] are currently looking into the antenna mounted on the side-frame of smartphones. These all have good MIMO performance. However, the height of the side frame is always greater than or equal to 6 mm in all of these designs. Therefore, it might limit those made for ultrathin smartphones. To overcome this, a MIMO system is presented [89] where, the antennas are mounted on 3 mm high side-frame. This was the lowest achieved side frame till now and is appropriate for extremely tiny cell-phones. However isolation is 10 dB, and it can be increased.

A compact MIMO system is proposed here, in response to the difficulties experienced by antenna designers when highly isolated antenna system for ultrathin smartphone application. Individual antenna is made up of loop like structures that covers LTE-42 band. As it is essential to check the behaviour of this MIMO system in user hand to fully understand its performance in the real life scenario, hence this study also includes the user hand effect on the individual antenna performance along with this, effect of installing few parts of the mobile-phone body are also discussed.

4.2 GEOMETRY DETAIL

Figure 4.1 shows the geometry of suggested side-edge printed antenna system. The PCB, which measures 150 ×78 ×0.8 mm^3, is constructed from a FR4 substrate with

tanδ=0.02 and ε_r=4.4 and a thickness of 0.8 mm. The primary circuit board's back is printed with a ground plane measuring 140 mm by 76 mm by 0.8 mm. The system ground's top and bottom sides each have a slot with a dimension of 78 mm by 5 mm. These are kept for 2G, 3G, and 4G antennas. The two side frames made up of FR4 substrates, with 0.8 mm thickness, height=3 mm are placed perpendicularly on the main PCB. There is a 1 mm gap between the ground-plane and side frames.

The side view of the suggested MIMO system is revealed in Figure 4.1(a). Four antennas are printed on each frame, with each antenna element having a 33 mm gap between them. Structure of single antenna structure is revealed in Figure 4.1(b). The external surface of the side frames is where the antenna is placed.

4.2.1 Single Antenna Structure

Figure 4.1(c) shows the feeding line dimensions. Feeding line is of length 12.2 mm and width 1.5 mm. Each antenna element's intricate structure is shown in Figure 4.1(d). In this case, the individual component is a grounded loop antenna.

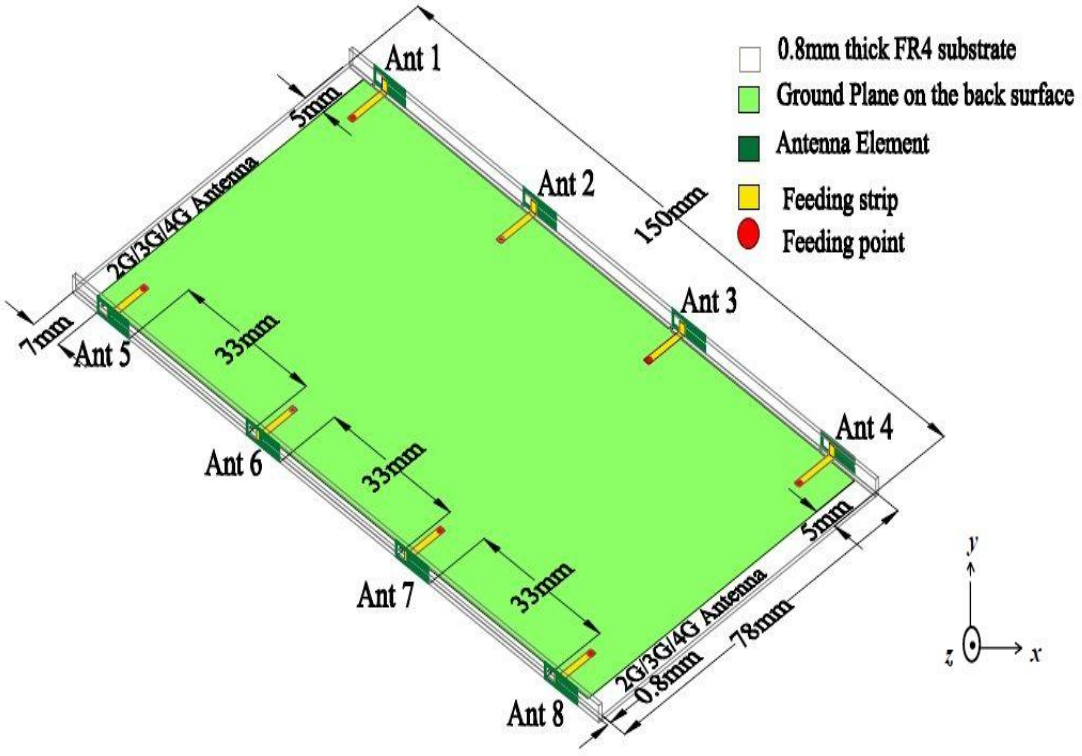

(a)

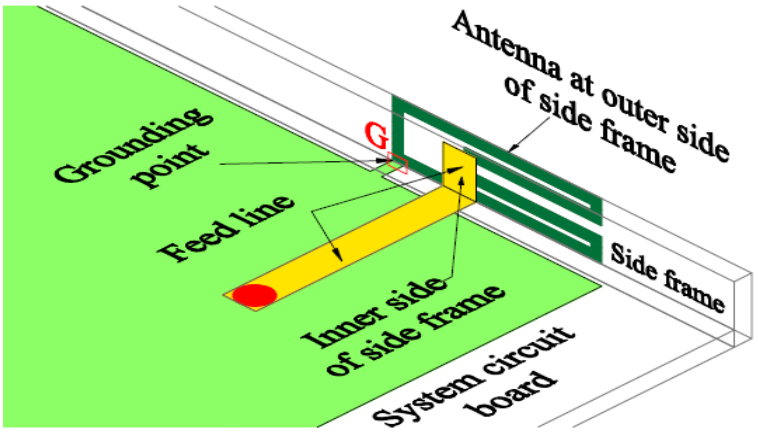

(b)

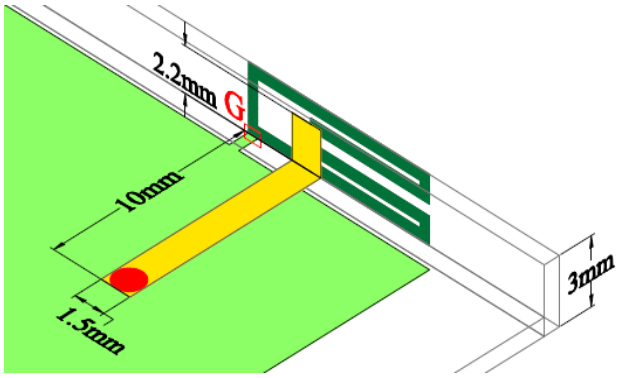

(c)

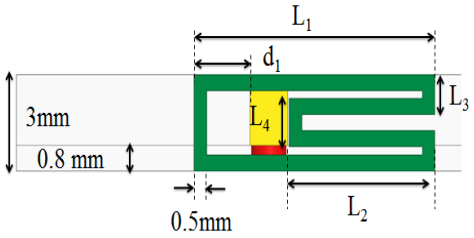

(d)

Figure 4.1 The overall geometry of compact side-edge printed antenna (a) Side view, (b) Side view of a single antenna, (c) Antenna feed dimension (d) Antenna element dimension.

At grounding point G, the loop antenna is attached to the ground. The antenna structure's L_1, L_2, L_3, and L_4 are, respectively, 9.5 mm, 6.25 mm, 1.25 mm, and 1.5 mm long. The feeding line offset, or d_1, is precisely calibrated for each antenna based on its position. It is measured in relation to the antenna. For Ants 1, 2, 3, and 4, the offset d_1 is, correspondingly, 2.2 mm, 2.3 mm, 1.9 mm, and 2.3 mm. The LTE 42 band is intended to be excited by the loop antenna.

4.2.2 Working principle and Parametric Study

The size of the individual antenna element is 0.11088 $\lambda_o \times$ 0.035 λ_o, where λ_o is the free space wavelength at 3.5 GHz. The structure that has been created here is a modified loop antenna that resonates in the half wavelength mode. The length (L_2) is drifted inward, resulting in a tailored loop structure, which reduces the antenna's total

size. The lengths L_1 and L_2 are utilized to modify the operating band and optimize the resonance frequency. Figure 4.2 shows the impact of changing two crucial factors, L_1 and L_2. Figure 4.2(a) shows that, changing the length L_1 has an impact on the resonance frequency and operating band. As length L_1 goes from 8.5 mm to 10.5 mm there is a movement in the resonant frequency is observed to the left side of the x-axis. This occurs because increase in L_1 causes the loop structure's overall length to grow, which change the resonance to a lesser frequency. The resonant frequency of closed loop structure is $f = 1/2\pi\sqrt{L_{eq}\,C_{eq}}$ and shifts towards the lower end of the spectrum as the overall length of the structure rises due to an increase in effective inductance and capacitance. The structure covers the LTE 42 and resonates at 3.5 GHz, when the L_1 is 9.5 mm. Consequently, this length was chosen. The length L_1 was fixed to 9.5 mm for the following parameter (L_2) change, and the length L_2 was then altered as shown in Figure 4.2(b). As length L_2 increases from 5.5 mm to 7 mm, it is apparent from Figure 4.2(b) that the resonance frequency shifts downward.

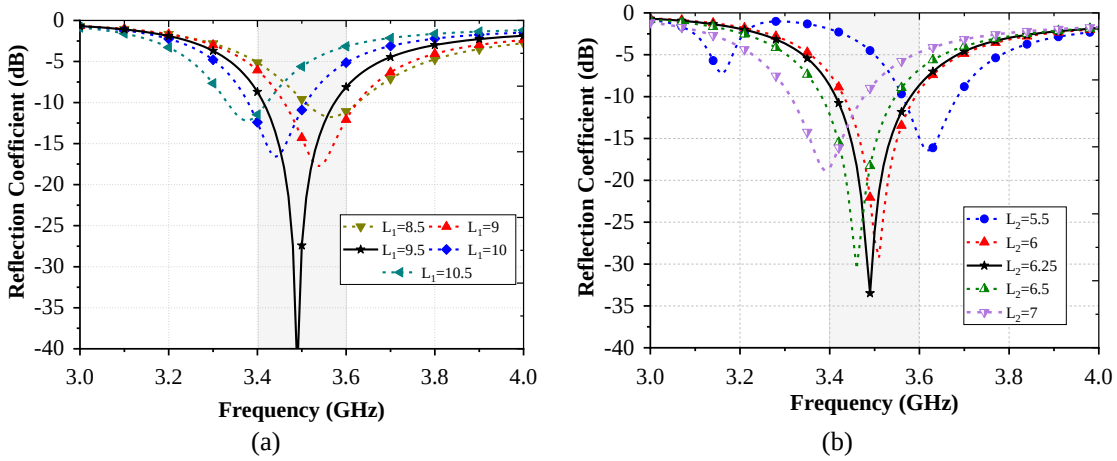

Figure 4.2 Simulated results (a) S-parameters for varying length L_1 (b) S-parameters for varying length L_2 when L_1=9.5 mm.

4.3 RESULT AND ANALYSIS

The reflection coefficients of proposed MIMO are presented in Figure 4.3 (a). In addition, Figure 4.3 (b) illustrates that the suggested antenna system provides better isolation (i.e 14.8 dB) between adjacent antenna elements over the entire band.

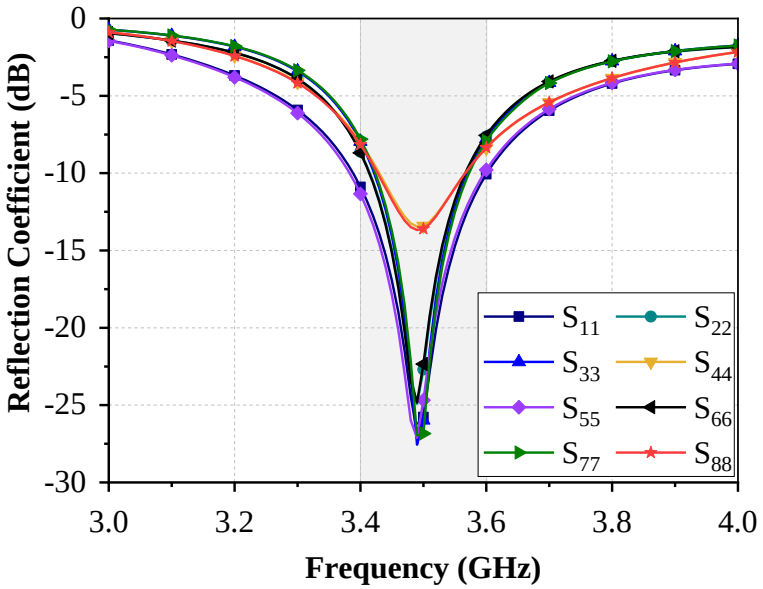

(a)

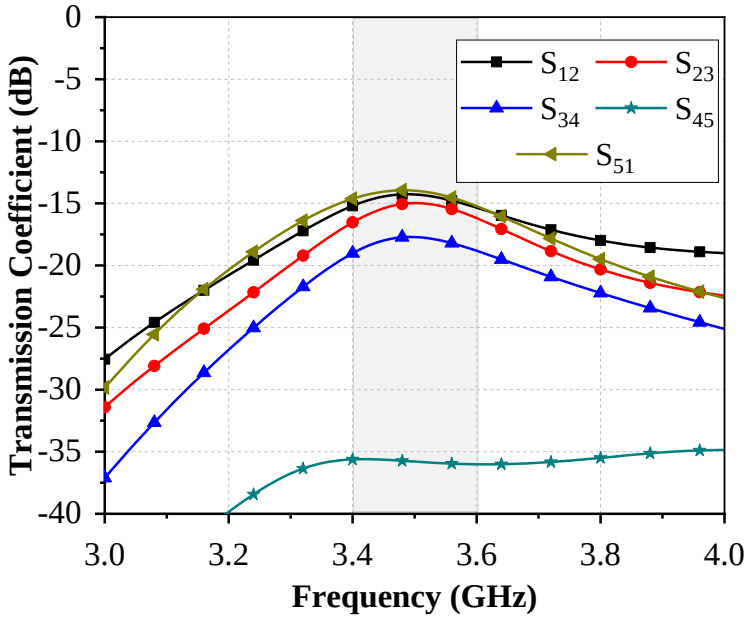

(b)

Figure 4.3 S-parameters (a) Simulated Reflection coefficients (b) Simulated Mutual coupling.

Without using any additional decoupling structure, the adequate distance (0.39 λo, , where λo is the 3.5 GHz free space wavelength), between neighbouring antenna parts, ensured acceptable isolation. Figure 4.4, which shows the distribution of current on the suggested array. As illustrated in Figure 4.4(a) and 4(b), two distinct cases are discussed: First case is when Ant1 is energized, and case two is when Ant2 is excited. Without a doubt, there is sufficient space between antenna elements for good isolation by preventing current from flowing toward the neighbouring port.

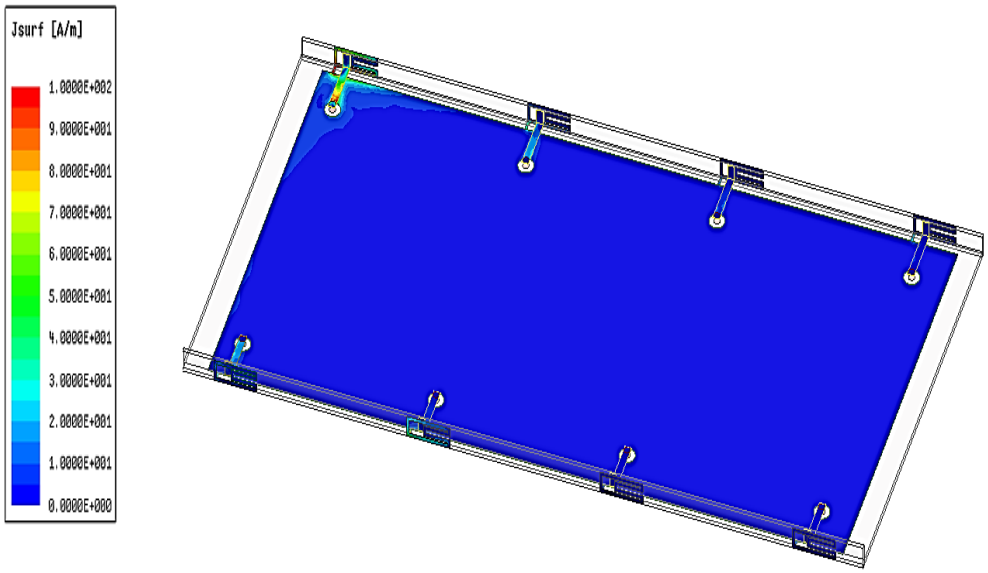

(a)

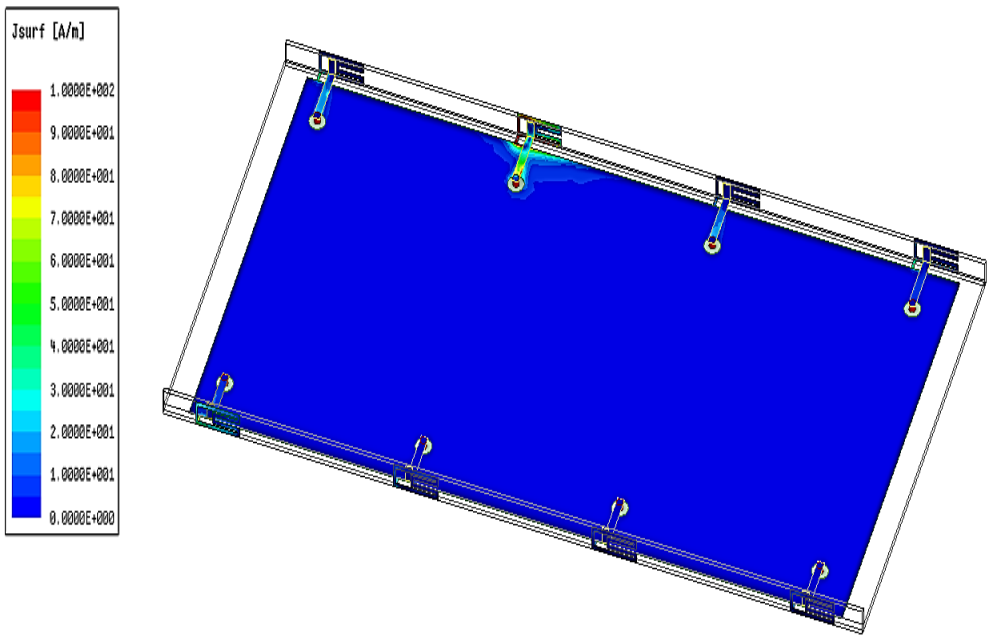

(b)

Figure 4.4 Surface current distribution (a) Case 1: Excitation of Ant 1 (b) Case 2: Excitation of Ant 2.

4.3.1 Measured Results

Figure 4.5 demonstrate the fabricated prototype of proposed MIMO system. The suggested antenna works in the LTE 42 band, as shown in Figure 4.6(a). It is possible to see the tiny variation in resonance frequency between the results of

simulation and measurement. Tolerance and fabrication could be the causes of this discrepancy. Figure 4.6 (b) shows the measured isolations between any two neighbouring antennas. Here, across the full 5G (3.4-3.6 GHz) spectrum, 15 dB isolation level is achieved. As Ant 4 and Ant 5 are at different corners, isolation between non-adjacent antennas, like S_{45}, is stronger than isolation between neighbouring antennas

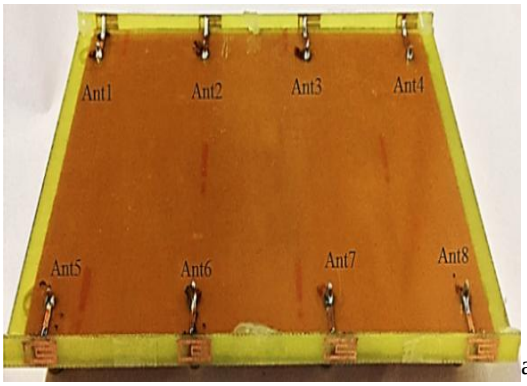

a)

(b)

(c)

(d)

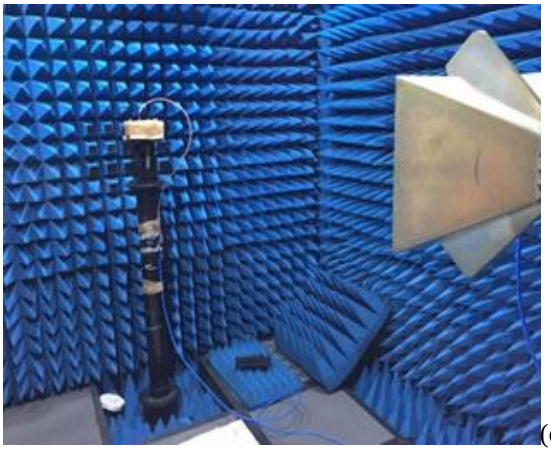

(e)

Figure 4.5 Proposed compact antenna system's fabricated prototype (a) Front view (b) Back view (c) zoom inner view (d) zoom outer(e) MIMO Antenna placement in anechoic chamber for radiation pattern testing.

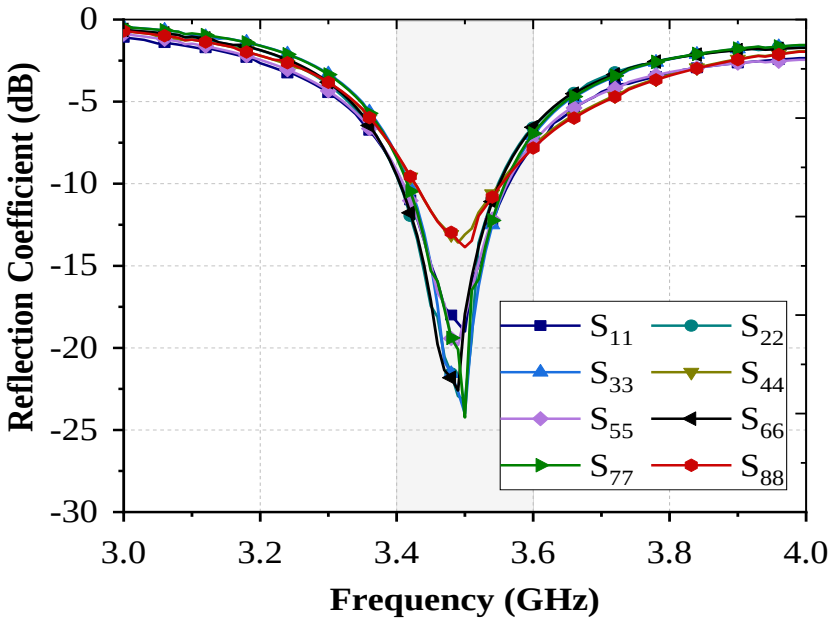

(a)

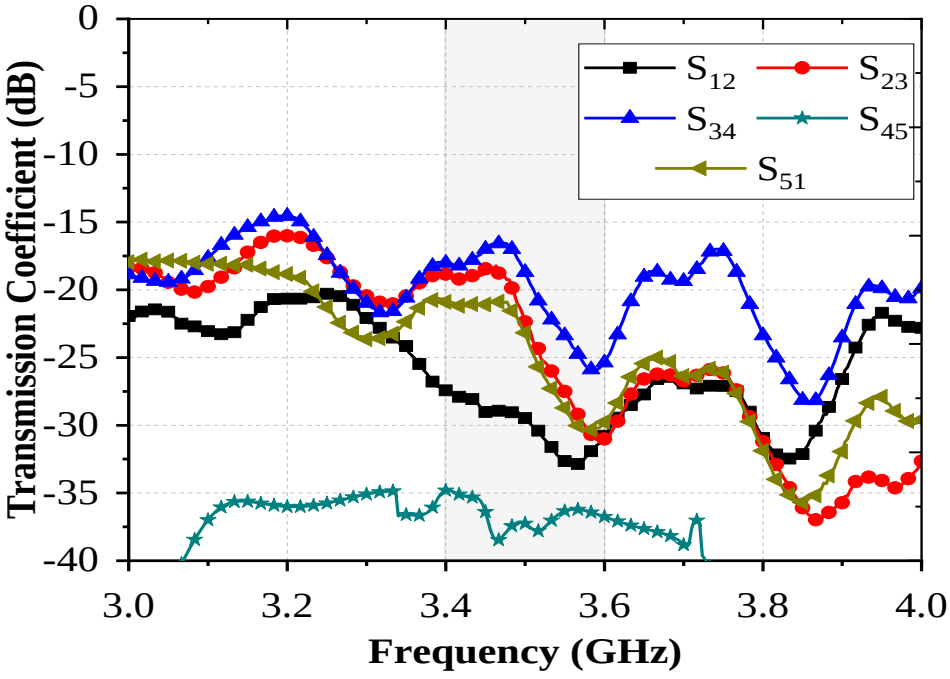

(b)

Figure 4.6 Measured (a) Reflection coefficient (b) Mutual coupling.

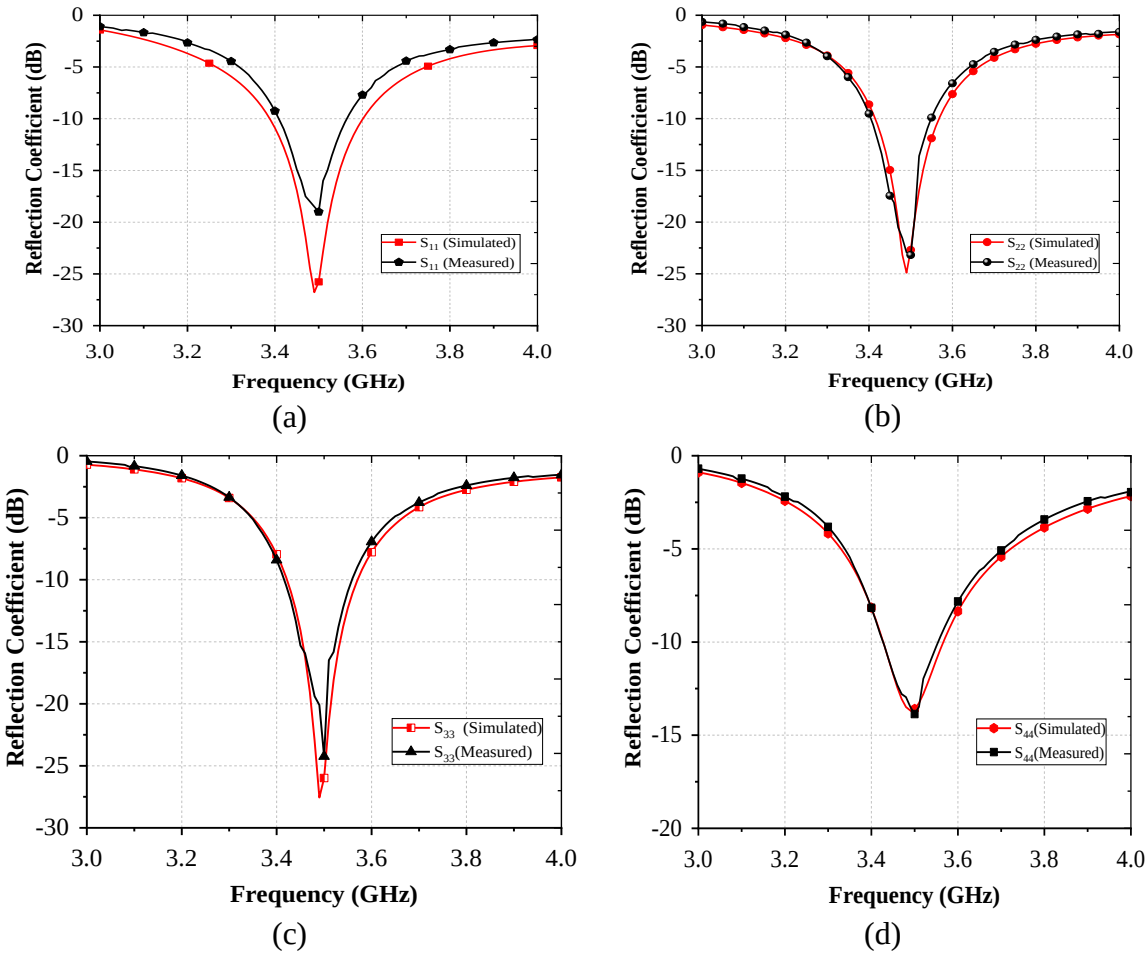

Figure 4.7 Comparison of the measured and simulated outcomes

For better visualization of results, the correspondence between simulated and measures outcomes for antenna 1,2,3, and 4 are presented in Figure 4.7. It is clear from this figure as well that there is decent matching between the two results.

4.3.1.1 Radiation performance

Figure 4.8 illustrates, the total simulated efficiency of the suggested MIMO system, which take accounts of the losses and may be estimated using equation 1.

$$\text{Total Efficiency} = \eta_{rad} * (1 - |r|^2) \qquad (4.1)$$

Where η_{rad} denote the radiation efficiency and r is the reflection coefficient.

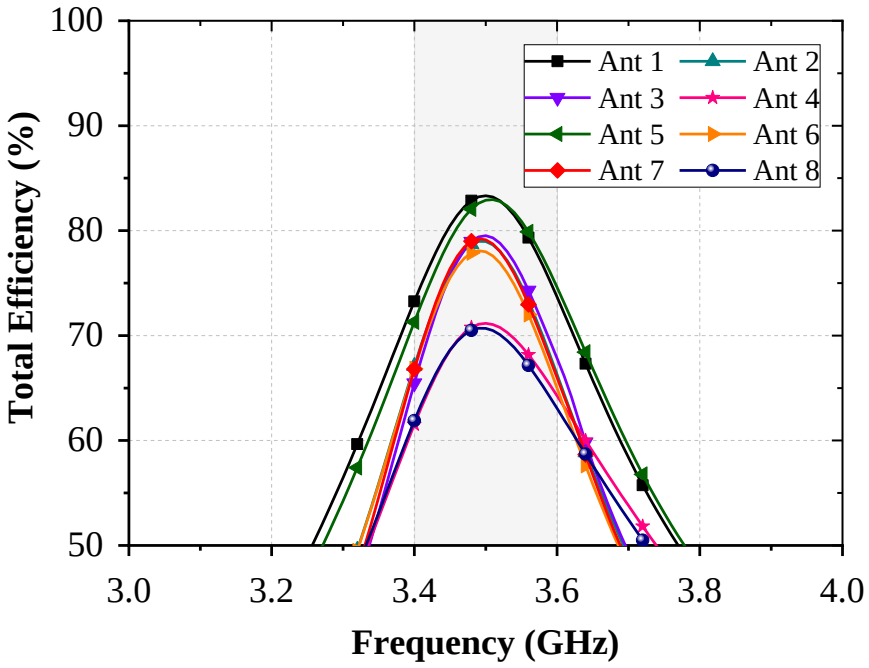

Figure 4.8 Total efficiencies of proposed compact MIMO system

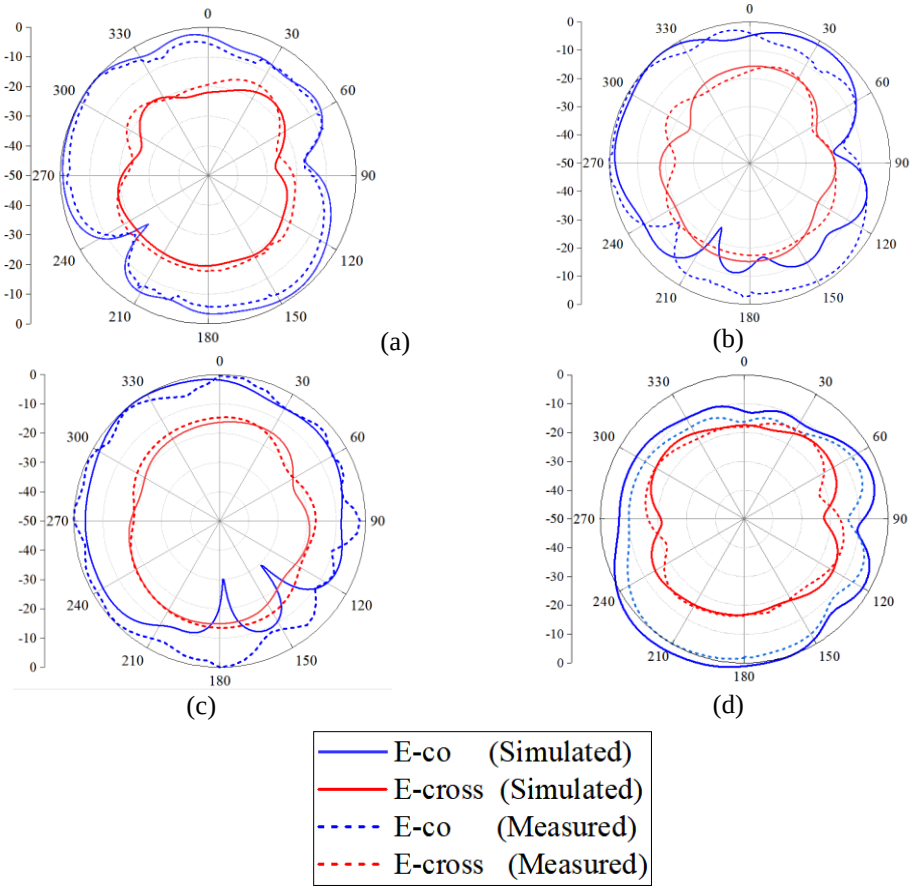

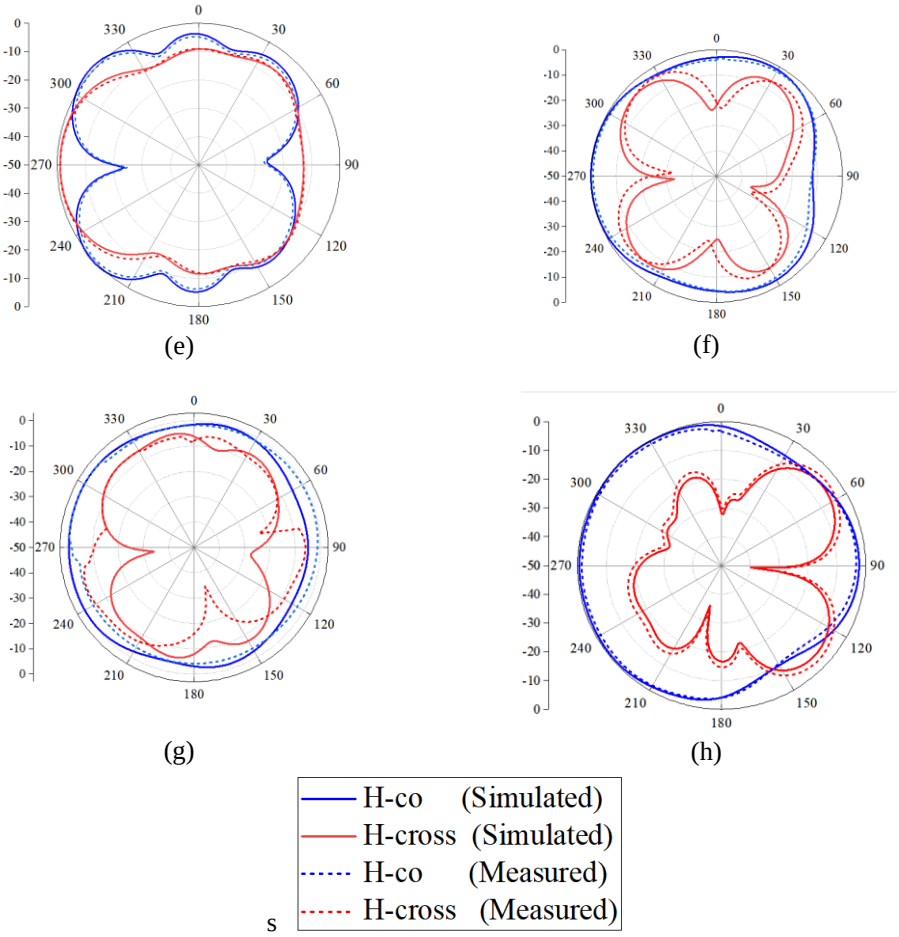

Figure 4.9: Measured and simulated radiation patterns in E-plane and H-plane for the proposed antenna elements. (a) Ant 1 – E-plane, (b) Ant 2 – E-plane, (c) Ant 3 – E-plane, (d) Ant 4 – E-plane, (e) Ant 1 – H-plane, (f) Ant 2 – H-plane, (g) Ant 3 – H-plane, (h) Ant 4 – H-plane.

In the 3.4-3.8 GHz range, the simulated total efficiency is the range 62% to 83%. Figure 4.9 shows the radiation pattern, simulated and measured. Figure 4.9 portrays a fine match between measured radiation patterns. The each antenna has different maximum radiation direction. The peak gain of antenna elements ranges from 3 to 5 dBi. This feature can help MIMO operations achieve good diversity performance. Eventually leading to increased channel capacity.

4.3.1.2 MIMO Performance

Figure 4.10 (a) and (b) show the two critical factors for analyzing the multiplexing and diversity properties of the proposed system. The ECC is determined using Equation 4.2

$$ECC = \frac{\left|\iint_{4\pi} E_i(\theta,\phi) * E_j(\theta,\phi)^* \partial\Omega\right|^2}{\iint_{4\pi}|E_i(\theta,\phi)|^2 \partial\Omega \iint_{4\pi}\left|E_j(\theta,\phi)\right|^2 \partial\Omega} \quad (4.2)$$

Where i and j are the two ports being excited.

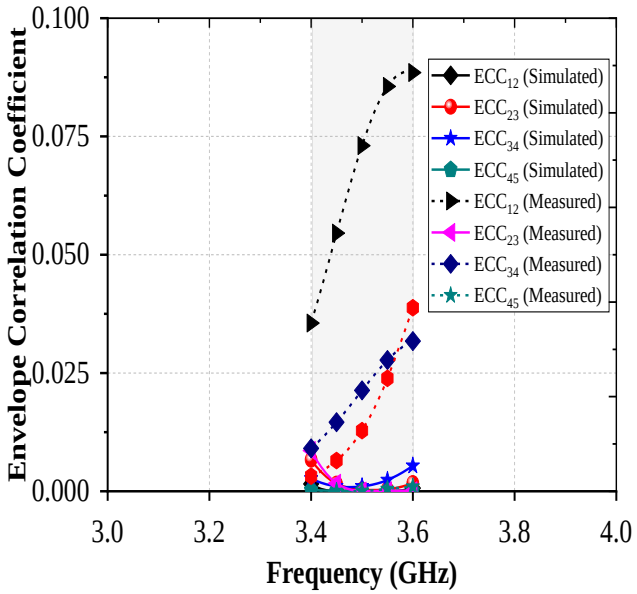

(a)

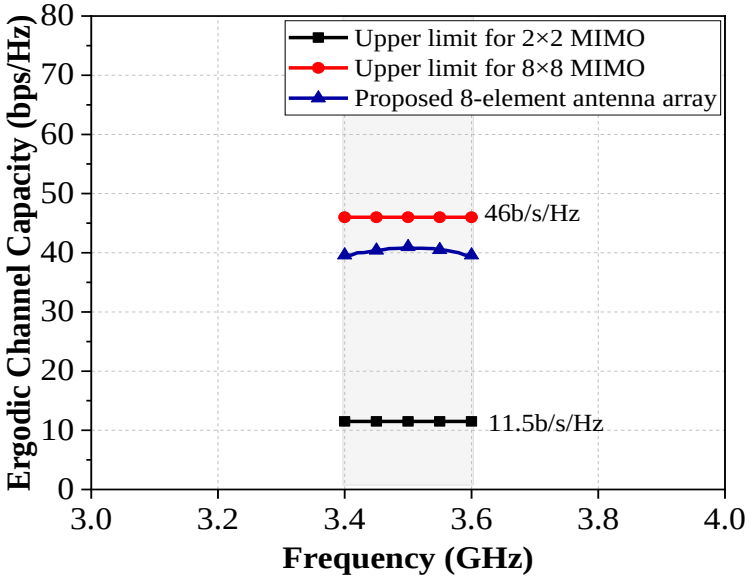

(b)

Figure 4.10 (a) Envelope correlation coefficient (b) Channel capacity.

The ECC among adjacent elements is presented in Figure 4.10 (a). This graph shows that all of the ECC values are lower than 0.1 across the complete working band due to symmetrical arrangement. The acceptable threshold for MIMO operation (ECC<0.5) is hence achieved by this design. This ensures a good diversity performance.

Figure 4.10 (b) depicts the channel capacity of suggested MIMO system, to evaluate multiplexing performance. It can be estimated using equation (4.1), assuming that the assigned power of each antenna is the same.

$$C = E\left\{log_2\left[det\left(I_N + \frac{\rho}{Nn_T} HH^H\right)\right]\right\} \quad (4.1)$$

Where number of transmitting antennas is n_T, I_N is identity matrix , Channel matrix is H and average SNR is ρ/N, and expectation is E. The channel used for rayleigh fading environment. SNR assumed is 20 dB. Comparison was made between proposed antenna design with ideal eight element MIMO system and two element MIMO systems. Peak channel capacity 41 b/s/Hz is achieved by the proposed design is, and it has lower capacity as compared to an ideal 8×8 MIMO by 1.12 times. However, it is 3.56 times more than the peak CC of a 2×2 MIMO (i.e. 11.5 b/s/Hz).

4.4 PRACTICAL APPLICATION ANALYSIS

This section studies the impact of the integration of different practical components on the suggested design performance. The impact of main mobile terminal components like as batteries and plastic frames is explored along with user hand effect.

4.4.1 User hand effect on the antenna performance

This section discusses the effect of the hand of the user on the performance of the proposed antenna system. Figure 4.11 depicts the proposed MIMO system in close contact to the user's hand, and Figure 4.12 (a) and (b) show the simulated

results. Figure 4.11 (b) and 11 (c) show two alternative side views of the proposed design when held in the user's hand for improved visualization.

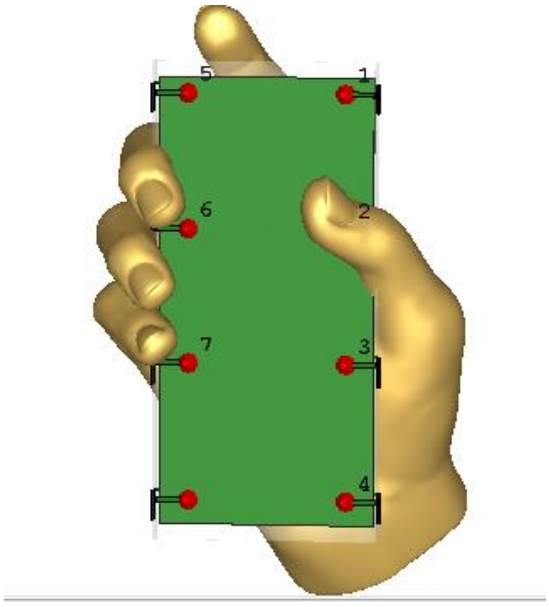

(a)

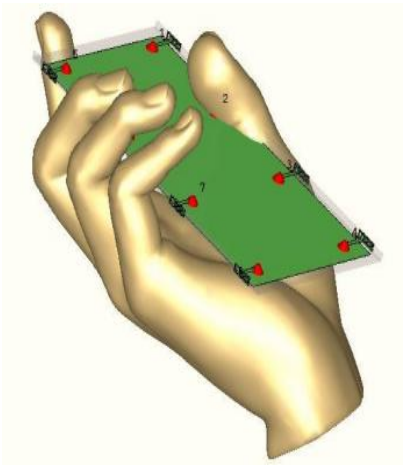

(b)

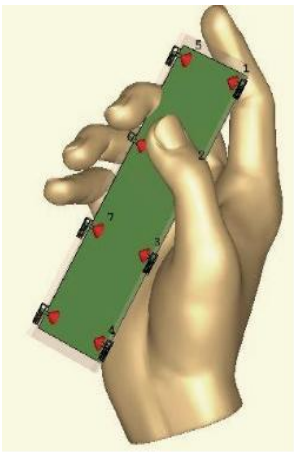

(c)

Figure 4. 11 View of antenna array under user's hand scenario (a) main view (b) Side view-1(c) Side view -2

It is evident from these Figure 4.12 that Ant-6 and Ant-2 are entirely roofed by the fingers and thumb, respectively, causing their performance to suffer greatly. Even

when Ant 7 is in close proximity to the fingers, it keeps its performance intact as the fingers do not cover the antenna.

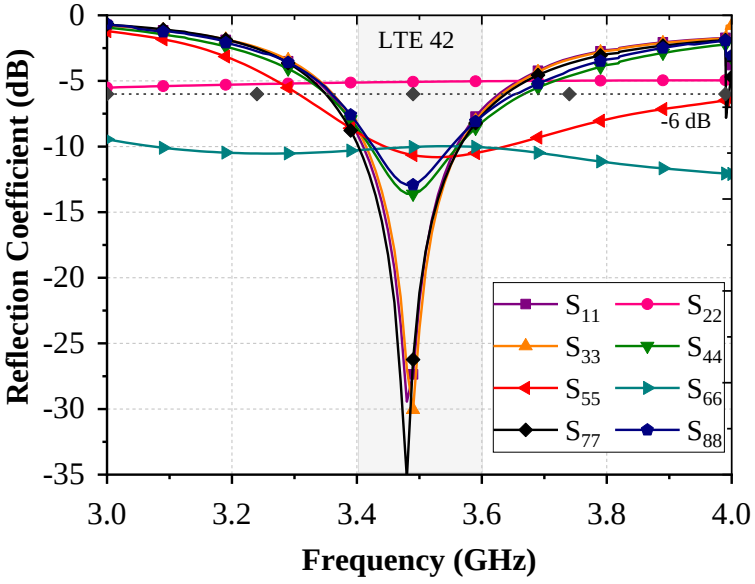

(a)

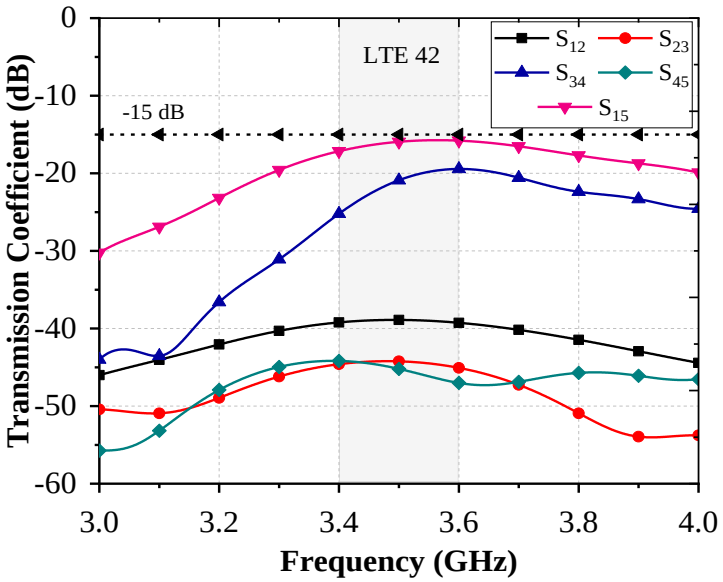

(b)

Figure 4.12 Results of single hand scenario (a) Simulated Reflection coefficient (b) Simulated Mutual coupling.

Figure 4.11 shows that the distance between the fingers and Antennas 1, 3, 4, 7, and 8 is quite significant. As depicted in Figure 4.12 (a) this results in a minimal impact on the reflection coefficient. Nevertheless, because of the fingers' closeness to Antennas 2, 6, and 5, their reflection coefficients are significantly impacted. However, Antenna

5 can still function within the desired frequency range. The isolation of the antenna array remains at a superior level of 15 dB or higher.

4.4.2 Impact of Battery

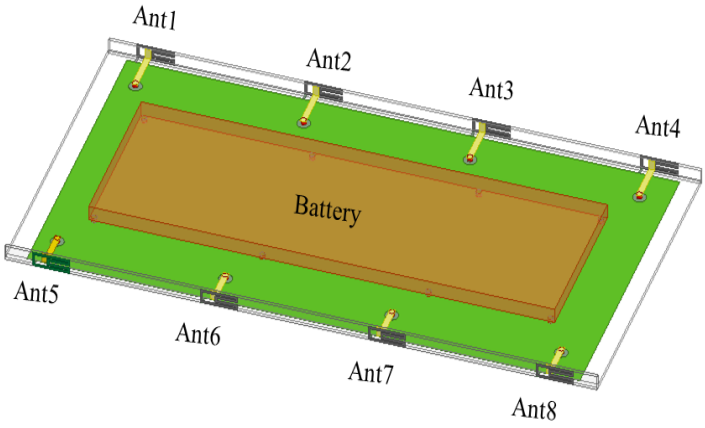

Figure 4. 13 Battery installation of the proposed MIMO system.

Battery module is installed on the proposed design and is showcased in Figure 4.13. In order to investigate the battery's impact, a metal of dimensions 118 × 40 ×3 mm^3 is positioned on the front side of PCB. The battery and ground plane are electrically connected via eight shorting pins. As Figure 4.14 demonstrates, proposed design with the battery module had little to no influence on its performance. The isolation was observed to exceed 14 dB

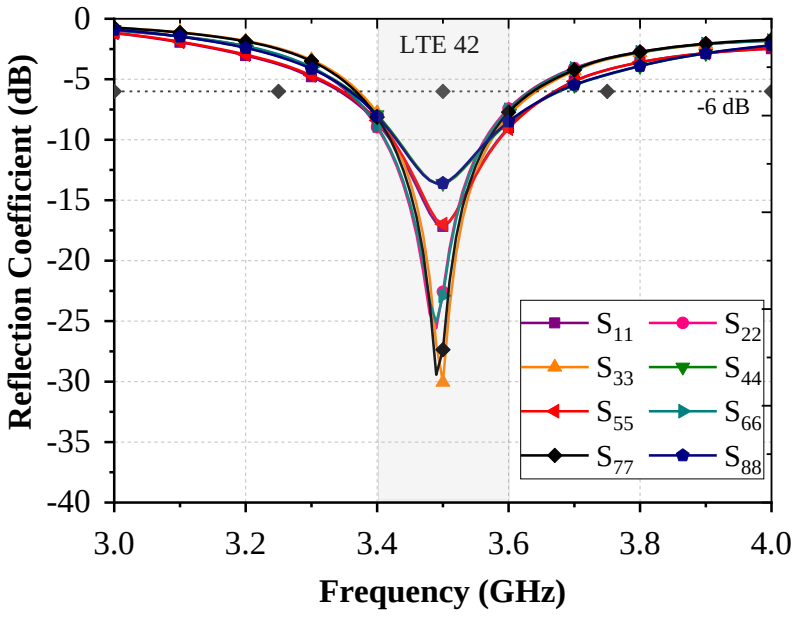

(a)

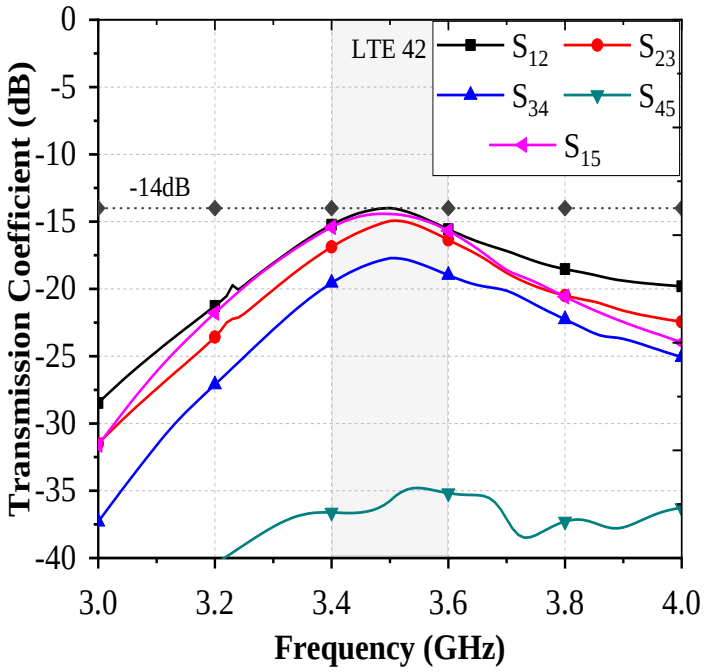

(b)

Figure 4.14 Results of proposed antenna with battery (a) Simulated Reflection coefficient (b) Simulated Mutual coupling

4.4.3 Impact of plastic frame

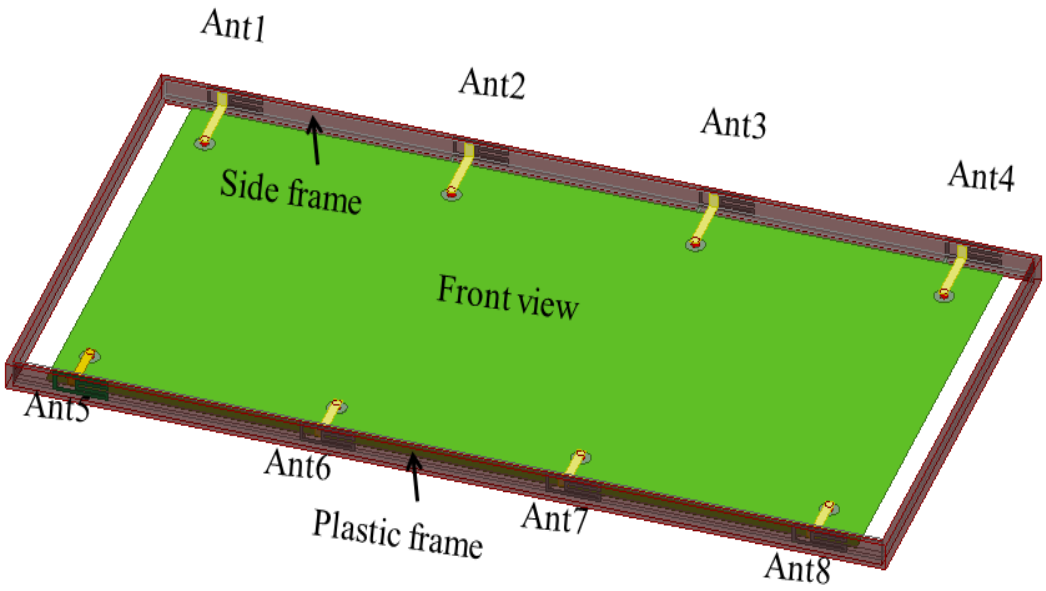

Figure 4.15 Plastic frame integrated with proposed design.

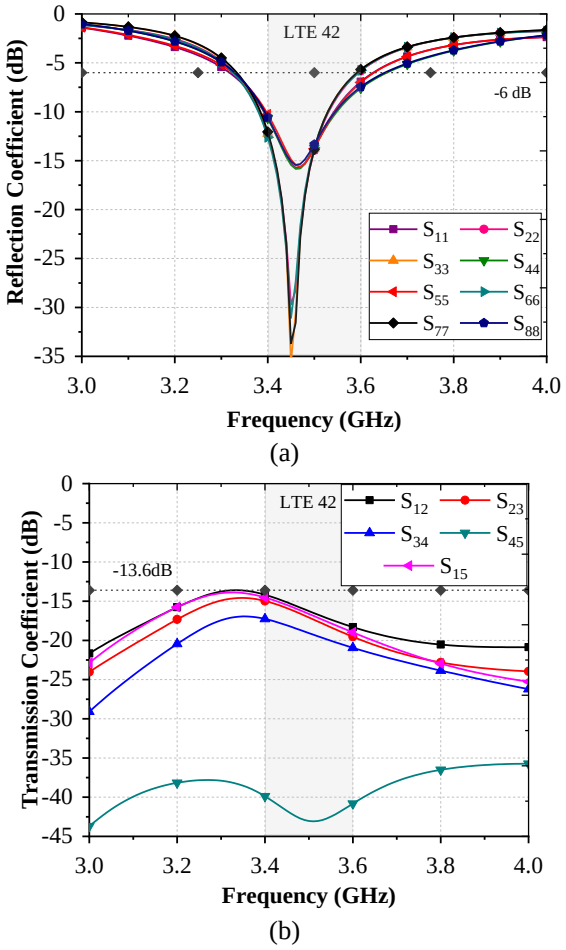

Figure 4.16 Simulated results (a) Reflection coefficient of plastic frame integrated model (b) Mutual coupling of plastic frame integrated model

Proposed design is enclosed by a 4 mm high plastic frame, (ε_r=3 and tanδ=0.01) (see Figure 4.15). Figure 4.16 illustrate the consequent results.

Figure 4.16 (a), one can observe a trivial shift in the resonance frequencies of the antennas towards the lower end of the spectrum. This interesting phenomenon can be caused by the glass frames situated in close contact to the antenna elements. When glass frames are situated in close proximity to the antenna elements, they introduce a change in the dielectric environment this is called dielectric loading. This change, in turn, affects the resonance frequencies of the antenna.

By fine-tuning specific parameters, such as L_1 and L_2, there is a chance to enhance the performance of this design. This adjustment can potentially neutralize the slight frequency shift caused by the dielectric loading, resulting in even better performance. It's important to note that Figure 4.16 (b) reveals a slight amend in the isolation level.

Though this change may seem insignificant, it remains superior to a value of 13.6 dB across 3.4-3.6 GHz band. This indicates that the MIMO antenna system, despite the influence of the glass frames, continues to perform admirably.

4.5 COMPARISON WITH STATE OF ART TECHNIQUES

The advantages offered by the proposed MIMO system with existing literature are discussed. A thorough comparison in Table 4.1 is conducted, considering factors such as multiband operation, MIMO order, isolation, efficiency, and size. Table 4.1 showcases the designs presented in [57], [89], [135], [13], and [137], all of which operate on multiband frequencies. It is worth noting that the MIMO order of these designs is generally eight or more, except for [57], where it is four. The number of antennas implanted in smartphones directly influences channel capacity. Consequently, a lower MIMO order, like in [57], results in lesser channel capacity compared to other mentioned designs. In the case of [137], the MIMO order matches that of the proposed design. However, it fails to achieve adequate isolation, even after incorporating neutralized lines, with an isolation value of only -9.7 dB in the lower band (2.496-2.69 GHz). On the other hand, both the proposed antenna system and those referred in Table 4.1 demonstrate decent isolation.

While the design in [57] provides decent isolation, its efficiency falls short when compared to the proposed design. Despite [135] has more antenna elements than the proposed design, but exhibit lower isolation value. In [135], the achieved isolation is 11 dB, which is less than what the suggested design offers. Therefore, for ultrathin smartphones the presented design proves to be appropriate.

4.5.1 Size Comparison

When it comes to size, the proposed design outshines the other mentioned work in table 1. It has compact 9.5×3 mm² antenna size for the operating band (3.4-3.6 GHz), which is the smallest among all the reported works. The vertical size of the frame in the proposed design is also remarkable, measuring only 3 mm. This vertical size is the minimum among the presented work in Table 1, except for [89]. The proposed structure, on the other hand, has the advantages of high efficiency, channel capacity along with good isolation. Furthermore, this isolation (>14.8 dB) has been achieved by

Table 4.1: Designcomparison with other 5G antenna array designs

Ref	**Working band (GHz)**	**Isolation (dB)**	**Size Of side frame (L ×H*)**	**MIMO Order**	**Antenna size (mm^2)**	**ECC**	**Channel Capacity (b/s/Hz)**	**Antenna Efficiency (%)**
[135]	3.4-3.8, 5.15-5.925	11	Without side frame	10	16×2.5	0.15 0.05	48 , 51.4	>42, >62
[13]	3.4-3.6, 4.8-5.1	>11.5	150×7	8	15×3.1, 7.2×3.1	<0.08, <0.05	38.5,38	>41, >40
[57]	3.4-3.6, 4.8-5	>17.5	150×7	4	10.4×7	<0.14, <0.12	>18.3	>50
[89]	3.3-3.8, 4.8-5, 5.150-5.925	>10.5	140×3	8	13×2, 15×3	<0.12	37.6	>43
[137]	2.496-2.69, 3.4-3.8	>9.7 >10.3	150×6	8	22×3	<0.2 <0.05	38, 38.3	>48
[93]	3.4-3.6	>10	150×7	8	10×7	<0.2	36	>40
[152]	3.26-4.48	>14.5	No side frame	8		<0.03	40	>60
Proposed	**3.4-3.6**	**>14.8**	**150×3**	**8**	**9.5×3**	**<0.1**	**41**	**>62**

the proposed antenna. The major contributions of this design are the compact size, good isolation, and small vertical side frame. Through careful comparison, it is clear that the proposed MIMO antenna system outperforms existing literature with respect to with size, isolation, efficiency, and channel capacity. Its small size, combined with its outstanding performance metrics, makes it an excellent choice for ultrathin smartphones with narrow frames.

4.6 CONCLUSION

This chapter presents an eight-element antenna module for 5G mobile phone applications in the 3.4-3.6 GHz sub-6 GHz spectrum. This innovative module has a one-of-a-kind design and excellent performance, making it a potential game changer in the world of smartphones. The individual element of this antenna module is a loop antenna fed by a 50 micro-strip line. Side frames with dimensions of $150\times3\times0.8$ mm^3 are used to accommodate the eight elements. On each side, four antenna elements are attached. This small arrangement makes optimal use of space without sacrificing performance, and the entire PCB is available for the installation of other electronic components. When operating at the specified frequency, this antenna module gives 14.8 dB of isolation. This isolation ensures minimum interference between nearby antenna parts, improving device performance. Furthermore, the antennas are extremely efficient, with a minimum efficiency of 62% across the band. This module's ability to obtain a low ECC of less than 0.1 is one of its primary advantages. This shows that the antenna elements have less correlation, resulting in greater MIMO performance. It is a strong contender for inclusion in the next generation of smartphones due to its excellent isolation, compact architecture, and remarkable MIMO performance. The next chapter of the thesis discuss about another MIMO design that is also utilizing the sideframes of the smartphone. However in this design the main importance was given to achieve multi-band coverage, while maintaining the similar or better performance than the previous design.

CHAPTER 5

A T-SHAPED MULTI-BAND MIMO SYSTEM FOR 5G SMARTPHONE APPLICATIONS

CHAPTER 5

A T-SHAPED MULTI-BAND MIMO SYSTEM FOR 5G SMARTPHONE APPLICATIONS

5.1 INTRODUCTION

Many nations view the 3.4–3.6 GHz spectrum (LTE 42 band) as the pioneer in the Sub-6 GHz range. Along with this frequency, contemporary 5G research is also concentrating on the unlicensed LTE band 46 (5.150–5.925 GHz) and the LTE 43 band (3.6–3.8 GHz). Multi-element system integration into a single mobile terminal module has increased in recent years, and this trend is being studied [132]. These MIMO systems can only operate on one band, so they fall short of meeting all of the demanding specifications needed for 5G multi-band communications. Other designs have been working to achieve dual band or multi-band operations or wide band [90-100]. Their ability to operate on all frequencies designated as part of the sub-6 GHz 5G spectrum is a benefit. Nonetheless, the antenna components are mounted in these designs using side frames that are 5 mm in diameter and larger. This may limit these designs' applicability to incredibly thin mobile devices. In design [139] side frame used to install antenna is 3 mm. Which is very less but it operates on single band. Hence, the design only focused on compactness of the overall smartphone and not on the multiband coverage. Each of the aforementioned designs emphasis on enhancing a single MIMO system's parameter; for example, some designs aim to improve isolation, others to provide multiband operation, and yet others are focused on miniaturization. However, only minority of the designs concurrently takes into account compactness, low ground clearance, LTE 42/46 band coverage, and improved isolation.

The goal of the proposed design is to construct a MIMO system which can reduces the overall amount of space taken up by the antenna that operates on multiple bands, and provides adequate isolation simultaneously. The basic T-shaped patch antenna serves as the basis for the evolved design idea.

5.2 GEOMETRICAL STRUCTURE

Figure 5.1 shows the T-shaped proposed MIMO system's whole geometric configuration. The suggested system is 150 × 75 × 0.8 mm^2 in dimension. FR4 substrate (tan δ = 0.02 and ϵ_r = 4.4) is utilized for the designing substrate and side frames. A T-shaped resonant structure operating on LTE 42/46 achieves dual band response. The antenna components are mounted on a 150 × 3.6 mm^2 sideframe with a thickness of 0.8 mm (see Figure 5.1(a)). The antenna components are inscribed on the exterior of the side frames as perceived from Figure 5.1(b). It is composed of two sections: a 3.6 mm vertical part located in the side-frame's internal side and a 10 mm horizontal piece located on top of the substrate.

The whole dimension attribute of an antenna element is displayed in Figure 5.1(c). The lengths of proposed antenna are 15.6 mm, 6.3 mm, 2.1 mm, and 1.5 mm for L_1, L_2, L_3, and W_1. The antennas (1 & 5), (2 & 6), (3 & 7), and (4 & 8) have width W_2 of 0.4 mm, 0.45 mm, 0.45 mm, and 0.454 mm, respectively. Each antenna has a feed line offset (d_1) of 2.95 mm.

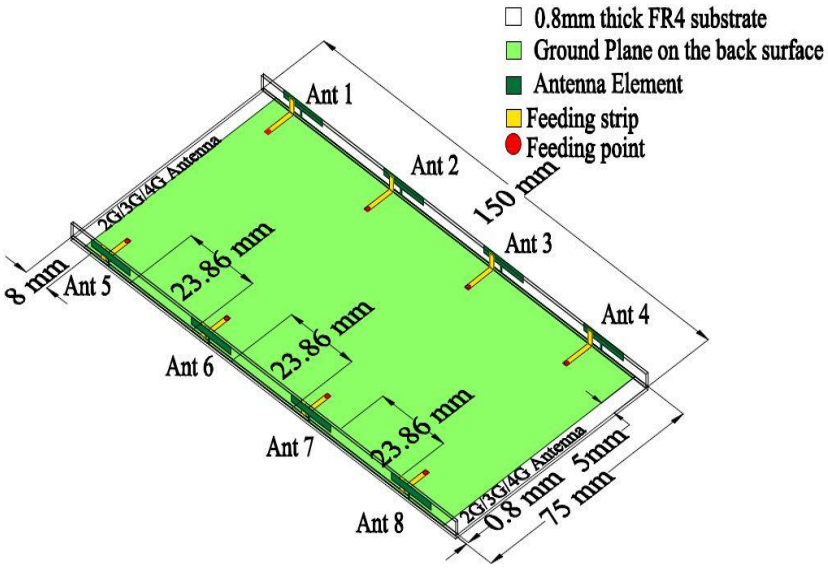

(a)

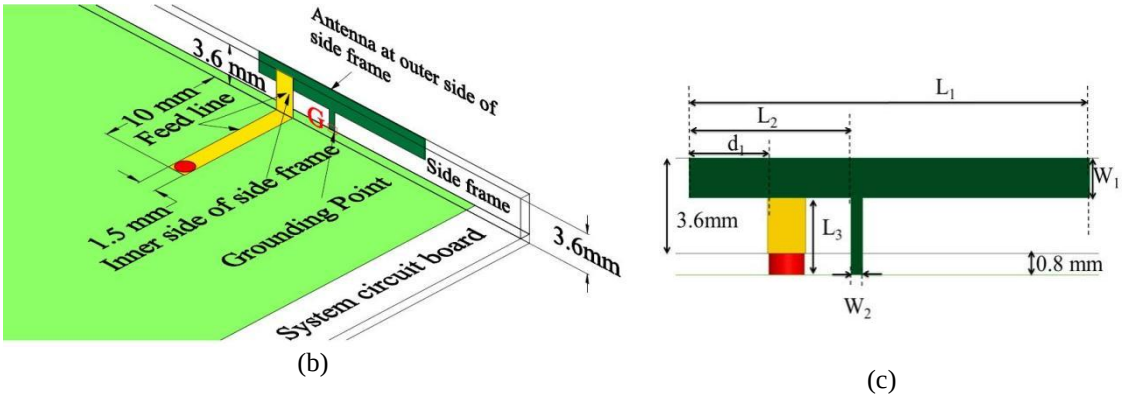

Figure 5.1 Geometry of the proposed multiband MIMO system (a) Complete view (b) Side frame with dimensions of feed line, (c) Individual element

5.3 MIMO ANTENNA SYSTEM PERFORMANCE

Figure 5.2 reveals the transmission and reflection response curves for the proposed MIMO antenna system. The lower band (resonates at 3.55 GHz) has bandwidth ranging from, 3.4 to 3.6 GHz, and the upper band (resonates at 5.5 GHz), is from 5.15 to 5.93 GHz, using -6 dB as a reference. It is possible to obtain 14 dB isolation for lower band and 25 dB isolation for non-adjacent antennas, such as S_{45}. The isolation for nearby and non-adjacent antennas in the upper band is 16.5 dB and 30 dB, respectively. As a result, the design has good isolation.

5.3.1 Analyzing parametric data and current distributions

Using the current distribution given in Figure 5.3, operational mechanism is investigated of proposed design.. The length L_1, L_2, L_3, W_1, and W_2 are, 15.6 mm, 6.3 mm, 2.1 mm, 1.5 mm, and 0.4 mm respectively. At 3.5 GHz current distribution is shown in Figure 5.3 (a), and at 5.5 GHz in Figure 5.3(b). The upper radiating element and the bottom element make form the antenna radiator. where the short element is connected to length L_3, and the top radiating element has length L_1.

The first resonance is caused by both the radiating elements. However, for the second resonance only the upper radiating part is included in the current path. The top radiating element's surface current varies by $\lambda/2$, which leads to the second resonance.

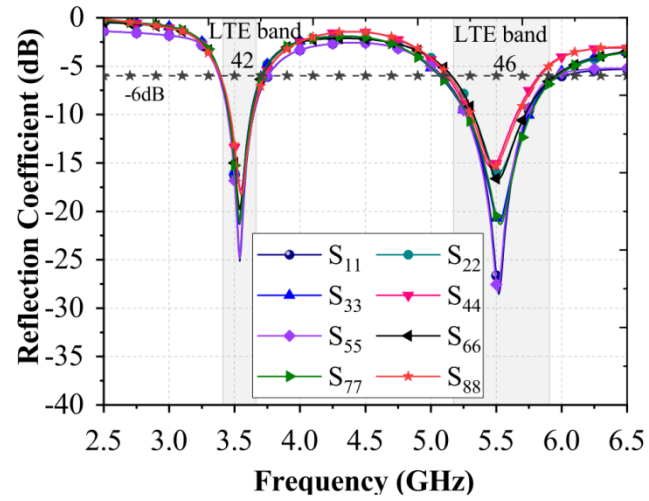

(a)

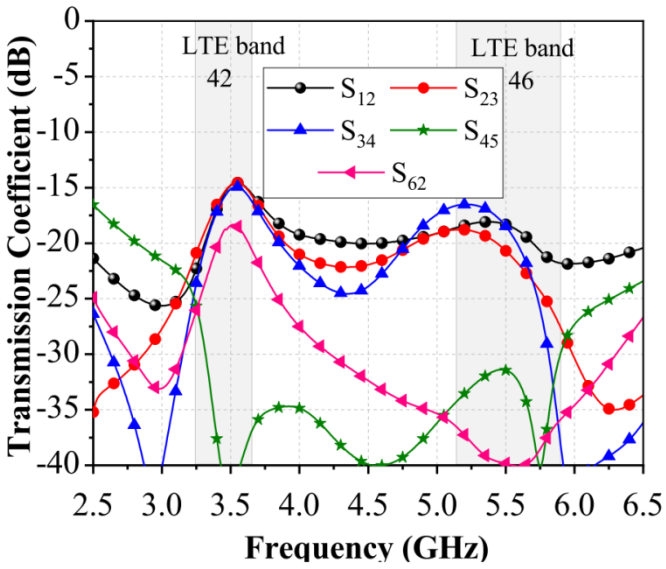

(b)

Figure 5.2 Simulation (a) Reflection coefficients, (b) Mutual coupling of proposed T-shaped MIMO system

To comprehend the impact of changing the antenna's length and breadth, L_1, W_1, and W_2 parameters are varied. The results show how these changes affect the resonance frequency and operating bandwidth, as shown in Figure 5.4 (a) and 5.4 (b). Both the upper and lower resonances moved to the lower frequency as L_1 length increased from 12 mm to 17 mm.

This was anticipated since the length L_1, which represents the entire horizontal length of proposed antenna, extend the current path of both resonant modes, hence reducing both resonances. The antenna covers the two needed bands when L_1 is 15.6 mm, which is why this length was chosen.

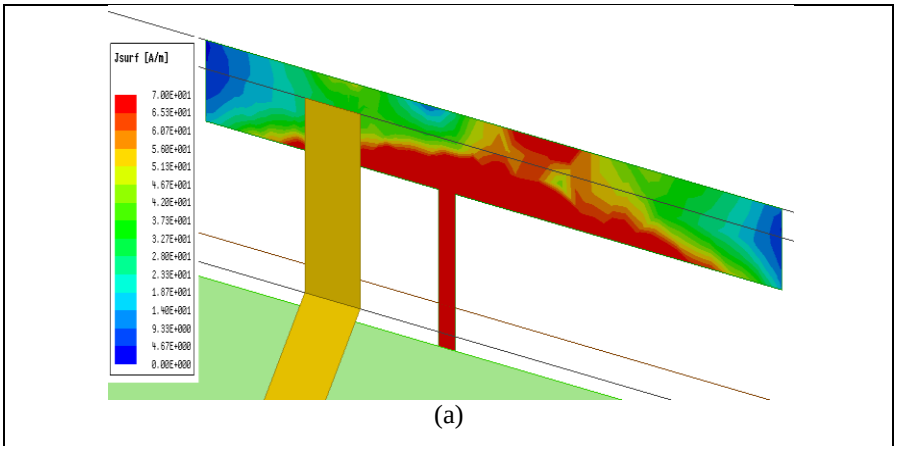

(a)

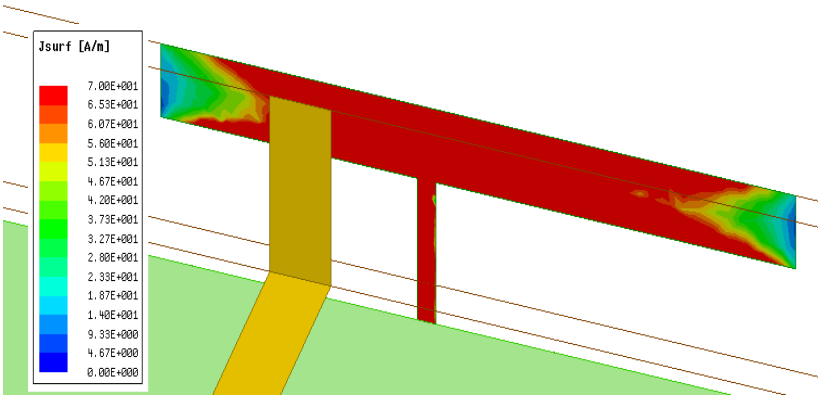

(b)

Figure 5.3 Surface current distribution (a) 3.5 GHz (b) 5.5 GHz

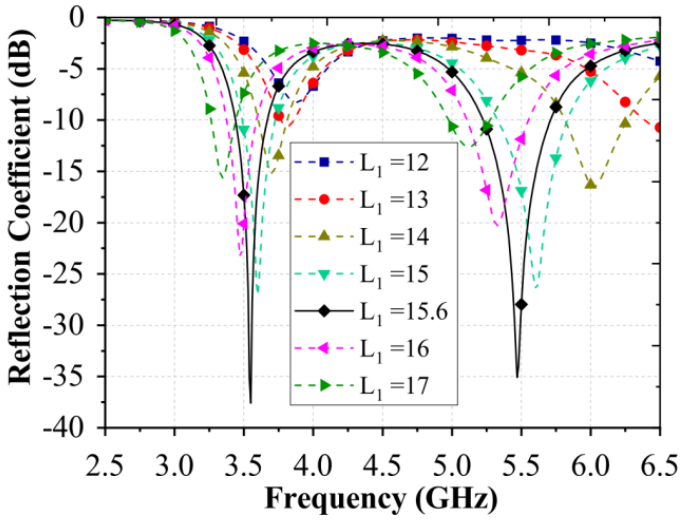

(a)

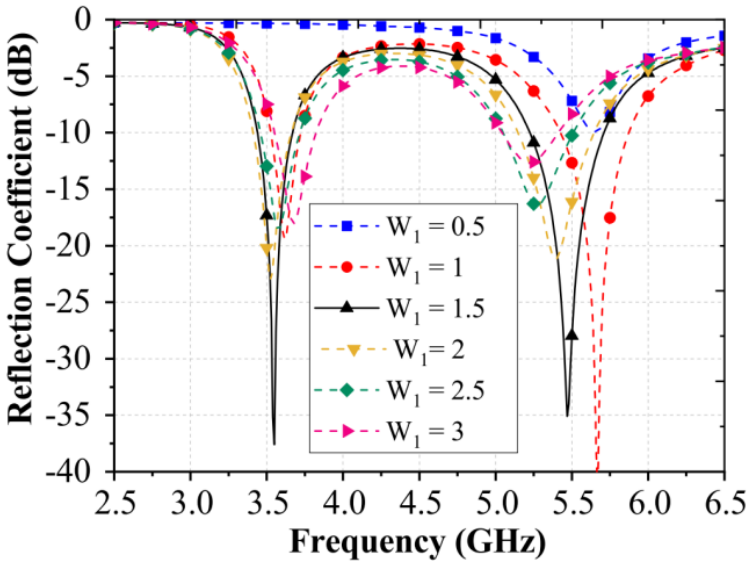

(b)

Figure 5.4 Variation of (a) Length L_1 (b) Width W_1 when L_1 is 15.6 mm

It became apparent that both resonances switched to the frequencies below when the width W_1 was increased from 0.5 to 1.5 mm.

The width W_1 was changed from 1 mm to 3 mm. The first resonance did, however, slightly alter at 2 mm, while the second resonance continued to migrate to the lower end of the spectrum. The first resonance began to move to a higher frequency while the second resonance shifted to a lower frequency as W_1 was further raised from 2.5 mm to 3 mm. This occurred because, once the width W_1 is expanded to 2 mm (the side-frame's height is fixed), doing so will cause the length L_3, which contributes to initial resonance, to decrease. The initial resonance will rise with any decrease in length L_3. Thus, when width W_1 is extended beyond a certain point, it sets the distance between the two resonant frequencies in addition to controlling the resonances of the two bands.

However, in this instance, we disregarded width W_1's additional capabilities and limited it to 1.5 mm. The initial resonance may be clearly affected by changing the width (W_2), and the lower band can be controlled using this parameter.

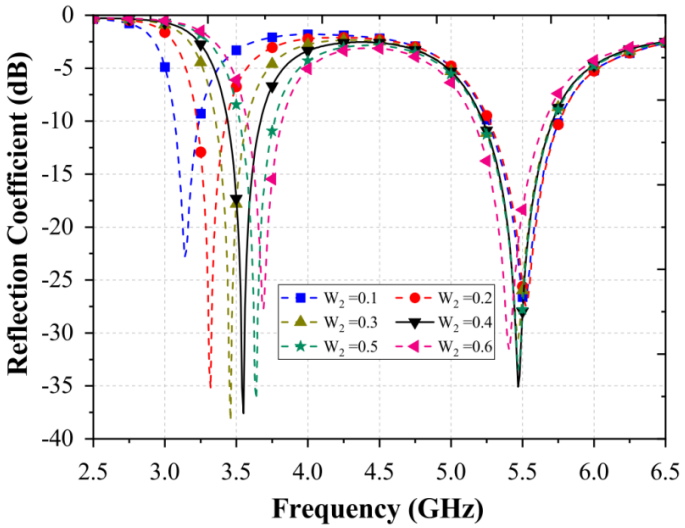

Figure 5.5 Variation of Width W_2 when L_1 is 15.6 mm.

5.4 RESULT AND DISCUSSION

Prototype was created in order to validate the simulated findings, as displayed in Figure 5.6.

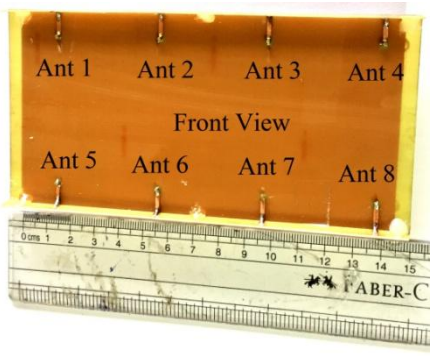

(a)

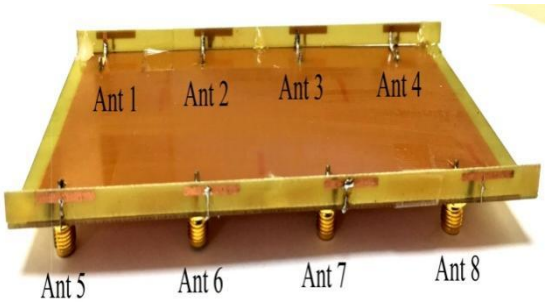

(b)

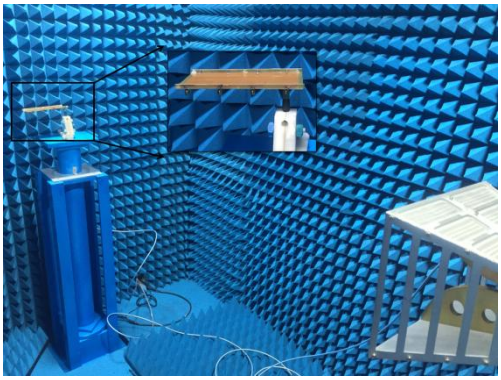

(c)

Figure 5.6 Image of fabricated design (a) Front view (b) Side view and (c) Measurement setup

According to the observed reflection coefficient revealed in Figure 5.7, the LTE bands 42/46 are the two band of operation achieved by proposed MIMO system. Because they are next to one another, the connections between ports 1 and 2, 2 and 3, and 3 and 4 are the strongest. For both bands, isolation is 14 dB between any two antenna pairs. The measured and simulated results agree rather well, with the exception of a few small variations caused by mismatch and manufacturing tolerance. The overall efficiencies are around 60%–81% in the lower and higher bands, respectively (see Figure 5.8). Figure 5.9 shows the co and cross radiation pattern of E and H plane of antenna 1 to antenna 4 at 3.5 GHz and 5.5 GHz. Because of the symmetry in the structure layout, radiation pattern of antenna 1 to antenna 4 are presented for the discourse. It is clear that the proposed design produces good radiation. The peak gain ranges from 2 to 4 dBi.

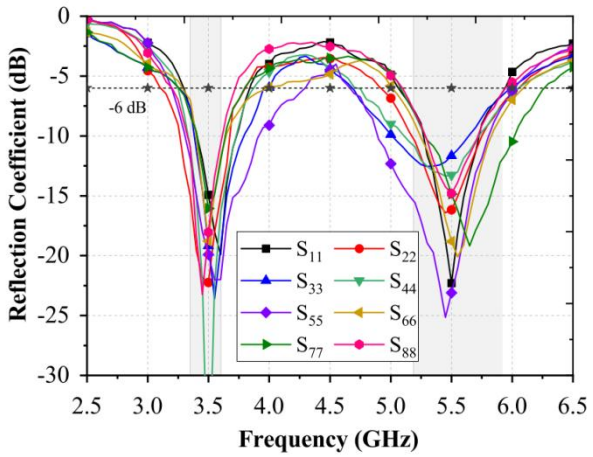

(a)

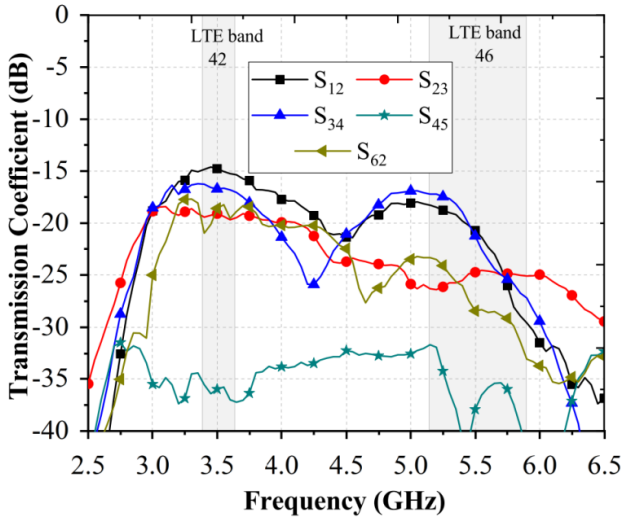

(b)

Figure 5.7 (a) Measured reflection coefficients results of proposed array (b) Measured Mutual coupling

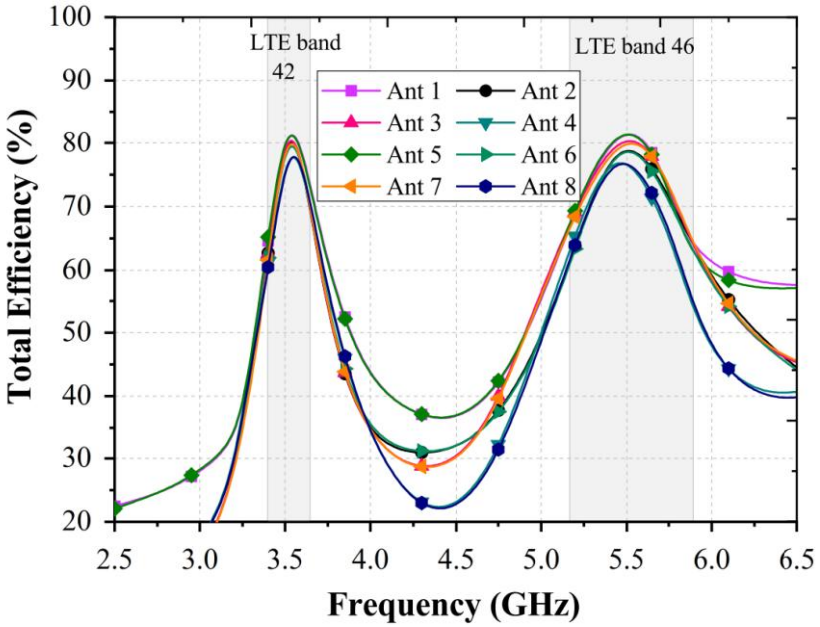

Figure 5.8 Simulation results of total efficiencies of ant 1-ant 8

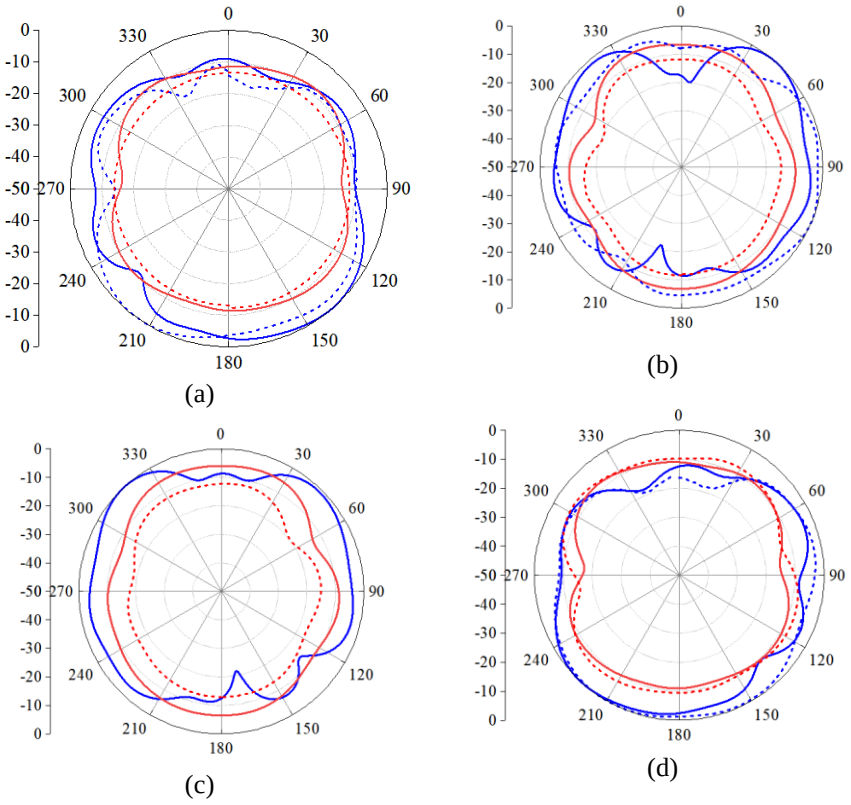

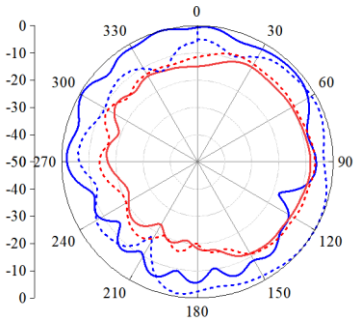
0
30
60
90
120
150
180
210
240
270
300
330
0
-10
-20
-30
-40
-50
-40
-30
-20
-10
0

(e)

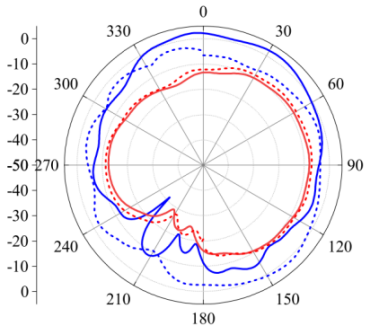
0
30
60
90
120
150
180
210
240
270
300
330
0
-10
-20
-30
-40
-50
-40
-30
-20
-10
0

(f)

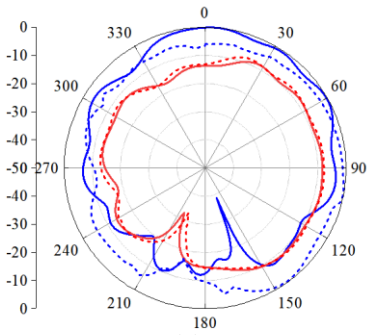
0
30
60
90
120
150
180
210
240
270
300
330
0
-10
-20
-30
-40
-50
-40
-30
-20
-10
0

(g)

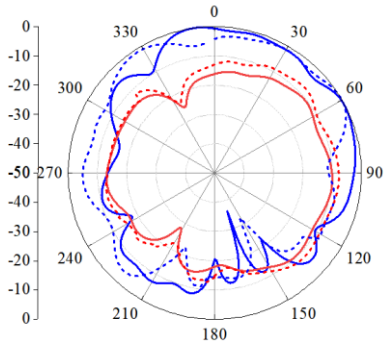
0
30
60
90
120
150
180
210
240
270
300
330
0
-10
-20
-30
-40
-50
-40
-30
-20
-10
0

(h)

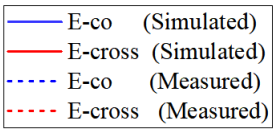
E-co (Simulated)
E-cross (Simulated)
E-co (Measured)
E-cross (Measured)

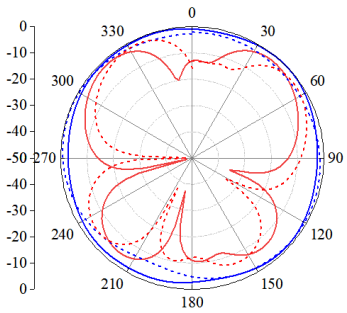
0
30
60
90
120
150
180
210
240
270
300
330
0
-10
-20
-30
-40
-50
-40
-30
-20
-10
0

(i)

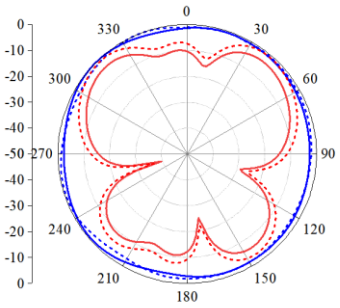
0
30
60
90
120
150
180
210
240
270
300
330
0
-10
-20
-30
-40
-50
-40
-30
-20
-10
0

(j)

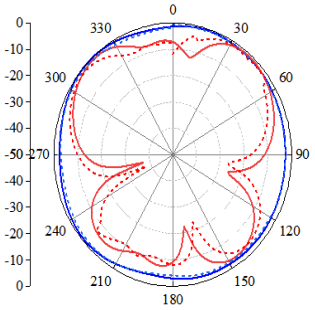
0
30
60
90
120
150
180
210
240
270
300
330
0
-10
-20
-30
-40
-50
-40
-30
-20
-10
0

(k)

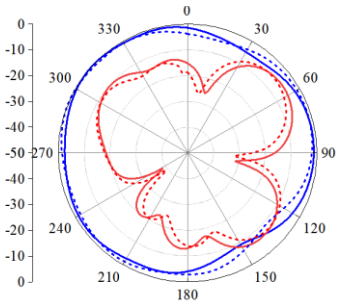
0
30
60
90
120
150
180
210
240
270
300
330
0
-10
-20
-30
-40
-50
-40
-30
-20
-10
0

(l)

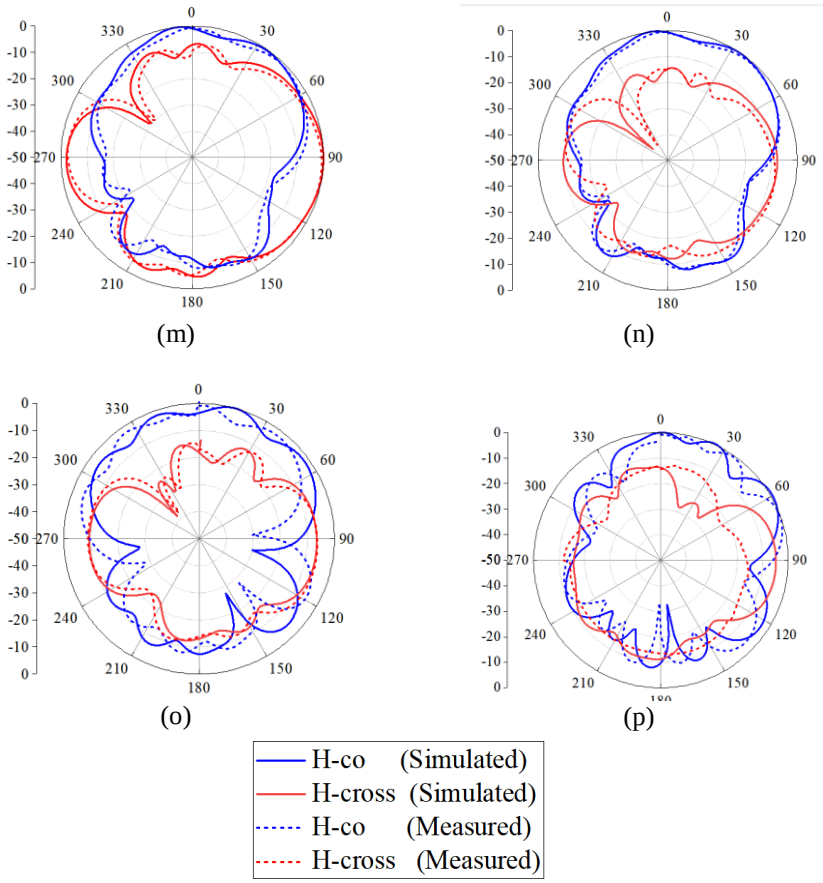

Figure 5.9 Simulated and measured radiation patterns of the proposed antenna array. E-plane radiation patterns:(a) Ant 1, (b) Ant 2, (c) Ant 3, (d) Ant 4 at 3.5 GHz,(e) Ant 1, (f) Ant 2, (g) Ant 3, (h) Ant 4 at 5.5 GHz. H-plane radiation patterns:(i) Ant 1, (j) Ant 2, (k) Ant 3, (l) Ant 4 at 3.5 GHz,(m) Ant 1, (n) Ant 2, (o) Ant 3, (p) Ant 4 at 5.5 GHz.

5.4.1 MIMO Performance

Figure 5.10 displays the ECC between antenna 1 and 2, antenna 2 and 3, antenna 3 and 4, antenna 4 and 5, and antenna 5 and 1. When half of the elements, namely antenna 1 to 4, are taken into consideration, ECC values are only displayed between these antenna pairs since they are the nearest to one another and, as a result, are prone to experience more intense radiation interference from one another. The ECC is determined using Equation 5.1.

$$ECC = \frac{\left|\iint_{4\pi} E_i(\theta,\phi) * E_j(\theta,\phi)^* \partial\Omega\right|^2}{\iint_{4\pi}|E_i(\theta,\phi)|^2 \partial\Omega \iint_{4\pi}\left|E_j(\theta,\phi)\right|^2 \partial\Omega} \quad (5.1)$$

i and j are the two ports being excited.

An excellent ECC of less than 0.075 and 0.05 is achieved across the lower and higher band respectively. In the event where the transmitter is unaware of the channel situation, the channel capacity for N×N MIMO system is determined using Equation 5.2. Every antenna receives the same quantity of power.

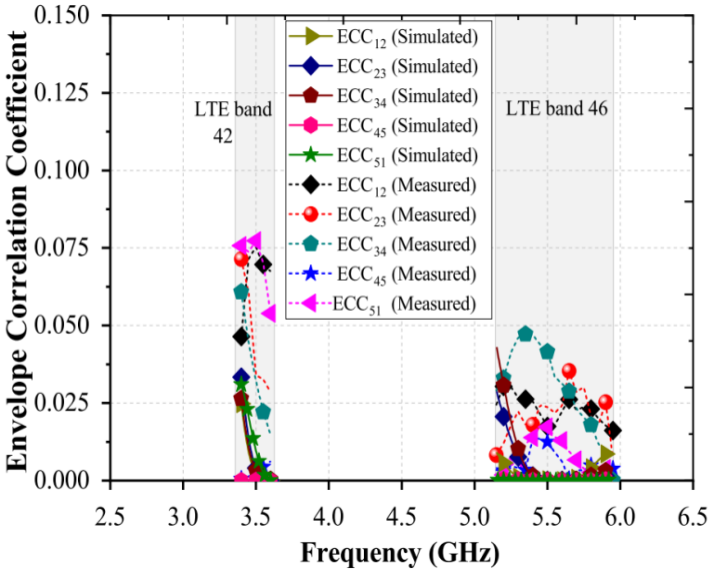

Figure 5.10 Measured and simulated ECC variations with frequency

$$C = E\left\{log_2\left[det\left(I_N + \frac{\rho}{Nn_T}HH^H\right)\right]\right\} \tag{5.2}$$

where H is a channel matrix (N×N), number of transmitting antennas n_T, E stands for expectation with respect to various channel realizations, and average SNR is ρ/N (in this case, 20 dB).

The channel has an identical distribution and is independent in a Rayleigh fading environment.

As seen in Figure 5.11, the proposed design achieves a channel capacity of 41 b/s/Hz and 43.6 b/s/Hz for LTE 42 and LTE 46 bands respectively.

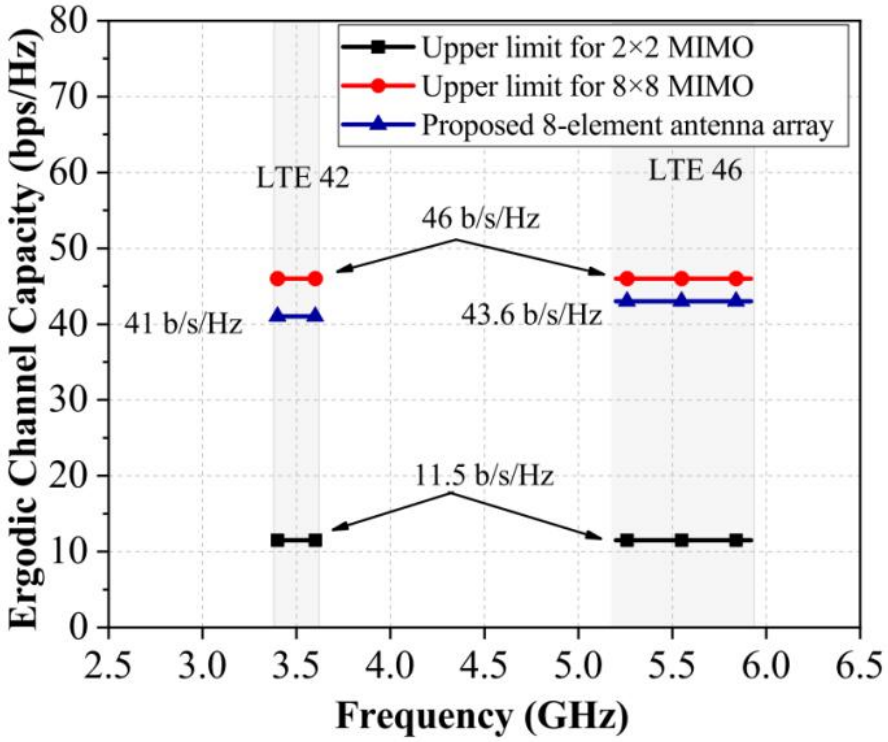

Figure 5.11 Proposed multiband compact system's Ergodic channel capacity

5.5 COMPARISON WITH OTHER RECENT DESIGNS

Table 5.1 presents a comparison of MIMO performance of proposed design with other state of the art methods. Every design listed in Table 5.1 covers. It is made on side frames larger than five millimeters and covers two or more 5G bands. With the exception of the design given in reference [88], it is larger than the suggested design. With a height of only 3 mm, the sideframe utilized in reference [88] is perfect for incredibly thin phones. When compared to this design, the suggested side-edge printed MIMO system offers the advantage of reasonable isolation and efficiency. The two 5G bands are covered by the design found in references [97] and [98], which also offers good isolation. Nevertheless, the reference [98] only has four MIMO orders, which may restrict the channel capacity. Although the design [102] operates at two 5G bands, the isolation and side-frame size can still be improved.

Table 5.1: Design comparison of T-shaped multiband MIMO system with state of the art 5G antenna design

Ref	**Length Height and thickness of side frame (L ×H*)**	**Operational band (GHz)**	**No. of antenna elements**	**Antenna Efficiency (%)**	**ECC**	**Isolation (dB)**	**Peak Channel Capacity (b/s/Hz)**
[13]	150×7×0.8	3.4-3.6, 4.8-5.1	8	>41, >40	<0.08, <0.07	>11.5	38.5, 38
[92]	150×5.2×0.8	3.4-3.6, 5.15-5.925	8	>50, >53	<0.1 <0.04	>12	38.8 39.7
[97]	150×6×0.8	3.3-5.95	8	>47	<0.11	>15	35.6-41.3
[98]	150×7×0.8	3.4-3.6, 4.8-5	4	-	<0.14, <0.12	>17.5	18.3
[100]	135×7×0.8	3.3-6	8	>46	<0.26	>11.4	-
[88]	150×3×0.8	3.3-3.8, 4.8-5, 5.150-5.925	8	>43	<0.12	>10.5	36.8 37 37.6
Proposed Design	**150×3.6×0.8**	**3.4-3.6, 5.15-5.925**	**8**	**>60**	**<0.075 <0.05**	**>14, >17.5**	**41 43.6**

Therefore, the suggested design excels because it simultaneously provides strong isolation, a small antenna size and dual band coverage, a feat that more recent designs were unable to accomplish.

5.6 Analysis Of Proposed MIMO Antenna For Its Practical Applications

The integration of a MIMO antenna system into a terminal device while including various components like a dielectric frame and a battery is a design issue. Because of this, modeling of a MIMO antenna system using these components is crucial and actual prototyping is insufficient. As a result, this section discusses the impact of the phantom hand, display screen, and frame (plastic) on the proposed MIMO performance.

5.6.1 Battery Effect on MIMO performance

As seen in Figure 5.12, the battery module combined with the main PCB. A metal that measures 118 mm × 40 mm × 3 mm is affixed to the main PCB to replicate the battery. Figure 5.13 presents the comparable results. The impact on the two resonances is minimal. The LTE 42/46 bands are still covered by the design, and the isolation is 14 dB.

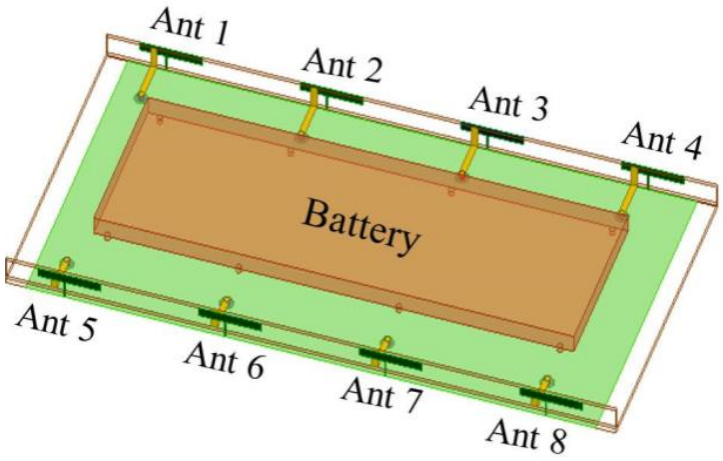

Figure 5.12 Battery installation with proposed MIMO system

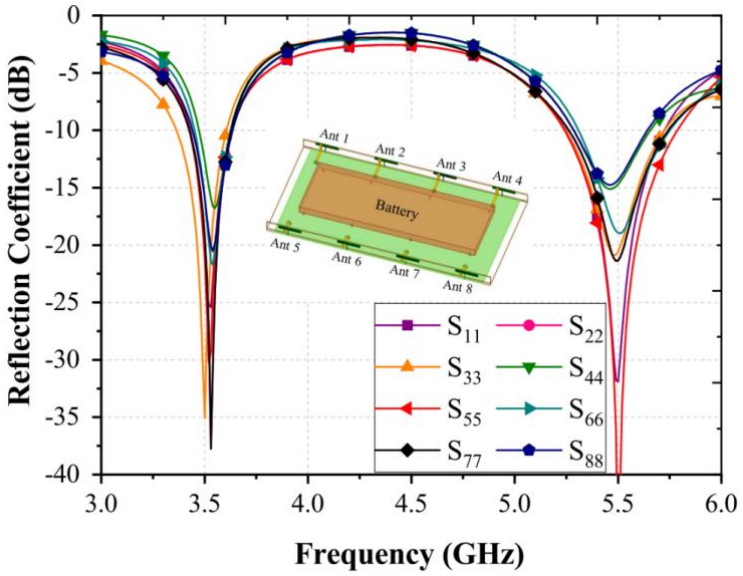

(a)

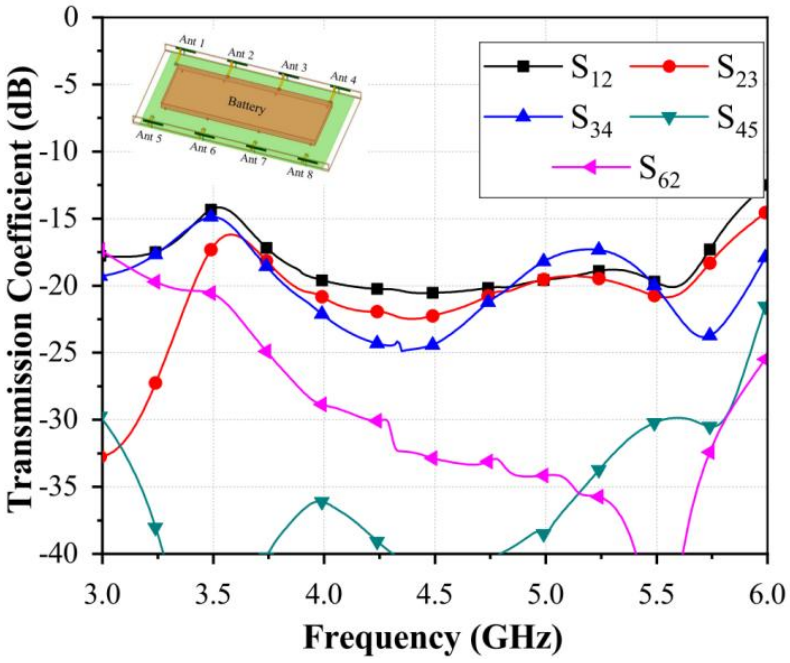

(b)

Figure 5.13 Simulation results of MIMO system with battery (a) Reflection coefficients (b) Mutual coupling

5.6.2 Performance analysis of MIMO with installation of plastic frame

As shown in Figure 5.14, a plastic frame of 4.6 mm in height ($\epsilon r = 3$ and $\tan \delta = 0.01$) encircled the antenna array. It is possible to observe the little change in the resonance frequency, which is 5.5 GHz to 5.4 GHz (see Figure 5.15). When plastic

frames are positioned all around the antenna array, dielectric loading happens because they are in close proximity to the antenna components. Still, the design features 14 dB isolation and functions on both bands.

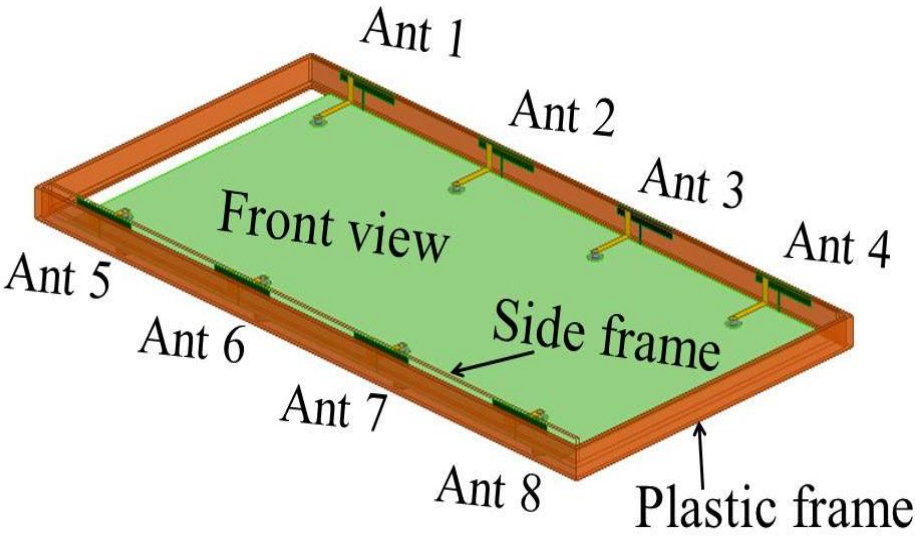

Figure 5.14 Proposed MIMO antenna with plastic frame

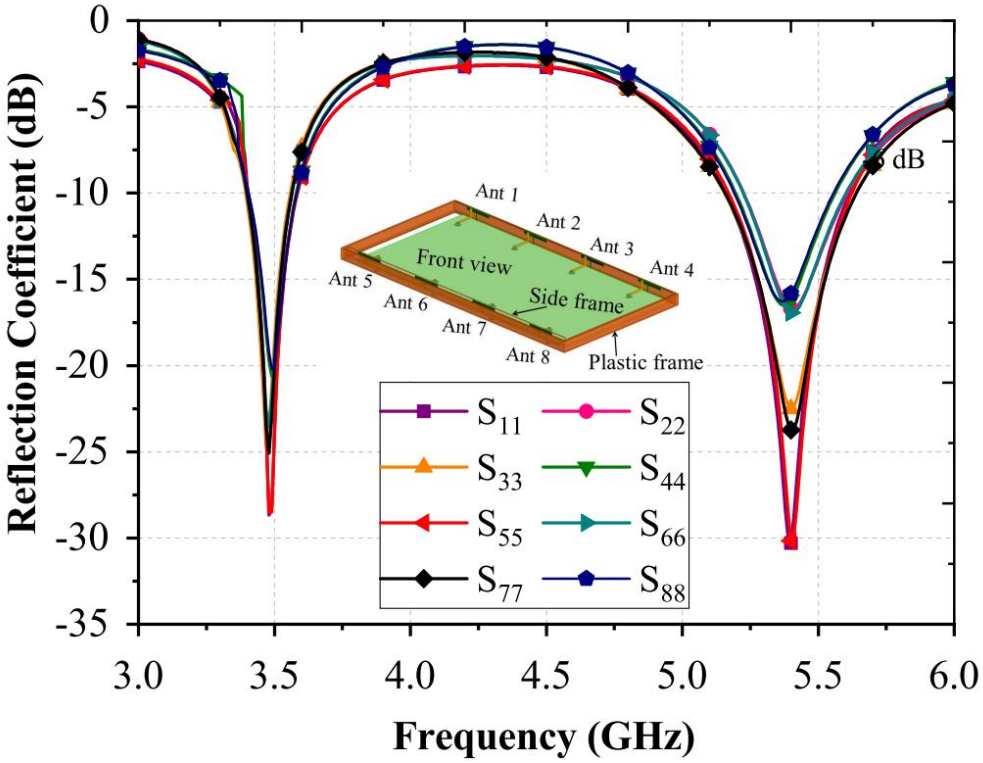

(a)

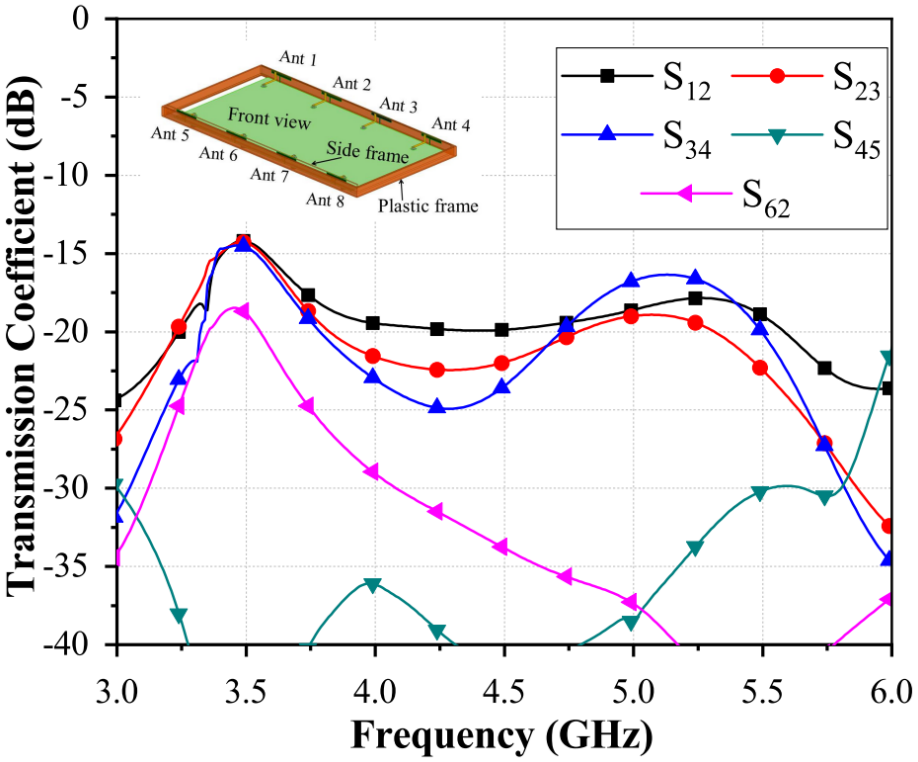

(b)

Figure 5.15 Plastic frame installed **(**a) Reflection coefficients (b) Transmission coefficients

5.6.3 Performance analysis of MIMO with user hand

The existence of the user hand in the near field of antenna elements may have an impact on a MIMO system since the human body has a property of being a lossy dielectric medium.

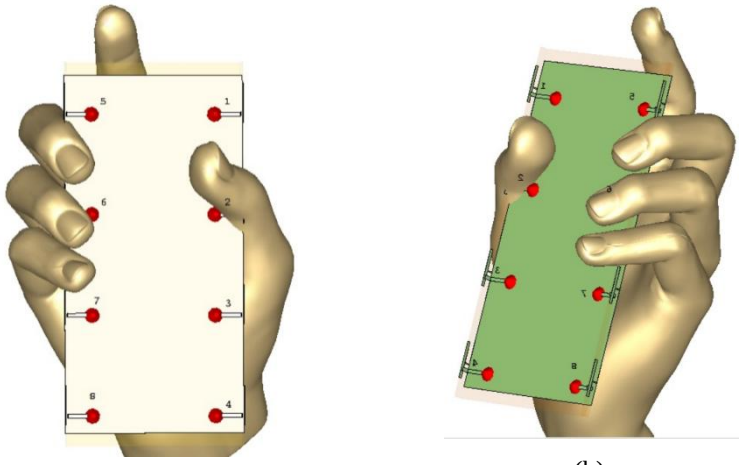

(a) (b)

Figure 5.16 Single hand usage scenario (a) Front View, (b) Side View

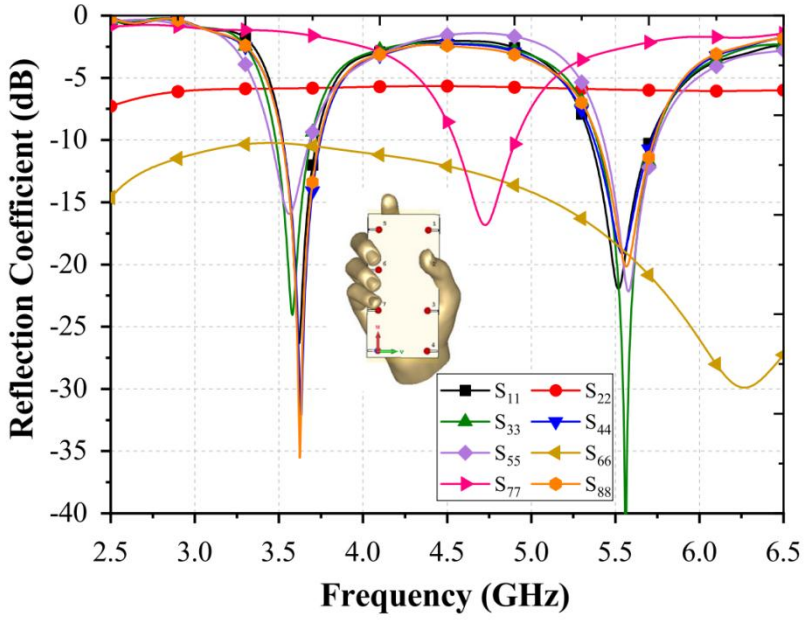

(a)

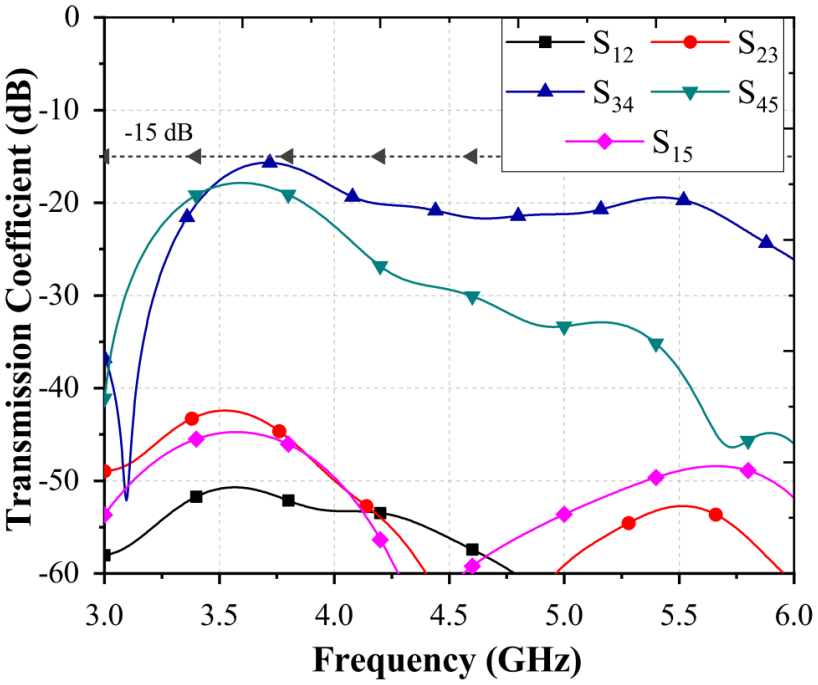

(b)

Figure 5.17 Single hand usage scenario (a) Reflection coefficients, (b) Mutual coupling

Living tissues have a higher relative permittivity than the air. The human hand's relatively high permittivity (while holding a cell phone) may result in an impedance change in the near field zone of the antenna. Consequently, antenna performance is affected by the inclusion of the hand model. The impact of the user hand on the MIMO system is revealed in Figure 5.17. The antenna 2, 6, and 7 are quite near to the

user's hand, as Figure 3.16 illustrates. Their performance suffers greatly as a result. Because they are not impeded by the user hand, the dual band ability of other antenna elements is maintained. The design provided 15 dB isolation.

5.7 CONCLUSION

Dual band antenna arrays are made using straightforward T-shaped designs. The suggested design uses side frames of just 150 mm × 3.6 mm, which are utilized to mount the antenna components. The isolation offered by proposed MIMO antenna system is better than 14 dB and operates on LTE 42/43 channels. The ECC for each of the two interest bands is less than 0.075. In the LTE 42/46 bands, the combined efficiency of all antennas is greater than 60%. The recommended antenna array performs better in terms of simultaneous dual band coverage, size reduction, and enhanced isolation. Though they may be added in the future, the performance of the system with additional mobile device components (such as the camera, speaker, etc.) has not yet been covered in this thesis. The suggested MIMO system has promise for use in incredibly small 5G devices, provided that the antenna is used practically. Further, after achieving the miniaturization and multiband coverage which can help in making the smartphone less bulky, tracking the appearance of the smartphone is also important as some customers are keen to buy metalbody smartphone. Therefore the next chapter of the thesis is dedicated to a MIMO system, which is designed for the smartphone with metal body.

CHAPTER 6

METAL-RIMMED 8-ELEMENT TRI-BAND MIMO SYSTEM WITH HIGH EFFICIENCY FOR MODERN 5G SMARTPHONES

CHAPTER 6

METAL-RIMMED 8-ELEMENT TRI-BAND MIMO SYSTEM WITH HIGH EFFICIENCY FOR MODERN 5G SMARTPHONES

6.1 INTRODUCTION

The physical design of smartphones and fast data rates have lately been the two foremost things that users are interested in before they make a choice of buying a phone. Modern mobile customers demand resilience and appealing appearances in addition to high performance from their smartphones. The body of a smart phone can now be designed in a variety of ways, such as, a glass body, a metal body or a hybrid metal-plastic design. The most common option from these is metal-rimmed cell-phones since they give the entire smart phone the needed mechanical strength and a decent appearance when installed. However, antenna performance gets noticeable influenced due to the mobile phone's metal chassis. The adverse effects of the metal frame affect the impedance matching, antenna efficiency, and other performance attributes. This happens because of the movement of current in the metal frames will interact with the current flowing in the antenna element itself. It is challenging to design an antenna that covers different sub-6 GHz bands assigned to 5G communication with acceptable performance under these rigid restrictions. One possible solution to this problem is given [140] in which use of grounded patches is done and the metal rim is modified by creating gaps to enhance antenna's performance. The alternate method entails employing the entire portion as antenna. Another approach is utilizing a section of the metal rim to construct the antenna. This can make it easier to design antennas.

For metal rim antennas, researchers have developed a number of intriguing designs. Creating an antenna radiator out of the metal rim is a common move towards getting adequate bandwidth and efficiency [101–123] and [141-142]. Unique method is presented [143] to improve radiation performance by using half square and circular loop. There were essentially two research gaps found in the open literature by the

authors and that are as follows. 1) Designs consider their bands at -6 dB impedance bandwidth. 2) Modern designs have significantly lower efficiency. The current research is motivated by these elements. In this study, inverted F antenna (IFA) and an open-slot antenna are presented that may be utilized with metal-frame smartphones to operate LTE in the bands of 42/43/46. The antenna uses a metal frame that also serves as the IFA. There is improvement in the impedance matching of the open-slot antenna due to the presence of metal-rim. This antenna is a strong contender for metal-rimmed smartphones.

6.2 GEOMETRY OF ANTENNA

For 5G mobile devices, a three-band (LTE 42/43/46) MIMO metal rimmed design is suggested, as shown in Figure 6.1. The 150 mm×75 mm×0.8 mm, circuit board has been designed using FR4 substrate (tan = 0.02, r = 4.4). There is metal ground on the backside. Two side frames are acting as the metal rim. They are placed on the circuit board's two longer sides. In order to match the metal rims of cellphones, the inside edges of the frames are copper-plated also they are electrically linked to the ground plane.

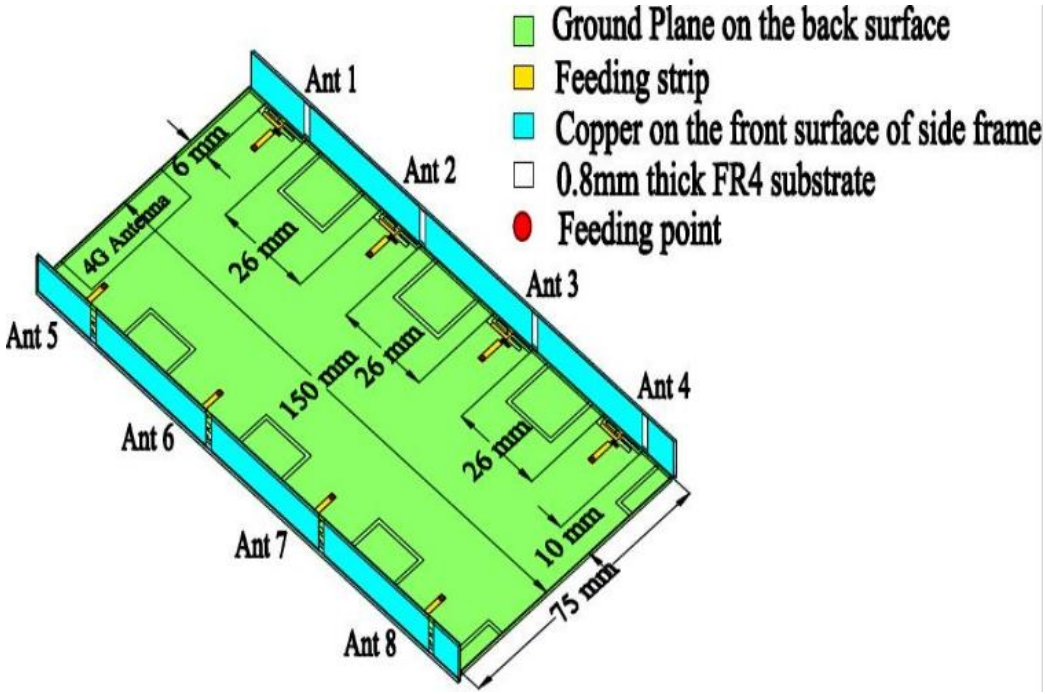

(a)

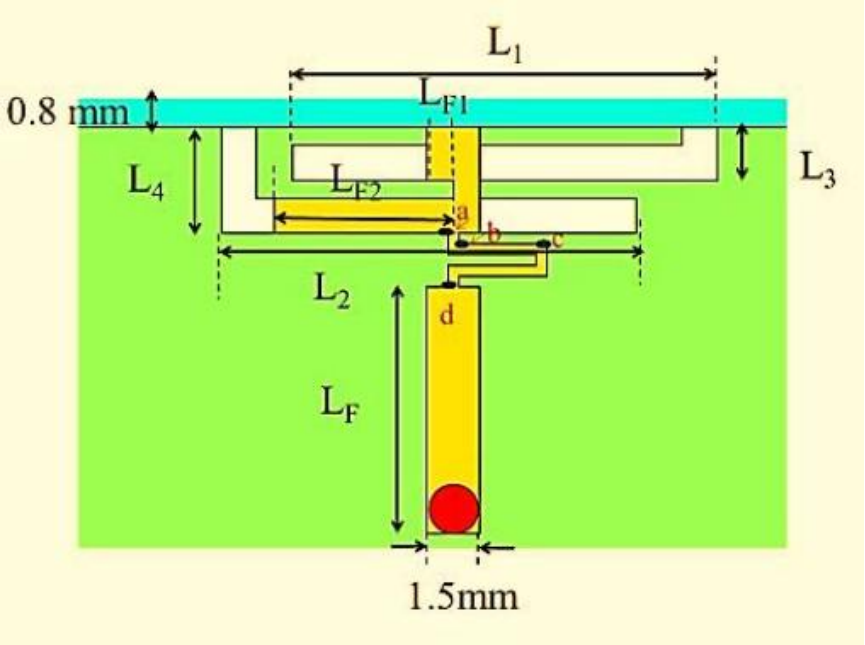

(b)

Figure 6.1(a) Complete structure of the proposed tri-band metal rimed MIMO system (b) Single antenna element

The spacing among radiating components or antenna structure is divided equally i.e. 26 mm. A rectangular defect made up of two L-shaped slots in the ground structure of a single antenna element is exploited to construct the proposed tri-band MIMO system. This defect is of 14 × 3 mm^2 dimension in total. The design specifications for the radiating element are shown in Figure 1(b), with L_1=12.3 mm, L_2=12 mm, L_3=1 mm, L_4=3 mm, L_F=7 mm, L_{F1}=1.5 mm, and L_{F2}=5.25 mm. The feeding for the antenna element is provided via a micro-strip line that is present on the inner side of metal rim. A tuning stub that can be compared to a capacitive loading is placed to the feeding line parallel to the metal rims. Points 'a' and 'd' are used to link a thin, 0.3 mm wide meandering line to the straight microstrip. In this mode, it acts as an impedance transformer. To maintain the robustness of the design the ground plane and metal-rim are electrically connected.

6.3 PERFORMANCE OF MIMO ANTENNA SYSTEM

Figure 6.2 displays the proposed slot antenna's reflection coefficients. The suggested tri-band metal rim design operates on 3.4 - 3.6 GHz and 3.6 - 3.8 GHz bands and resonates at 3.6 GHz. These two bands are covered with -10 dB impedance bandwidth which an infrequent occurrence in contemporary MIMO antenna designs

for smartphones. This design also works on LTE 46 (-6 dB impedance bandwidth) band (I.e 5.1 - 5.8 GHz). The proposed tri-band metal rim MIMO antenna arrangement achieves isolation of 12 dB.

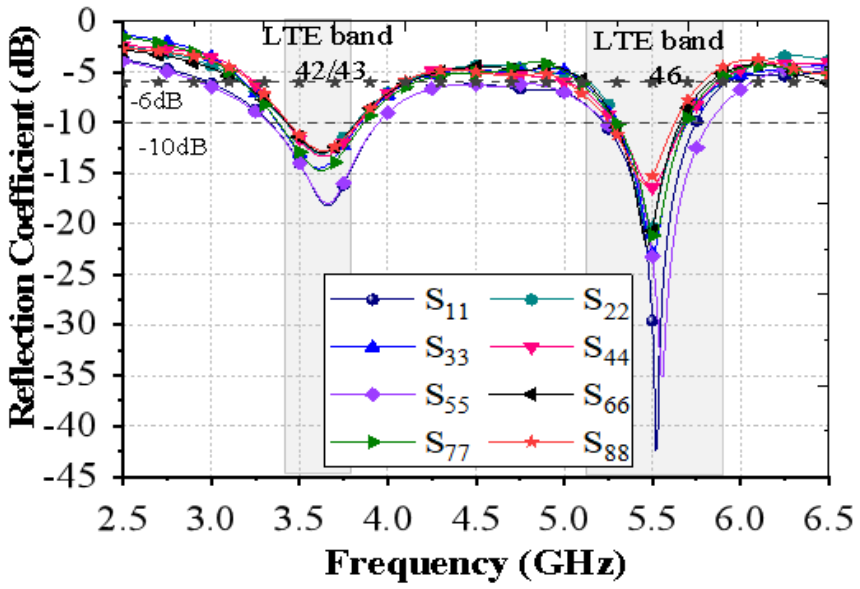

(a)

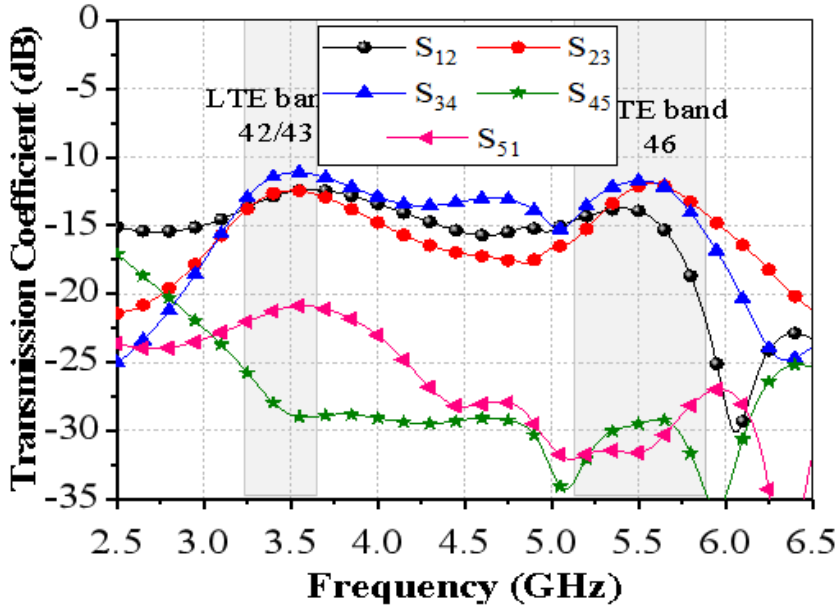

(b)

Figure 6.2 S-parameter of tri-band metal rim MIMO system (a) Simulated reflection coefficients (b) Simulated Mutual coupling.

6.3.1 Design Process

The proposed tri-band metal rim antenna's design progress is broken down into four stages. Only the open slot and feed line are visible in step 1. Impedance transformer is inserted in step 2. Stub is added in step 3 along with the impedance transformer are both present. To create the suggested design, step 4 involves adding another slot. The reflection coefficient of all design steps is presented in Figure 6.4. The only mode produced in first step is the open slot mode, which has a resonance at 4 GHz. The second stage entails the addition of an impedance transformer, and alters the impedance to bring the resonance down to 3.8 GHz. This meandered structure act as a LC tank.

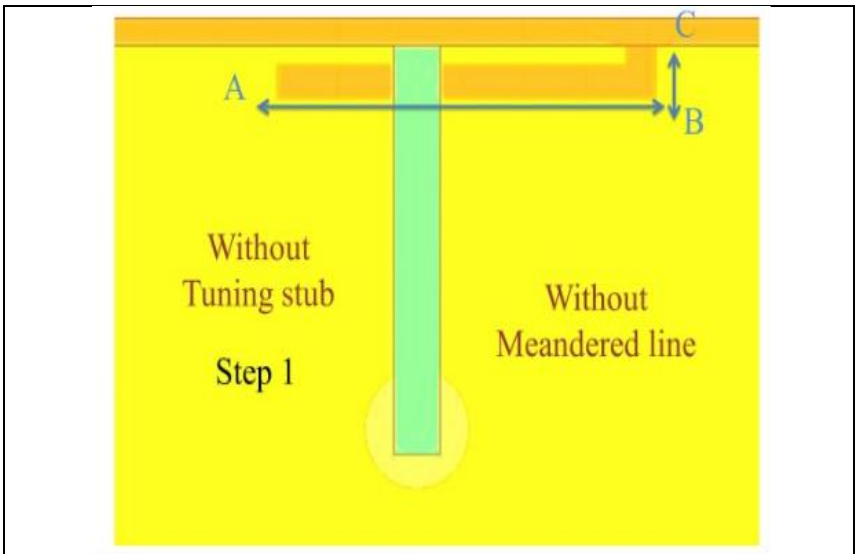

(a)

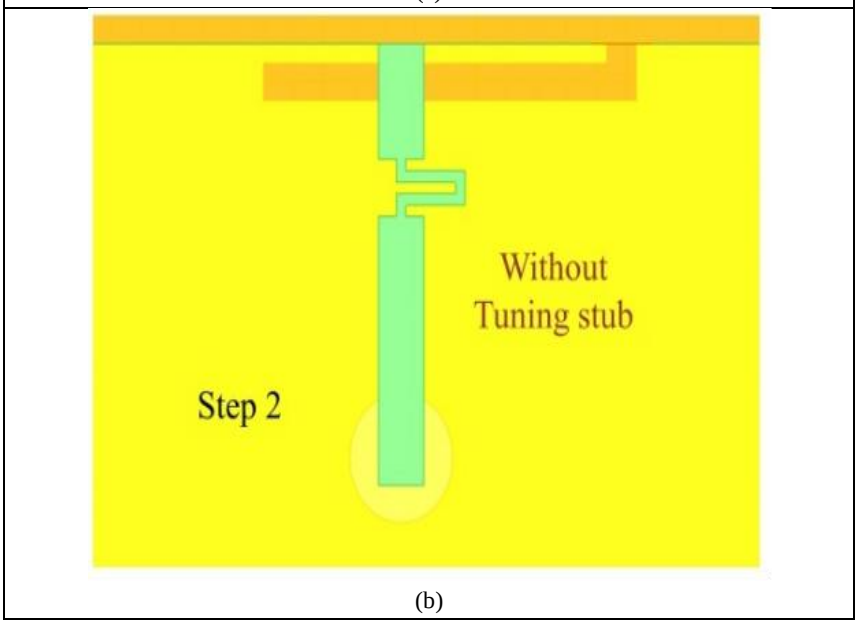

(b)

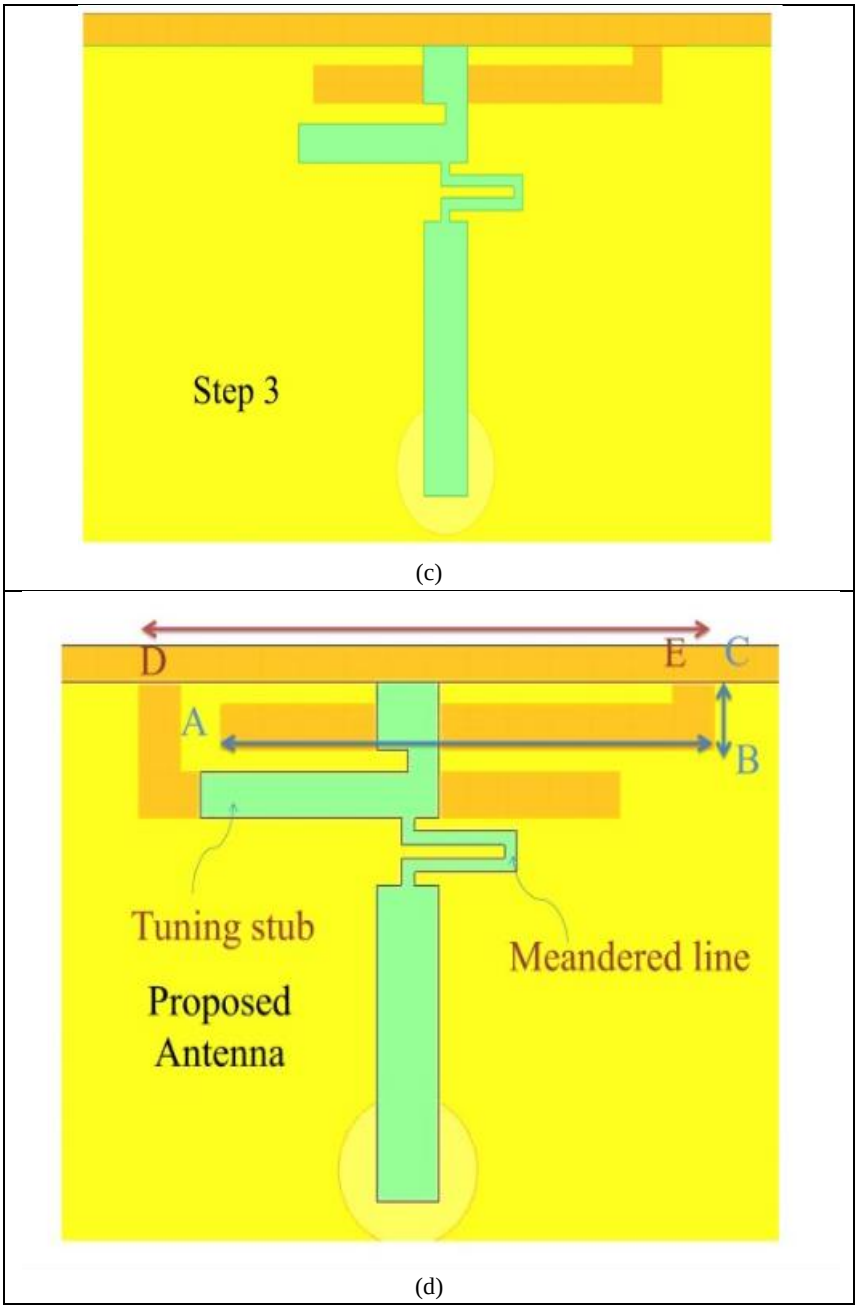

Figure 6.3 The suggested antenna's design steps include (a) 1 (b) 2 (c) 3 (d) 4, respectively

At about 8 GHz, there is a new resonance which is a result of IFA mode excitation and it is caused by the feed line and metal rim working together. The transmission line is given a stub in step 3, which causes capacitance between the metal rim and transmission line. The mode that is excited at 5.5 GHz is IFA mode, when this stub is introduced, but up until this stage this design is not working on the desired frequency bands.

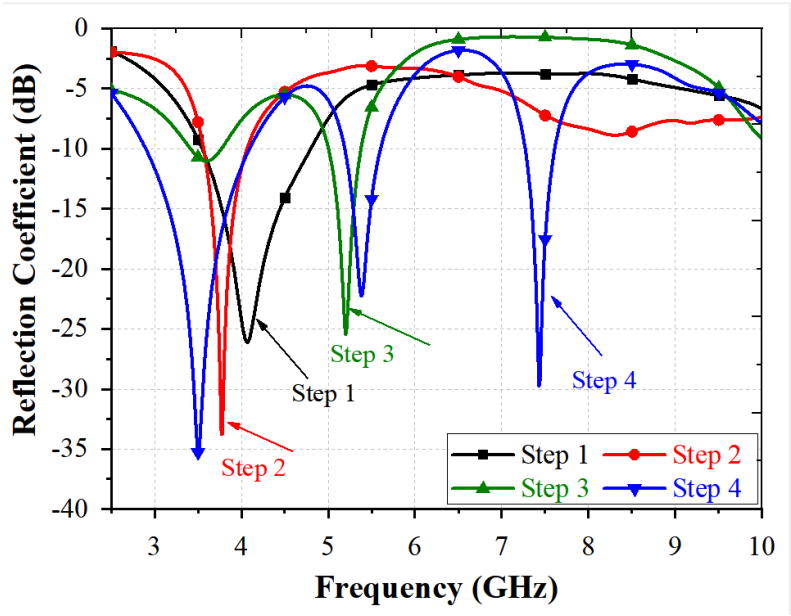

Figure 6.4 Evolution process in terms of reflection coefficient

Last but not the least, a new slot is added to assist in relocating the resonance frequency to the relevant frequency range. An additional resonance is appearing at 7.5 GHz, however for the respective thesis this is not the area of concern.

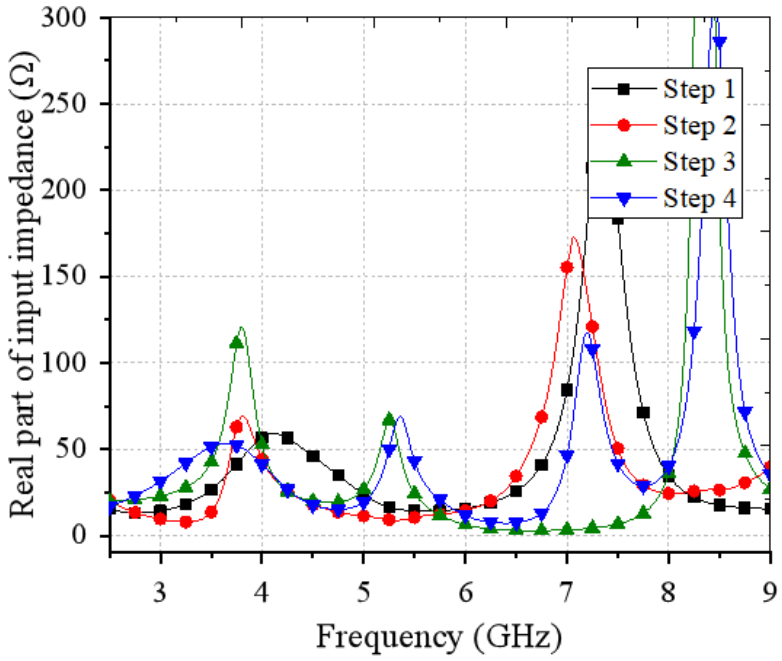

(a)

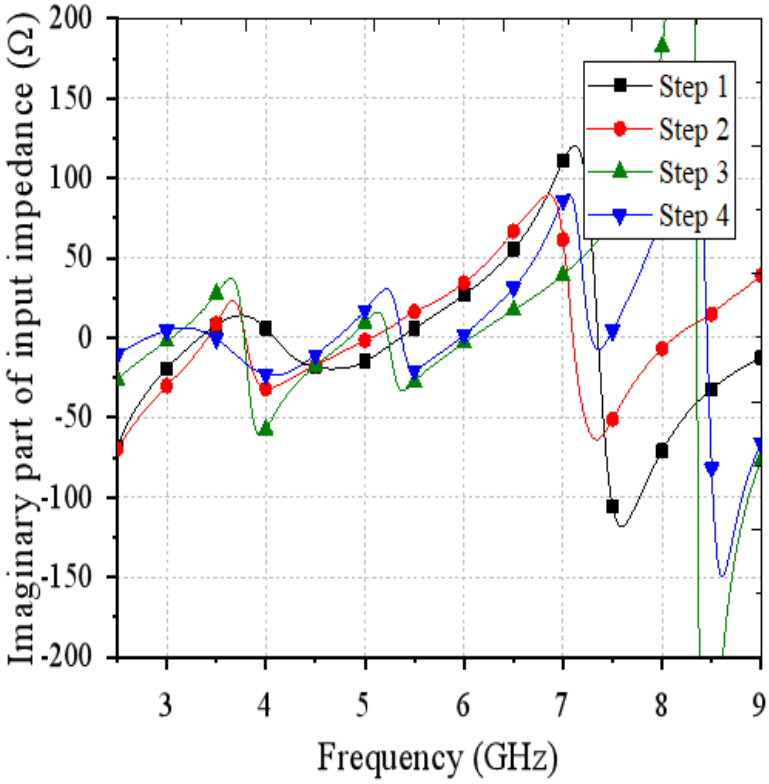

(b)

Figure 6.5 Input impedance of the different steps (a) real part (b) imaginary part

Input impedance of all the steps is depicted in Figure 6.5. At step one, the only excited mode operating at 4 GHz is the open slot mode, where the real component depicted in Figure 6.5(a) is around 50Ω and the imaginary part is approximately zero. The resonance frequency at the lower band is moved downward in step 2. This phenomenon occurred as the input impedance of antenna is altered as a result of the LC loading. The imaginary component decreases and the IFA frequency shifts to 5.4 GHz in step 3 as a result of capacitance, but the design still does not cover the target bands.So, the final stage includes the addition of slot 2. As a result, the IFA mode can be correctly tuned to the required band.

6.3.2 Operating principle

Two modes are produced by a single antenna. The slot mode comes first, followed by IFA mode. At 3.6 GHz, less amount of current is present at the open end and higher amount of current at the closed end of the slot (see Figure 6.6 (a)).

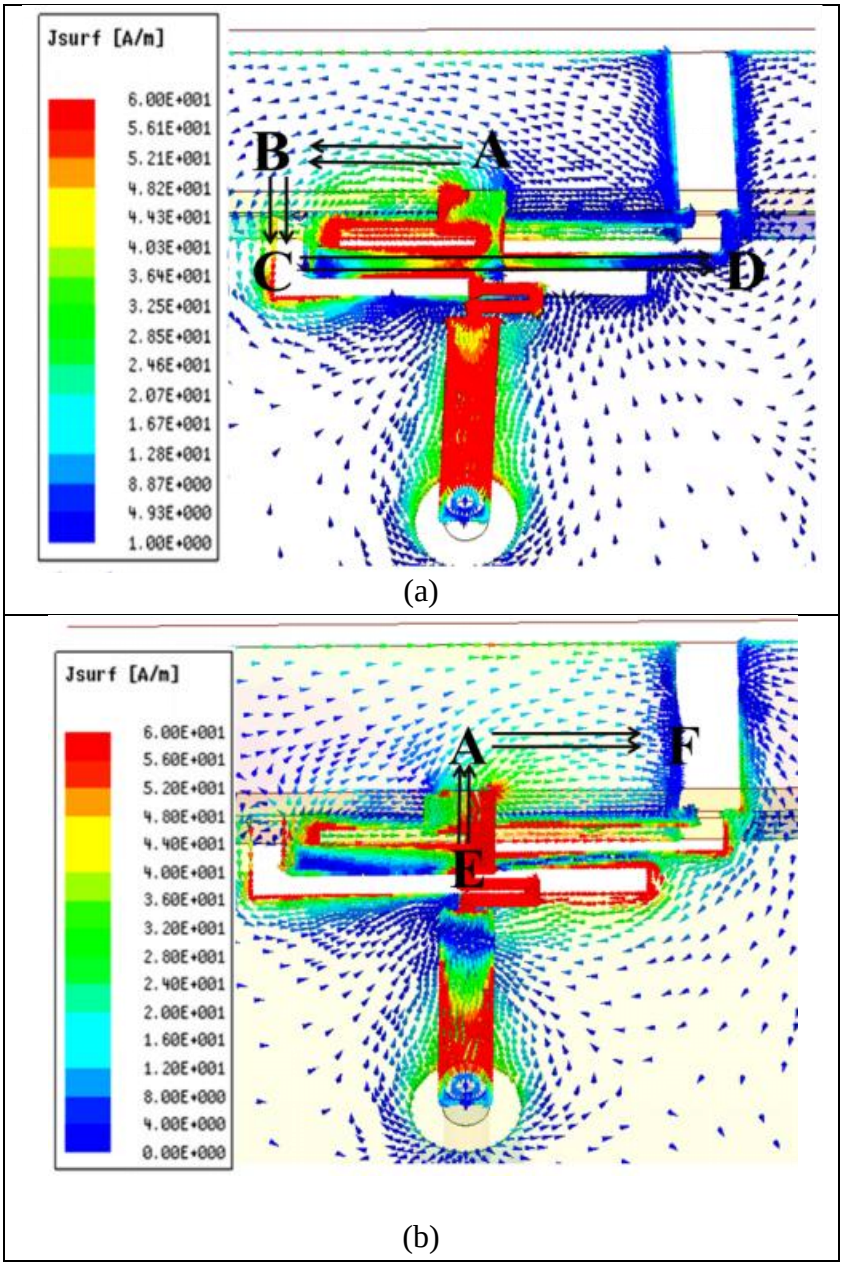

Figure 6.6 Distribution of current (a) 3.6 GHz (b) 5.5 GHz

The current route of length L, follows the path ABCD, where ABCD = 5.5 mm+3 mm+12.3 mm=20.8 mm≈ 0.25 λ. It is a open slot antenna operating at 0.25 wavelength. As demonstrated in Figure 6.6 (b), the 0.25 IFA mode is the cause of the second resonance. Points EAF are included in the present route.

It is crucial to comprehend how design factors affect the functionality of the antenna array. As a result, the suggested design must undergo a parametric analysis. The impact of changing the length L_1 of slot 1 (which is L_1 + L_3) is seen in Figure 6.7(a). The resonance frequency decreases as L_1 length increased.

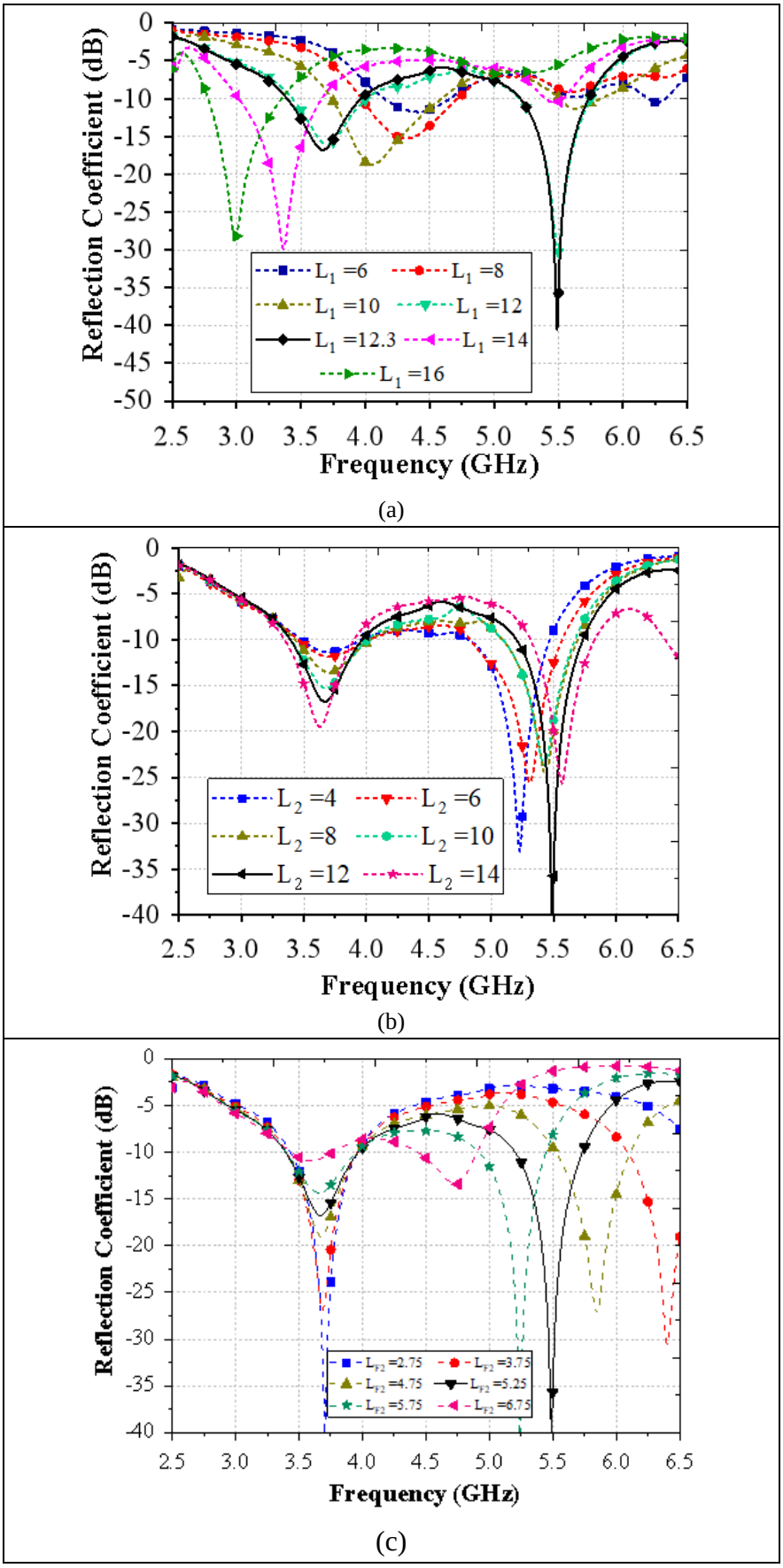

Figure 6.7(a) Length L_1 variation,(b)Variation in length L_2 when length L1 is 12.3 mm (c) Variation in Stub length L_F2 when length L_1 is 12.3 mm and L_2 is 12 mm.

Open slot mode produced by slot 1 is responsible for first resonance. At 0.25, the open slot resonant. However, because the FR4 substrate fills the open slot in this configuration, the slot resonates at 0.16 as a outcome of the loading effect. Figure 6.7 (b) shows the impact of changing the length of slot 2 ($L_2 + L_4$).

Feed line and metal-rim, are an essential component of the IFA mode. The second resonance's impedance is controlled by slot length L_2. Therefore, Figure 6.7(b) shows the impact of changing the length of L_2 on the second resonance. Unlike the metal rim's set length, the stub length can be altered. The metal rim's breadth and length are fixed. As the stub length varies, the capacitance between the metal rim and the stub will rise (see Figure 6.7(c)). As a result, capacitance will increase by lengthening the stub and push the second resonance frequency downward. The two frequencies can be tuned with this approach without having a major impact on the other resonant frequency.

6.4 FINDING AND ANALYSIS

As shown in Figure 6.8, a prototype is fabricated with thick FR-4 substrate (0.8 mm), utilizing PCB technology to validate the outcomes of simulations. Anechoic chamber testing is used to assess the manufactured prototype's radiation performance, and is depicted in Figure 6.11.

For the sake of simplicity, the antenna element's findings from antenna 1 to antenna 4 are reported, as there is symmetry in the placement of individual elements along two sides of PCB. The prototype's measured reflection coefficient is shown in Figure 6.9. The presented MIMO antenna system may operate between 3.4 to 3.8 GHz (with -10 dB impedance bandwidth) and between 5.19 to 5.8 GHz (with -6 dB impedance bandwidth).The predicted and observed results match well, but there is small deviation in the resonance freq -uencies due to fabrication tolerance and mismatch

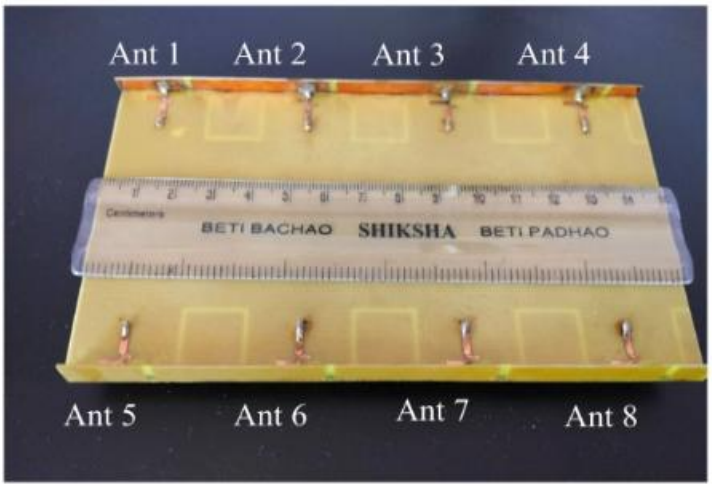

(a)

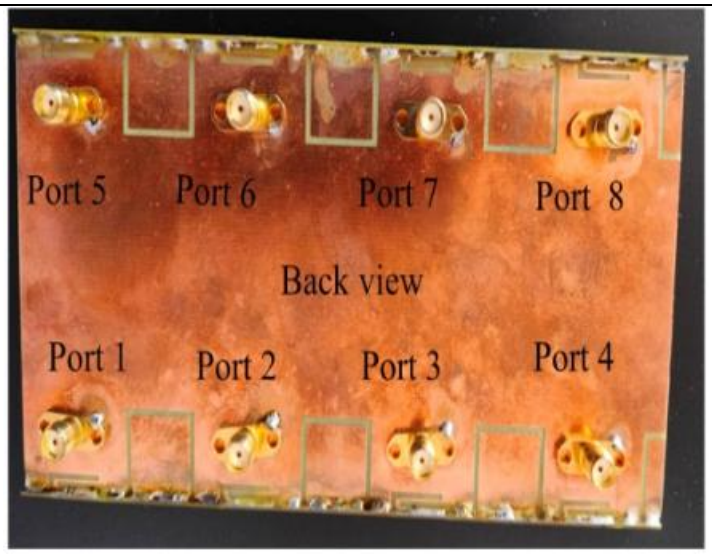

(b)

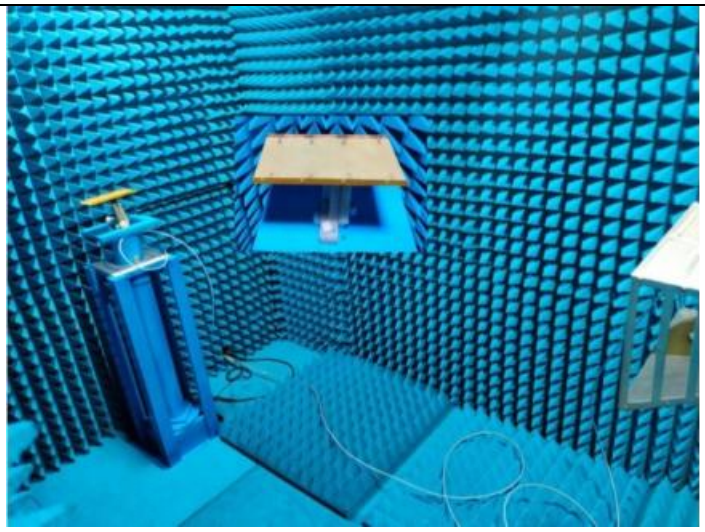

(c)

Figure 6.8 Fabricated prototype (a) side view (b) back view (c) Measurement setup in Anechoic chamber

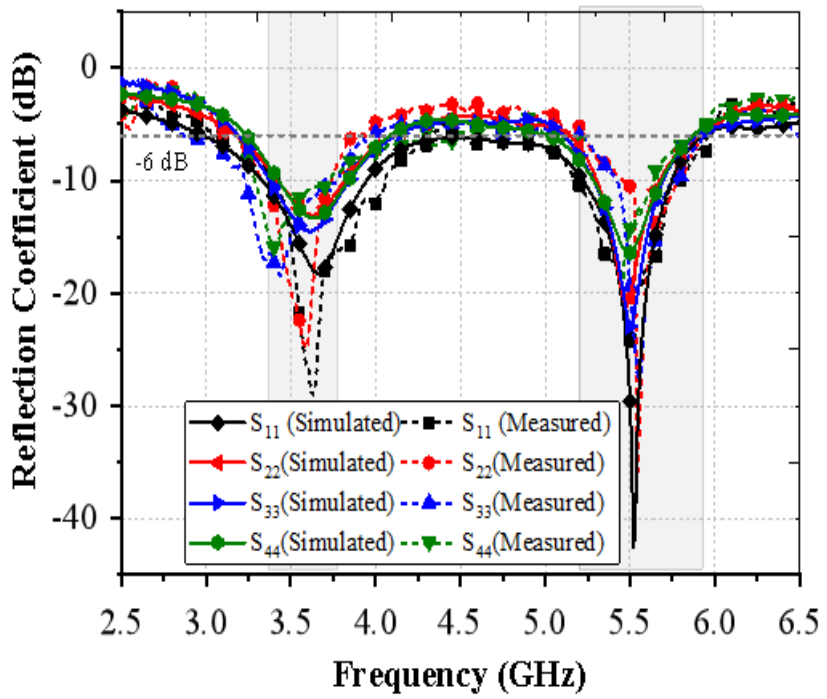

(a)

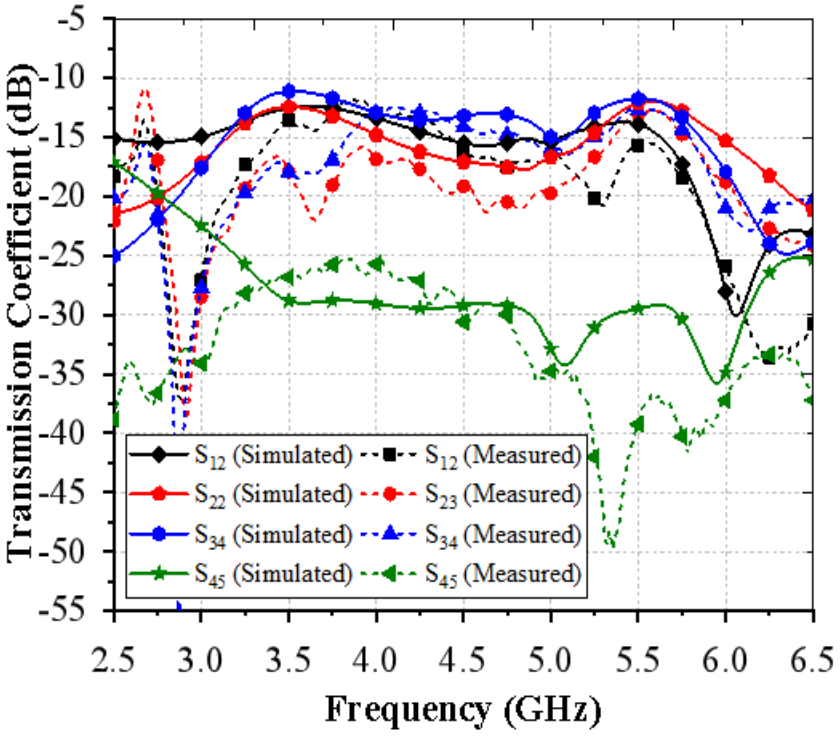

(b)

Figure 6.9 The suggested metal rim antenna array's (a) reflection coefficient and (b) mutual coupling measured.

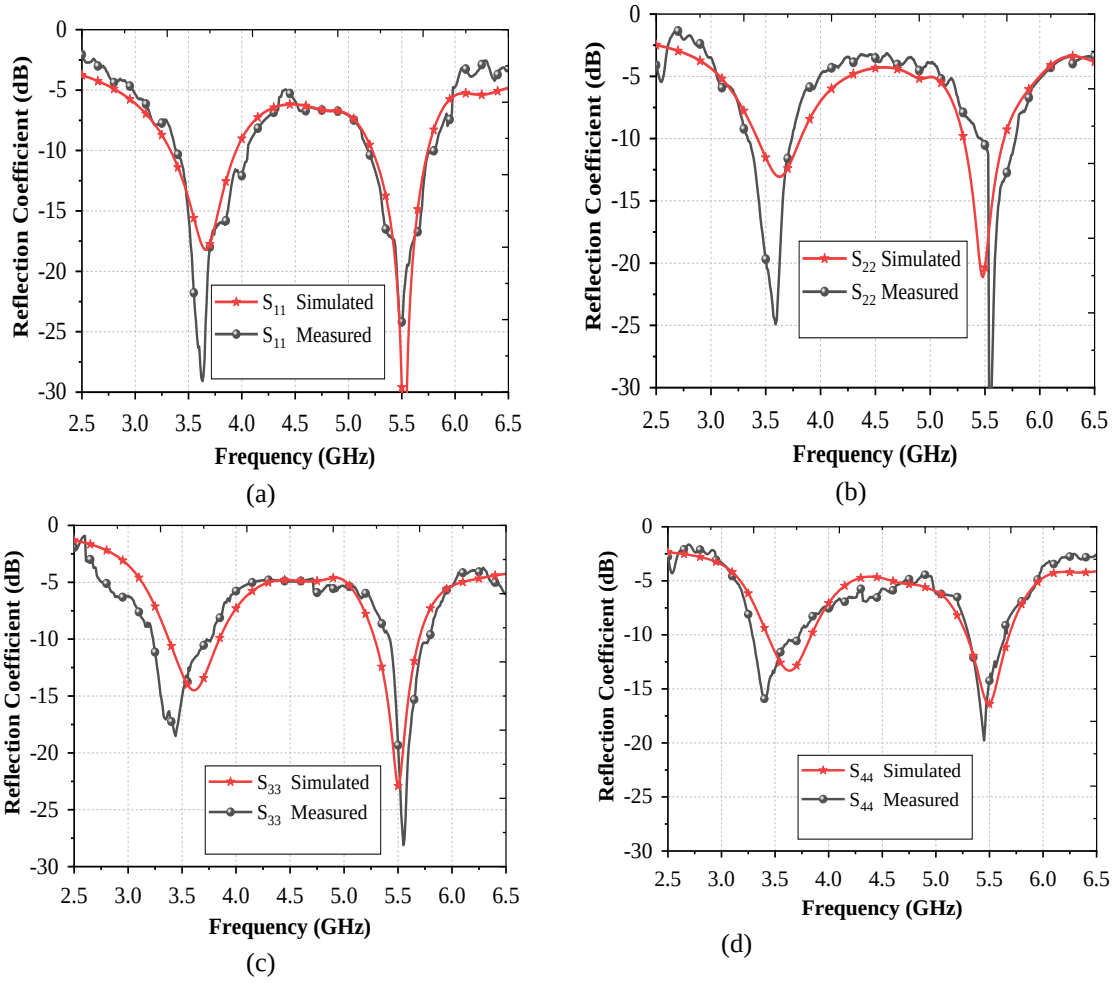

Figure 6.10 Comparison between simulated and measured results of proposed metal rimmed antenna

For better visualization of the result, comparison between measured and simulated results of proposed metal rimmed antenna is presented in Figure 6.10. Results of antenna 1, 2, 3 and 4 are presented in Figure 6.10 (a), (b), (c) and (d) respectively. It is clear from the figure that matching between the two results is decent.

6.4.1 Radiation performance analysis of proposed design

When compared to current recent techniques mentioned in literature, simulated efficiency of antenna is 80%-91%, which is quite good, according to Figure 6.11 overall efficiency graph. For the LTE 46 band, the simulated total efficiency ranges from 70% to 92 %.

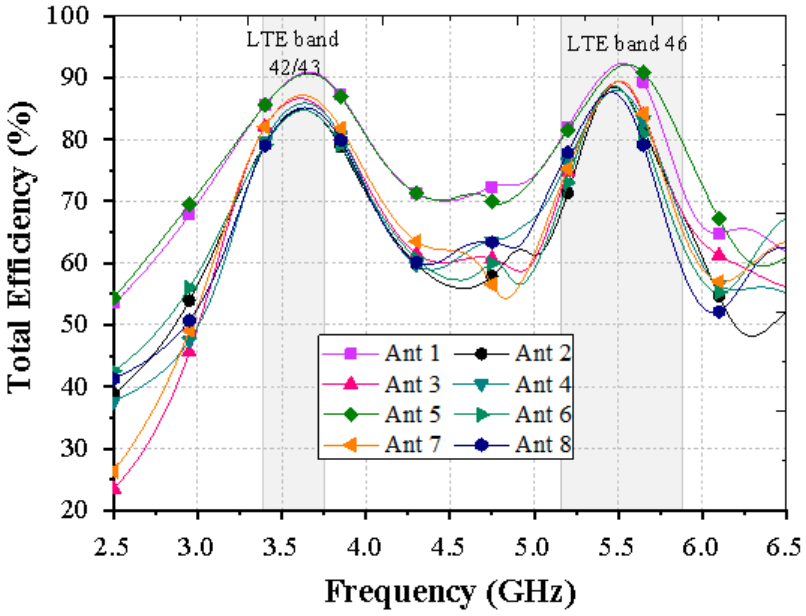

Figure 6.11 Simulated total efficiency

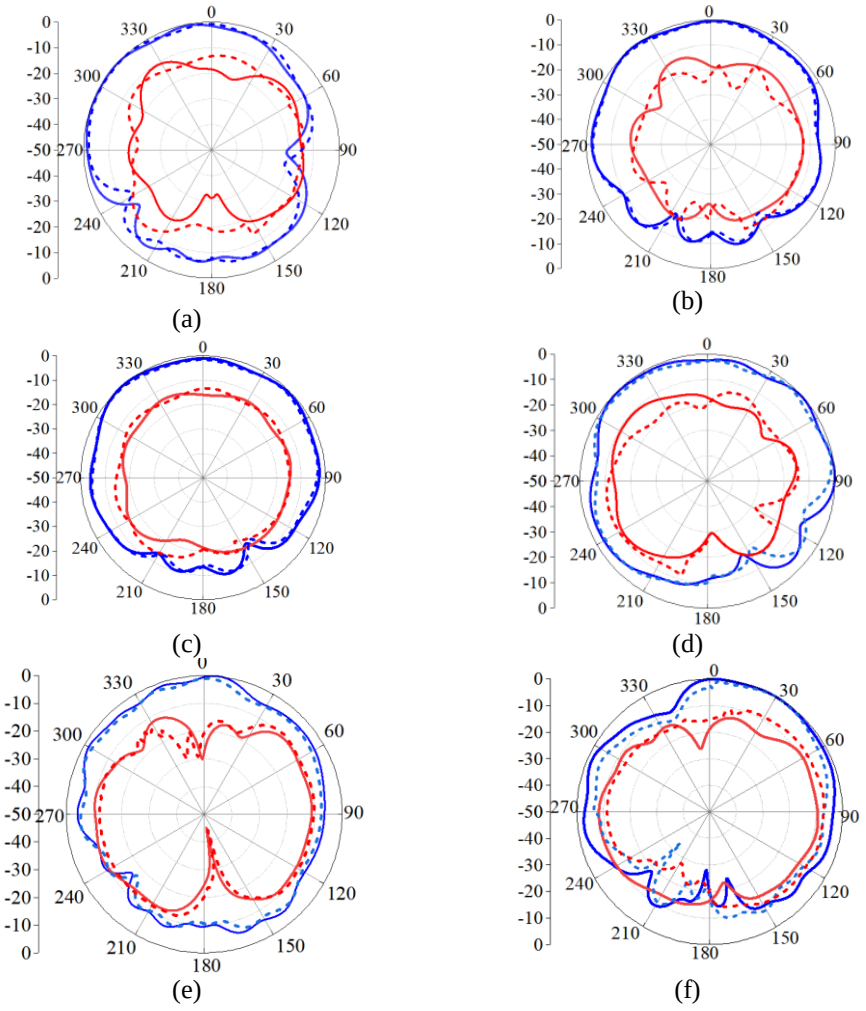

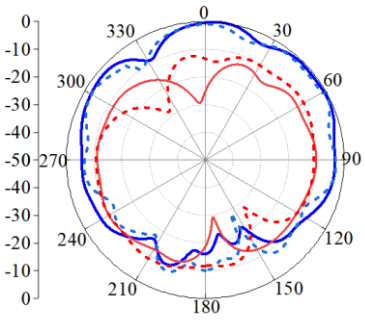
0
30
60
90
120
150
180
210
240
270
300
330
0
-10
-20
-30
-40
-50

(g)

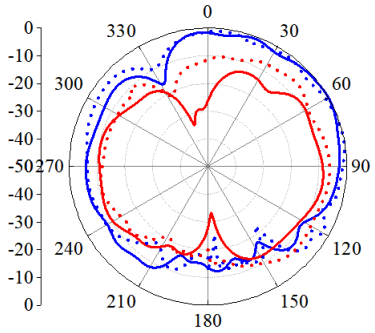
0
30
60
90
120
150
180
210
240
270
300
330
0
-10
-20
-30
-40
-50

(h)

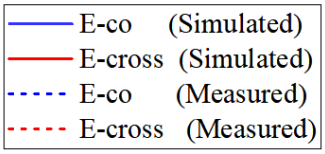
E-co (Simulated)
E-cross (Simulated)
E-co (Measured)
E-cross (Measured)

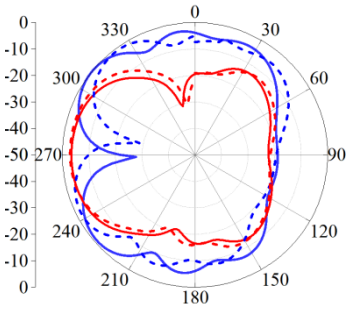
0
30
60
90
120
150
180
210
240
270
300
330
0
-10
-20
-30
-40
-50

(i)

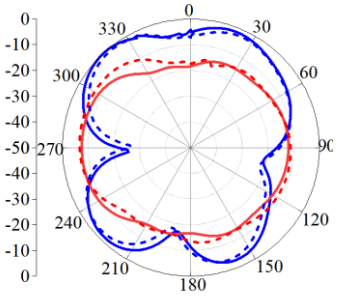
0
30
60
90
120
150
180
210
240
270
300
330
0
-10
-20
-30
-40
-50

(j)

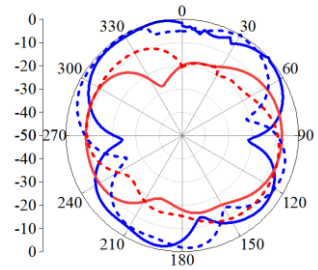
0
30
60
90
120
150
180
210
240
270
300
330
0
-10
-20
-30
-40
-50

(k)

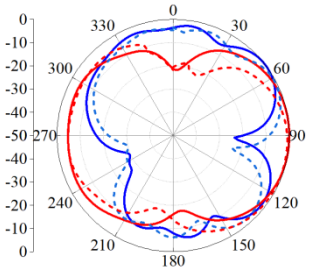
0
30
60
90
120
150
180
210
240
270
300
330
0
-10
-20
-30
-40
-50

(l)

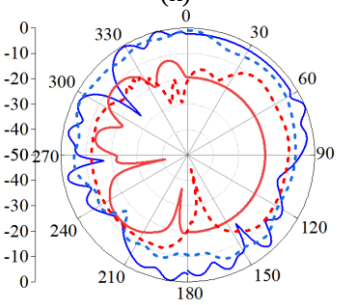
0
30
60
90
120
150
180
210
240
270
300
330
0
-10
-20
-30
-40
-50

(m)

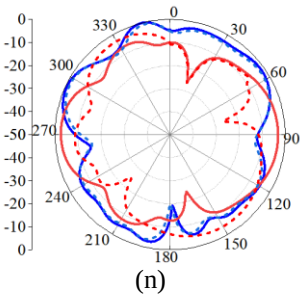
0
30
60
90
120
150
180
210
240
270
300
330
0
-10
-20
-30
-40
-50

(n)

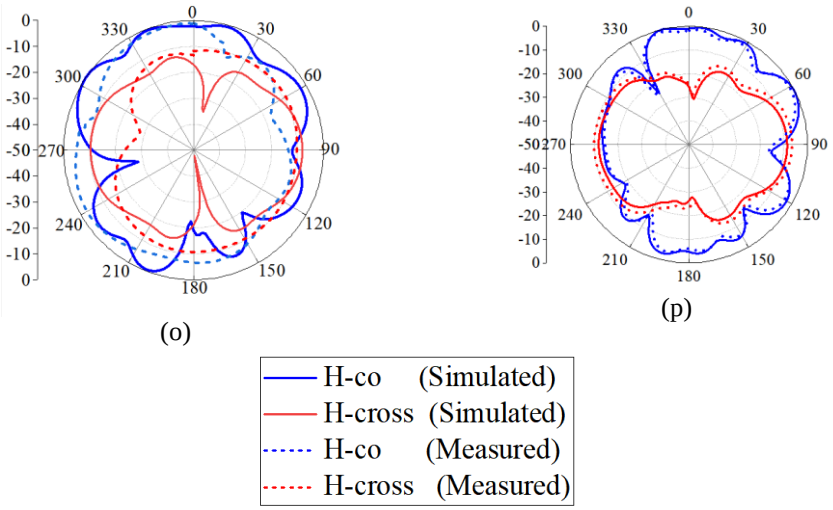

Figure 6.12: Measured and simulated 2D E-plane and H-plane radiation patterns of the proposed antenna elements at 3.6 GHz and 5.5 GHz. E-plane radiation patterns:(a–d) Ants 1–4 at 3.6 GHz,(e–h) Ants 1–4 at 5.5 GHz, .H-plane radiation patterns:(i–l) Ants 1–4 at 3.6 GHz, (m–p) Ants 1–4 at 5.5 GHz.

Figure 6.12 depicts the radiation patterns of antenna 1, 2, 3, and 4 at 3.6 GHz and 5.5 GHz, respectively for e-plane and h-plane. The recommended antenna elements have radiation characteristics that are almost omnidirectional with direction of maximum radiation pointing in different directions. The peak gain lies between 3 to 4.2 dBi. Although the general patterns of the two outputs are similar, there are minor differences in the two pattern due to the fabrication loss and other factors such as test environment are the main causes of this.

6.4.2 MIMO parameters response analysis

Diversity and multiplexing performance is presented in this section. The ECC of diverse antenna pairs is examined and shown in Figure 6.13. The calculated and simulated ECC values are below 0.15 and 0.05, respectively between antenna 1 and 2. It is below 0.05 and 0.1 for antenna 2 and 3. All components have ECC value under 0.15. Next, the ergodic channel capacity is investigated at high signal-to-noise ratios (SNRs), i.e., 20 dB. A Rayleigh fading environment was assumed to calculate the channel capacity. The following gives a description of the ergodic channel capacity C.

$$C = E\left\{log_2\left[det\left(I_N + \frac{\rho}{Nn_T}HH^H\right)\right]\right\} \tag{6.1}$$

Where E stands for expectation, channel matrix is H, (N×N), and average SNR is ρ/N, identity matrix is I_N, and transmitting antennas is n_T.

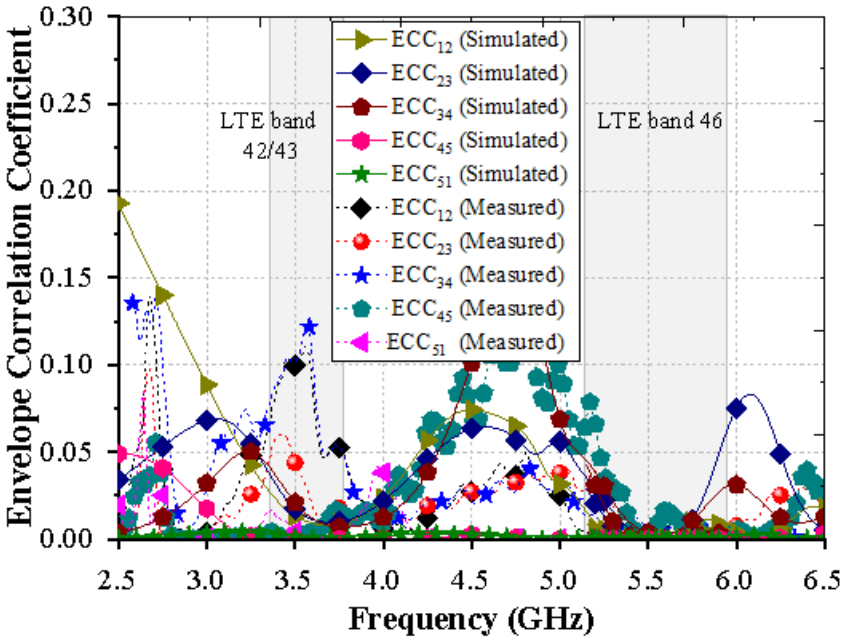

(a)

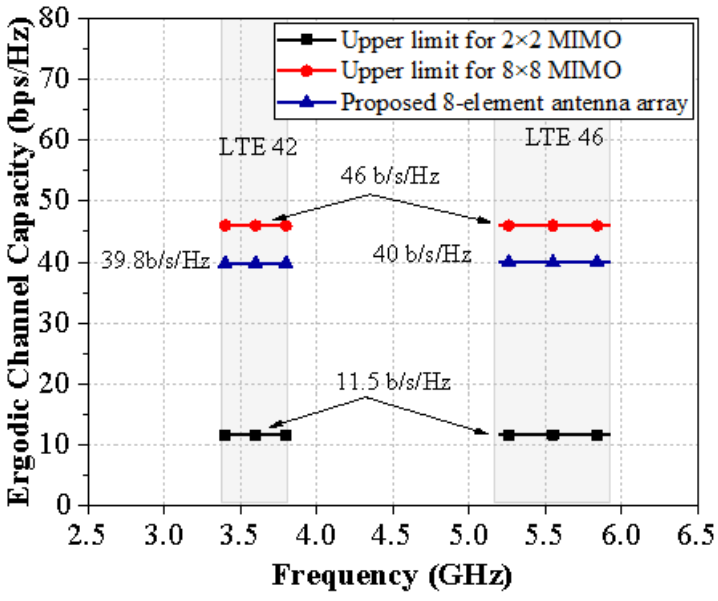

(b)

Figure 6.13 (a) Simulated and measured ECC (b) Ergodic channel capacity

The realized channel capacity in the lower and upper band is 39.8 b/s/Hz and 40 b/s/Hz respectively (shown in Figure 6.13 (b)).

The user hand can impact the antenna performance. Consequently, for use in real-world scenarios, the effect on antenna due to the presence of hand of user in the antenna vicinity is investigated (see Figure 6.14).

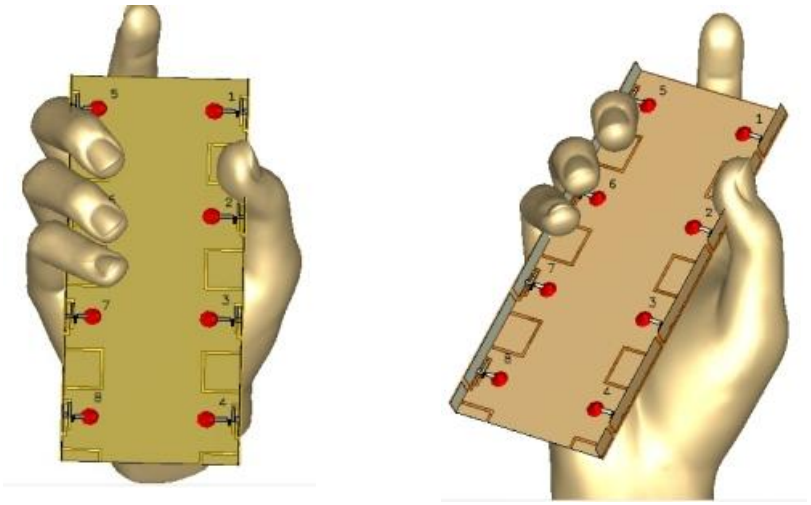

(a) (b)

Figure 6.14 Single hand mode (a) top, (b) side view

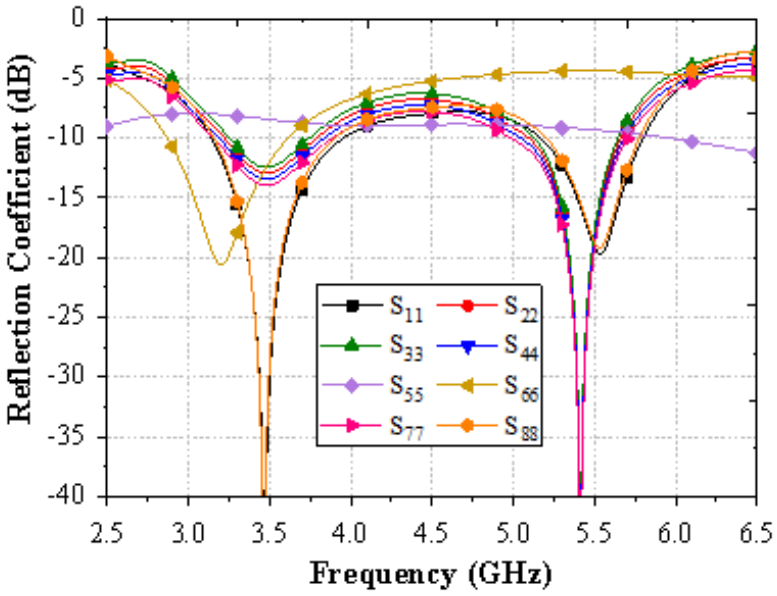

(a)

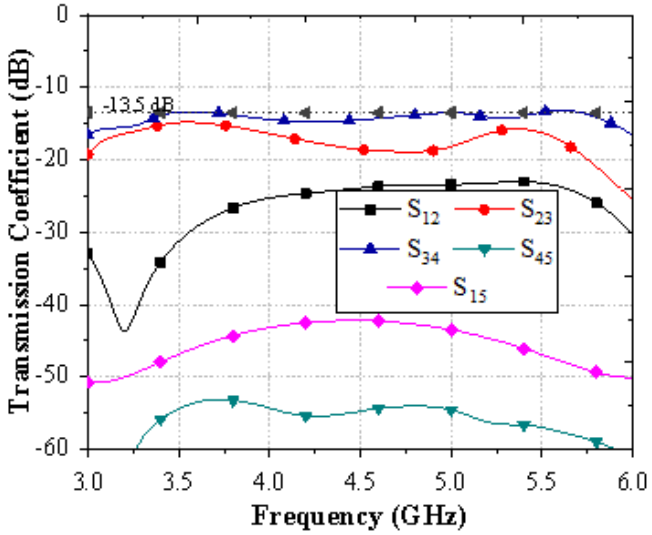

(b)

Figure 6.15 Simulation of S-parameters for a single-hand application (a) Reflection coefficients (b) Transmission coefficient

As seen in Figure 6.15, their performance is significantly reduced that are close to the user's finger and thumb. Even thought thumb is close to the Ant 2, open slot and the metal rim slots are not blocked by the thumb, so the Ant 2's performance is unaffected. The other antennas can preserve their dual band features due to the reason that the user's hand is not covering the other antennas. The design still provides isolation that is superior to 13.5 dB.

6.5 COMPARISON OF PROPOSED METAL-RIM ANTENNA WITH OTHER MIMO SYSTEM IN LITERATURE

In order to emphasize the benefits offered by the proposed design smartphones, modern techniques are evaluated to the suggested design in table 6.1. The designs that can provide a multiband response are suggested in references [121], [122], [88], [141], and [137]. Reference [121] does not emphasize covering the LTE 46 band, though. Despite covering the LTE 42 and 46 bands, [122] and [138] do not include the LTE 43 band. Future 5G phones will require all three of the bands. Additionally, because they were not created for metal rim cellphones, as designs in reference ([121], [122], and [138]) are not appropriate metal rim smartphones. Rest of the designs aside from these two is appropriate for 5G devices with metal rims.

Table 6.1: Comparison of recent 5G antenna's performance with proposed metal rimmed MIMO system

Ref	Operating band(GHz)	Metal Frame	Isolation (dB)	No. of antenna element	ECC	Peak Channel Capacity (b/s/Hz)	Efficiency of Antenna(%)
[121]	3.1-3.85,5.6-7.20 (-6 dB)	Without	>10	14	<0.15	60.6 70.5	>41,>61
[122]	3.3-3.55,4.2-6.2 (-10 dB)	Without	>15	8	<0.1	40.2	>58
[88]	2.496-2.69, 3.3-3.7 (-6 dB)	With	>10.5	8	<0.11	38.9	>41
[91]	3.4-3.6 (-6 dB)	With	>12.7	4	<0.13	-	>29.2
[141]	3.3-4.2,4.4-5, 5.15-5.95 (-6 dB)	With	>11	8	<0.1	40	>40
[142]	3.4-3.6 (-6 dB)	With	>10	8	<0.15	-	>42
[138]	3.4-3.6,5.12-5.925 (-10 dB)	Without	11.2	8	0.1	36.9	>51, >62
Proposed Design	**3.4-3.6, 3.6-3.8** (-10 dB) **5.15-5.925** (-6 dB)	**With**	**>11.5, >12**	**8**	**<0.15 <0.13**	**38.8, 40**	**>80 >70**

Reference [91] has only 4 antenna elements, hence high data rate demands may not be met by these designs in the future. The only 5G band that Reference [88] and [142] are operating with is one. Despite the fact that the citation [141] is intended for metal rimmed and encompasses all bands. However, the suggested design offers greater efficiency. The suggested design has a -10 dB impedance bandwidth, which is significantly less than the most recent work and covers the LTE42/LTE43 frequencies. Additionally, the proposed design's antenna efficiency is higher than other designs presented in Table 6.1.

6.6 CONCLUSION

A tri-band, highly efficient metal rim MIMO system that offers excellent overall efficiency and can operate in the 3.4 to 3.8 GHz and 5.1 GHz to 5.8 GHz frequency ranges is given in this study. The slot present in the metal rim serves two purposes. First is it providing the isolation between two neighboring antenna elements and second is that it helps in exciting the IFA mode. The slots in the metal-rim along with the U-shaped slots in the ground plane are used in the proposed MIMO system for isolation enhancement. The analysis of the proposed configuration shows that it is applicable to contemporary metal rimmed 5G smart phone applications.

Performance Comparison of the Latest 5G Smartphones with the Proposed Designs: Table 6.2. presents a performance comparison between the latest 5G smartphones and the proposed designs. The comparison is based on the number of bands covered, the number of antenna elements, and the thickness of the device (data readily available from the internet). To account for the outer cover (radome) of the smartphone, one millimeter is added to each design. It is evident from the table that the latest phones, such as the iPhone 16, have only four 5G antenna elements, while the proposed designs feature a minimum of eight antenna elements. While the smartphones in the comparison cover the sub-6 GHz band, only Design 4 supports the LTE-46 band. Additionally, the thickness of the proposed designs is significantly less than that of leading smartphones, demonstrating that the proposed designs achieve compactness—an essential factor for developing ultra-thin smartphones.

Table 6.2: Performance Comparison of Latest 5G Smartphones with Proposed Designs

Design	No of Antennas	Sub-6 GHz Band Coverage	Thickness (mm)
Design 1	12	LTE42/43	0.8 mm + 3 mm
Design 2	8	LTE42	3 mm + 1 mm
Design 3	8	LTE42/46	3.6 mm + 1 mm
Design 4	8	LTE42/43/46	7 mm + 1 mm
iPhone 16	4	LTE42/43	7.8 mm
Samsung Galaxy S24	4	Yes (Sub-6 GHz and mmWave)	7.6 mm
OnePlus 11R 5G	4	Yes (Sub-6 GHz and mmWave)	8.7 mm
Vivo T3 Lite	4	LTE42/43	8.4 mm

This thesis primarily focuses on the providing better solution for the future mobile phones. For this purpose different designs have been presented that provides unique solution to unique problem. Results obtained by the proposed system surpass those of the present state-of-the-art systems, according to a comparative validation of the proposed models with other designs presented in the literature. Even with all of the efforts made to create different methods and approaches to aid in the development of the antenna system for 5G smart phone applications, there is still need for more research. One of the methods involves using a neutralized line between antenna elements, which can create an additional coupling path to cancel out the coupled current from antenna 1 when excited. However, the length and width of the neutralized line must be chosen carefully to avoid mismatch, and optimizing these dimensions can indeed be a complex task. Space diversity is although effective, but is challenging to implement in mobile devices due to the physical space limitations and the necessity of maintaining at least $\lambda/2$ spacing between elements, which, is not feasible at 3.5 GHz for a compact smartphone.

In Design 1, four antennas were placed on the shorter side, and eight antennas were placed on the longer side of the device. This configuration, coupled with polarization diversity, effectively reduced mutual coupling without the need for additional space-consuming decoupling structures. Therefore, achieving decent isolation without decoupling structures was one of the key contributions [148] of all the design proposed in the thesis.

Moreover, there are additional methods found in the literature, such as the use of cross-line fences [149], in-phase and out-of-phase excitation modes [34], wave trap methods [150], and slotted elements in the ground plane [151], all of which offer potential solutions for reducing mutual coupling. However, as discussed in the chapters, these methods often require additional physical space or modifications to the antenna structure, which can lead to an increase in the overall profile of the device.

CHAPTER 7

CONCLUSION AND FUTURE SCOPE

CHAPTER 7

CONCLUSION AND FUTURE SCOPE

In the world of rapidly advancing technology, the quest for faster and more efficient wireless communication has led to groundbreaking developments. Fourth generation was no longer capable to deal with with the demand of higher datarates. Fifth generation of mobile communication can provide the user with higher datarate and low latency. MIMO technology is the most suitable option for datarate enhancement in sub6-GHz range.

This thesis covers various designs to achieve the demand of 5G smartphone applications. One such development is the investigation of a twelve-element MIMO antenna system using a slot antenna for LTE 42/43 bands. This novel MIMO antenna system has shown promising results in fulfilling the needs of 5G smartphones. By utilizing orthogonal placement and embracing the concept of space diversity, the isolation of 14.8 dB is achieved. This means that interference between the antenna elements is minimized, providing a more reliable and efficient communication experience. With an ECC of less than 0.05, ensures a high level of accuracy and reliability in data transmission. Moreover, the MIMO system boasts an impressive channel capacity of 61.9 b/s/Hz, enabling faster and smoother data transfer. The proposed MIMO antenna system is poised to meet the demanding needs of 5G smartphones.

As the era of 5G smartphones dawns upon us, the demand for ultra slim mobile phones continues to grow. Side-edge of the smartphone was seen as a new place to install antenna elements. The proposed design is a compact loop-based MIMO system that can fit into an ultrathin smartphone. which covers the LTE-42 band. The size of the side-frame needed to mount the antenna components is just 9.5 × 3 mm2. This indicates that, when compared to the design offered in the literature, it is the smallest size attained to date and can fit in the 3 mm high side frame. With a respectable isolation of 14.8 dB, the structure resonates at 3.5 GHz.

Further, in order to create dual band MIMO system, simple T-shaped designs are used that works on LTE 42/43 bands. The antenna components are mounted on side frames measuring only 150 mm by 3.6 mm in the proposed design. In each of the

interest bands, the ECC is less than 0.075 and isolation is better than 14 dB. The total antenna efficiency in the LTE 42/46 bands is more than 60%. Size reduction, improved isolation, and simultaneous dual band coverage are all improved by the proposed MIMO antenna system. Several components have been explored to assess the effectiveness of the proposed design that includes investigating the performance of the proposed design after installing side frames, and batteries also the effect of user hand.

There are a lot of materials used to design the body of the smartphone. Few examples can be metal, glass or plastic body. Among which metal is that element that can severely affect the performance of antenna. However metalrim smartphones are still widely used as it provide needed mechanical strength to the overall design. Another MIMO antenna system has been developed for metalrim smartphones by using combination of IFA and slot antenna.There are two uses for the slot in the metal rim. It first offers separation between two nearby antennas. Secondly, it facilitates the activation of the IFA mode. The design covers tri-band (LTE42/43/46), 3.4 to 3.8 GHz and 5.1 GHz to 5.8 GHz frequency bands. It also delivers good total efficiency of 80 % and 70 % efficiency at LTE42/43 and LTE 46 bands respectively.

Due to spatial constraints, the need to meet aesthetic requirements and the widespread demand for full edge-to-edge displays with metal bezels in today's handheld devices, integrating all necessary antennas is highly challenging. This doctoral thesis presents solutions to optimize the use of available space in mobile devices.

Table 7.1 clearly indicate the Design-1 (D1) introduces a compact twelve-element MIMO slot antenna system that enhances channel capacity while reducing mutual coupling. The space limitation in mobile devices is addressed in Design-2 (D2) and 3 by relocating the antenna to a novel position — the side edge of the PCB. Although this location poses challenges, such as the potential for a bulky device due to large antenna size, miniaturized structures with good performance are demonstrated in both Design-2 and 3. Design-2 employs a loop antenna as the base element for an eight-element MIMO system, while Design-3 uses a monopole structure. Notably, adequate isolation is achieved without the use of decoupling structures, making the designs more suitable for cost-effective mass production.

Since smartphones are consumer electronics, their visual appearance is critical in the design process. Consumers have extensive preference of smartphones with edge-to-edge screens and metal rims, making antenna integration even more difficult. Design-4 (D4) presents a MIMO system specifically designed for smartphones with metal rims.

The main contribution of Design-2 (D2) is the miniaturized antenna design for ultra-thin smartphones, while Design-2 (D2), D3, and D4 demonstrate integration of multiple 5G communication bands.

As space in mobile devices becomes increasingly limited, the solutions proposed in this thesis offer viable approaches to antenna integration. These approaches are also applicable to future sixth-generation (6G) mobile technologies, which will face similar design constraints

Table 7.1 Performance Summary of MIMO Antenna Designs

Ref	WB (GHz)	Iso. (dB)	SF/MR (L × H*)	MO	ECC	CC (b/s/Hz)	AE (%)
D1	3.3–3.8	>14.8	No / No	12	<0.1	61.9	>74
D2	3.4–3.6	>14.8	150 × 3 / No	8	<0.1	41	>62
D3	3.4–3.6, 5.15–5.925	>14, >17.5	150 × 3.6 / No	8	<0.075, <0.05	41, 43.6	>60
D4	3.4–3.6, 3.6–3.8 (–10 dB); 5.15–5.925 (–6 dB)	>11.5, >12	150 × 7/ Yes	8	<0.15, <0.13	38.8, 40	>80, >70

Ref: Design Reference, WB: Working Band, Iso.: Isolation, SF/MR: Side Frame / Metal Rim (Length × Height in mm), MO: MIMO Order, ECC: Envelope Correlation Coefficient, CC: Channel Capacity, AE: Antenna Efficiency

The following list contains the topics that this research project may investigate in the future.

- The work present in the thesis is limited to the implementation of MIMO antenna system for sub-6 GHz range only. Extension of the research work on millimeter wave is yet to be performed as this frequency range is also a part of

5G band and as the demand of higher data-rate increase the sub-6 GHz range band assigned for 5G communication may no longer will be able to fulfil this high demand. By exploring the antenna designs that can work on these bands can lead to future increase the datarate.

- Addressing isolation and efficiency problems causing a poor performing MIMO system, ultimately leading to performance degradation of any antenna system.

- As the study primarily focuses on the MIMO operation in the sub-6 GHz frequency range, which is predominantly used for data transmission, This thesis did not include the effect of the user's head, as it is not relevant during data mode usage. In talk mode, the phone is typically held near the user's head, but the multi-port MIMO operation is designed for data transmission, where the antenna performance is primarily influenced by the proximity of the user's hand, rather than the head. This is why the effects of the user's head were excluded in our study, as it falls outside the scope of sub-6 GHz MIMO performance in data mode . However it can be done in future to study the safety aspect of the designs

- Deployment of deep learning based antenna designing approach to provide better optimization to the design parameters.
- Incorporating emerging technologies such as beamforming and machine learning algorithms could greatly enhance the optimization of antenna performance, especially in dynamic environments. Hence exploration of these cutting-edge technologies specifically, beamforming techniques can be employed to improve signal strength and directivity, enhancing the performance of antenna systems, especially in complex environments. Additionally, machine learning algorithms could be applied for real-time optimization of antenna parameters, allowing for adaptive and intelligent performance adjustments based on varying environmental conditions and user requirements.
- Also environmental effect such as temperature and moisture on the performance of proposed designs are not discussed in this thesis.
- Although the demand of higher data rate is never ending next generation after 5G will continue to work on more better and sophisticated designs to enable ultra low latency communication [144].

LIST OF PUBLICATIONS

LIST OF PUBLICATIONS

JOURNALS

1) V. Thakur, N. Jaglan and S.D. Gupta, "Design of a Dual-band 12-Element MIMO Antenna Array for 5G Mobile Applications," *Progress in Electromagnetics Research Letters*,vol.95, pp. 73-81, 2021 . doi: *10.2528/PIERL20102004*

(ESCI/Scopus)

2) V. Thakur, N. Jaglan and S.D. Gupta, "Side Edge Printed Eight-element Compact MIMO Antenna Array for 5G Smartphone Applications," *Journal of Electromagnetic Waves and Applications*, pp. 1-17, Feb 2022. doi: 10.1080/09205071.2022.2040057

(SCI with impact factor: 1.3)

3) V. Thakur and N. Jaglan, "Metal rimmed 8-Element Multi-band MIMO System with high efficiency for Modern 5G Smartphones," *InternationalJjournal of Microwave and Wireless Technologies, Cambridge University Press*, pp,1-11, June,2023. doi:10.1017/S1759078723000661

(SCI with impact factor: 1.4)

4) V. Thakur and N. Jaglan, "A T-Shaped compact dual-band MIMO antenna system for 5G smartphone applications," *Wireless Networks*, Nov 2023. doi:https://doi.org/10.1007/s11276-023-03597-x
(SCI with impact factor: 3)

CONFERENCES

1) V. Thakur, N. Jaglan and S. D. Gupta, "A Review on Antenna Design for 5G Applications," 2020 6th International Conference on Signal Processing and Communication (ICSC), Noida, India, 2020, pp. 266-271, doi: 10.1109/ICSC48311.2020.9182774.

2) V. Thakur, N. Jaglan and S. D. Gupta, "Compact ten element antenna array for thin 5G smartphone applications," 2021 6th International Conference on Signal Processing, Computing and Control (ISPCC), Solan, India, 2021, pp. 29-33, doi: 10.1109/ISPCC53510.2021.9609508

3) V. Thakur and N. Jaglan, "Eight-Element Low-Profile MIMO System for Thin 5G Smartphone Applications," 2023 9th International Conference on Signal Processing and Communication (ICSC), NOIDA, India, 2023, pp. 557-561, doi: 10.1109/ICSC60394.2023.10441208.

REFERENCES

REFERENCES

[1] N. Bhandari, S.Devra and K.Singh, “Evolution of Cellular Network: From 1G to 5G,”*International Journal of Engineering and Technique,* Vol. 3 Issue 5, Sep - Oct 2017.

[2] K. Pandya , “Comparative Study on Wireless Mobile Technology: 1G, 2G, 3G, 4G and 5G,” *IJRTER,* vol. 1, no.1, pp. 24-7, 2015

[3] S.Koul, Shiban & G.S, Karthikeya & A. Poddar, “ Compact Antennas for Future 5G Smartphones”*Microwave journal,* pp.3-28, 2021.

[4] He *et al.,* "D2D-V2X-SDN: Taxonomy and Architecture Towards 5G Mobile Communication System," in *IEEE Access,* vol. 9, pp. 155507-155525, 2021, doi: 10.1109/ACCESS.2021.3127041.

[5] M. S. Sharawi, A. T. Hassan, and M. U. Khan, “Correlation coefficient calculations for MIMO antenna systems: A comparative study,” Int. J. Microw. Wireless Technol., vol. 9, no. 10, pp. 1991–2004, 2017.

[6] M. S. Sharawi, “Current misuses and future prospects for printed multiple-input, multiple-output antenna systems,” IEEE Antennas Propag. Magn., vol. 59, no. 2, pp. 162–170, Apr. 2017.

[7] R. Tian, B. K. Lau, and Z. Ying, “Multiplexing efficiency of MIMO antennas,” IEEE Antennas Wireless Propag. Lett., vol. 10, pp. 183–186, 2011.

[8] M. S. Sharawi, “Printed multi-band MIMO antenna systems and their performance metrics [wireless corner],” IEEE Antennas Propag. Mag., vol. 55, no. 5, pp. 218–232, Oct. 2013.

[9] M. A. Jensen and J. W. Wallace, ‘‘A review of antennas and propagation for MIMO wireless communications,’’ IEEE Trans. Antennas Propag., vol. 52, no. 11, pp. 2810–2824, Nov. 2004.

[10] T. Svantesson, ‘‘Correlation and channel capacity of MIMO systems employing multimode antennas,’’ IEEE Trans. Veh. Technol., vol. 51, no. 6, pp. 1304–1312, Nov. 2002

[11] S. Zhang, S. Khan, and S. He, ‘‘Reducing mutual coupling for an extremely closely-packed tunable dual-element PIFA array through a resonant slot antenna formed in-between,’’ IEEE Trans. Antennas Propag., vol. 58, no. 8, pp. 2771–2776, Aug. 2010.

[12] J.-Y. Lee, S.-H. Kim, and J.-H. Jang, ‘‘Reduction of mutual coupling in planar multiple antenna by using 1-D EBG and SRR structures,’’ IEEE Trans. Antennas Propag., vol. 63, no. 9, pp. 4194–4198, Sep. 2015.

[13] J. L. Guo, L. Cui, C. Li, and B. H. Sun, ‘‘Side-edge frame printed eight-port dual-band antenna array for 5G smartphone applications,’’ IEEE Trans. Antennas Propag., vol. 66, no. 12, pp. 7412–7417, Dec. 2018.

[14] D. Gangwar, J. Malik and A. Patnaik, "Enhanced Isolation 4×4 MIMO Antennas on Cross-Substrate for Vehicular Communications," in *IEEE Antennas and Wireless Propagation Letters*, vol. 22, no. 11, pp. 2715-2719, Nov. 2023, doi: 10.1109/LAWP.2023.3314212.

[15] S. Kumar *et al*., "Wideband Circularly Polarized Textile MIMO Antenna for Wearable Applications," in *IEEE Access*, vol. 9, pp. 108601-108613, 2021, doi: 10.1109/ACCESS.2021.3101441.

[16] P. Mondal, D. Dhara and A. R. Harish, "A Partially Reflective FSS-Based Superstrate as a Decoupling Structure for Reducing the Mutual Coupling of Circularly Polarized Antennas," in *IEEE Transactions on Antennas and Propagation*, vol. 72, no. 4, pp. 3652-3661, April 2024, doi: 10.1109/TAP.2024.3364750.

[17] M. Agarwal and M. K. Meshram, "Isolation improvement of 5 GHz WLAN antenna array using metamaterial absorber,"*2016 URSI Asia-Pacific Radio Science Conference (URSI AP-RASC)*, Seoul, Korea (South), 2016, pp. 1050-1053, doi: 10.1109/URSIAP-RASC.2016.7601144.

[18] C.Mao, M. Khalily, R. Tafazolli and A. Kishk, "Wideband Dual Circularly Polarized Helical Antenna With Reduced Mutual Coupling for MIMO Applications," in *IEEE Transactions on Antennas and Propagation*, vol. 72, no. 4, pp. 3766-3771, April 2024, doi: 10.1109/TAP.2024.3367499

[19] I. Ahmed, M. A. Abdalla, A. B. A-Rahman, and H.FA Hamed. "Compact MIMO antenna with optimized mutual coupling reduction using DGS." International Journal of Microwave and Wireless Technologies 6, no. 2 ,pp.173-180,2014.

[20] A. K. Gautam, L. Kumar, B. K. Kanaujia and K. Rambabu, "Design of Compact F-Shaped Slot Triple-Band Antenna for WLAN/WiMAX Applications," in *IEEE Transactions on Antennas and Propagation*, vol. 64, no. 3, pp. 1101-1105, March 2016, doi: 10.1109/TAP.2015.2513099.

[21] M. Harbel, J. Zbitou, M. Hefnawi and M. Latrach, "Mutual Coupling Reduction in MmWave Patch Antenna Arrays Using Mushroom-like EBG Structure,"*2020 IEEE 2nd International Conference on Electronics, Control, Optimization and Computer Science (ICECOCS)*, Kenitra, Morocco, 2020, pp. 1-3, doi: 10.1109/ICECOCS50124.2020.9314440.

[22] K. L. Wong and J.Y. Lu, "3.6-GHz 10-antenna array for MIMO operation in the smartphone," Microwave Opt. Technol. Lett., vol. 57, no. 7, pp. 1699–1704, Apr. 2015.

[23] N. O. Parchin *et al*., "Eight-Element Dual-Polarized MIMO Slot Antenna System for 5G Smartphone Applications," in *IEEE Access*, vol. 7, pp. 15612-15622, 2019, doi: 10.1109/ACCESS.2019.2893112.

[24] J. Huang and J. Liu, "Six-Element MIMO Slot Antenna for 5G Metal-Frame smartphones,"*2020 13th UK-Europe-China Workshop on Millimetre-Waves and Terahertz Technologies (UCMMT)*, Tianjin, China, 2020, pp. 1-2, doi: 10.1109/UCMMT49983.2020.9296032.

[25] N. O. Parchin *et al*., "A New Multiple Slot Antenna System for Sub 6 GHz Smartphones,"*2022 International Telecommunications Conference (ITC-Egypt)*, Alexandria, Egypt, 2022, pp. 1-4, doi: 10.1109/ITC-Egypt55520.2022.9855691.

[26] I. Ishteyaq, I. S. Masoodi and K. Muzaffar, "Six-Element MIMO Antenna With Slot Ring Radiators for Future 5G Hand-Held Mobile Applications,"*2020 IEEE*

Bangalore Humanitarian Technology Conference (B-HTC), Vijiyapur, India, 2020, pp. 1-4, doi: 10.1109/B-HTC50970.2020.9298006.

[27] M. Ikram, N. Nguyen-Trong and A. Abbosh, "Hybrid Antenna Using Open-Ended Slot for Integrated 4G/5G Mobile Application," in *IEEE Antennas and Wireless Propagation Letters*, vol. 19, no. 4, pp. 710-714, April 2020, doi: 10.1109/LAWP.2020.2978181.

[28] D. Q. Liu, M. Zhang, H. J. Luo, H. L. Wen and J. Wang, "Dual-Band Platform-Free PIFA for 5G MIMO Application of Mobile Devices," in *IEEE Transactions on Antennas and Propagation*, vol. 66, no. 11, pp. 6328-6333, Nov. 2018, doi: 10.1109/TAP.2018.2863109.

[29] C. -Y. -D. Sim, H. -Y. Liu and C. -J. Huang, "Wideband MIMO Antenna Array Design for Future Mobile Devices Operating in the 5G NR Frequency Bands n77/n78/n79 and LTE Band 46," in *IEEE Antennas and Wireless Propagation Letters*, vol. 19, no. 1, pp. 74-78, Jan. 2020, doi: 10.1109/LAWP.2019.2953334.

[30] Q. Cai, Y. Li, X. Zhang and W. Shen, "Wideband MIMO Antenna Array Covering 3.3–7.1 GHz for 5G Metal-Rimmed Smartphone Applications," in *IEEE Access*, vol. 7, pp. 142070-142084, 2019, doi: 10.1109/ACCESS.2019.2944681.

[31] D. Q. Liu, H. J. Luo, M. Zhang, H. L. Wen, B. Wang and J. Wang, "An Extremely Low-Profile Wideband MIMO Antenna for 5G Smartphones," in *IEEE Transactions on Antennas and Propagation*, vol. 67, no. 9, pp. 5772-5780, Sept. 2019, doi: 10.1109/TAP.2019.2908261.

[32] W. -F. Zeng, F. -C. Chen and Q. -X. Chu, "Bandwidth-Enhanced 5G Mobile Phone Antenna Pair With Tunable Electric Field Null," in *IEEE Transactions on Antennas and Propagation*, vol. 71, no. 2, pp. 1960-1964, Feb. 2023, doi: 10.1109/TAP.2022.3232748.

[33] Z. Ji *et al*., "Low Mutual Coupling Design for 5G MIMO Antennas Using Multi-Feed Technology and Its Application on Metal-Rimmed Mobile Phones," in *IEEE Access*, vol. 9, pp. 151023-151036, 2021, doi: 10.1109/ACCESS.2021.3126640.

[34] W. Hu *et al*., "Dual-Band Antenna Pair With High Isolation Using Multiple Orthogonal Modes for 5G Smartphones," in *IEEE Transactions on Antennas and Propagation*, vol. 71, no. 2, pp. 1949-1954, Feb. 2023, doi: 10.1109/TAP.2022.3233458.

[35] D. Serghiou, M. Khalily, V. Singh, A. Araghi and R. Tafazolli, "Sub-6 GHz Dual-Band 8 × 8 MIMO Antenna for 5G Smartphones," in *IEEE Antennas and Wireless Propagation Letters*, vol. 19, no. 9, pp. 1546-1550, Sept. 2020, doi: 10.1109/LAWP.2020.3008962.

[36] M. Bridges, M. Khalily, M. Abedian, D. Serghiou, P. Xiao and R. Tafazolli, "High Isolation 8×8 MIMO Antenna Design for 5G Sub-6 GHz Smartphone Applications,"*2020 International Conference on UK-China Emerging Technologies (UCET)*, Glasgow, UK, 2020, pp. 1-4, doi: 10.1109/UCET51115.2020.9205450.

[37] C. -Z. Han, L. Xiao, Z. Chen and T. Yuan, "Co-Located Self-Neutralized Handset Antenna Pairs With Complementary Radiation Patterns for 5G MIMO

Applications," in *IEEE Access*, vol. 8, pp. 73151-73163, 2020, doi: 10.1109/ACCESS.2020.2988072.

[38] Jiang, Y. Cui, B. Liu, W. Hu and Y. Xi, "A Dual-Band MIMO Antenna With Enhanced Isolation for 5G Smartphone Applications," in *IEEE Access*, vol. 7, pp. 112554-112563, 2019, doi: 10.1109/ACCESS.2019.2934892.

[39] M. Y. Li, Y. L. Ban, Z. Q. Xu, C. Y. D. Sim, K. Kang, and Z. F. Yu, "Eight-port orthogonally dual-polarized antenna array for 5G smartphone applications," IEEE Trans. Antennas Propag., vol. 64, no. 9, pp. 3820–3830, Sept. 2016

[40] Y. L. Ban, C. Li, C. Y. D. Sim, G. Wang, and K. L. Wong, "4G/5G multiple antennas for future multi-mode smartphone applications," IEEE Access, vol. 4, pp. 2981–2988, Jun. 2016

[41] A. Zhao and Z. Ren, "Multiple-input and multiple-output antenna system with self-isolated antenna element for fifth-generation mobile terminals," Microwave Opt. Technol. Lett., vol. 61, no. 1, pp. 20–27, Jan. 2019.

[42] S. S. Alja'afreh *et al.*, "Ten Antenna Array Using a Small Footprint Capacitive-Coupled-Shorted Loop Antenna for 3.5 GHz 5G Smartphone Applications," in *IEEE Access*, vol. 9, pp. 33796-33810, 2021, doi: 10.1109/ACCESS.2021.3061640.

[43] W. Hu *et al*., "Wideband Back-Cover Antenna Design Using Dual Characteristic Modes With High Isolation for 5G MIMO Smartphone," in *IEEE Transactions on Antennas and Propagation*, vol. 70, no. 7, pp. 5254-5265, July 2022, doi: 10.1109/TAP.2022.3145456

[44] A. Ren, H. Yu, L. Yang, Z. Huang, Z. Zhang and Y. Liu, "A Broadband MIMO Antenna Based on Multimodes for 5G Smartphone Applications," in *IEEE Antennas and Wireless Propagation Letters*, vol. 22, no. 7, pp. 1642-1646, July 2023, doi: 10.1109/LAWP.2023.3257182.

[45] M. R. S. K. Sinha and Savita, "Wideband Technology Design with the Novel Based Technogy : An Antenna Systems,"*2023 International Conference on Power Energy, Environment & Intelligent Control (PEEIC)*, Greater Noida, India, 2023, pp. 1475-1479, doi: 10.1109/PEEIC59336.2023.10451357.

[46] Y. Fang, Y. Liu, Y. Jia, J. Liang and H. H. Zhang, "Reconfigurable Structure Reutilization Low-SAR MIMO Antenna for 4G/5G Full-Screen Metal-Frame Smartphone Operation," in *IEEE Antennas and Wireless Propagation Letters*, vol. 22, no. 5, pp. 1219-1223, May 2023, doi: 10.1109/LAWP.2023.3236782.

[47] S. Li, T. Chi, Y. Wang and H. Wang, "A Millimeter-Wave Dual-Feed Square Loop Antenna for 5G Communications," in *IEEE Transactions on Antennas and Propagation*, vol. 65, no. 12, pp. 6317-6328, Dec. 2017, doi: 10.1109/TAP.2017.2723920.

[48] A. Ren, Y. Liu and C. -Y. -D. Sim, "A Compact Building Block With Two Shared-Aperture Antennas for Eight-Antenna MIMO Array in Metal-Rimmed Smartphone," in *IEEE Transactions on Antennas and Propagation*, vol. 67, no. 10, pp. 6430-6438, Oct. 2019, doi: 10.1109/TAP.2019.2920306.

[49] Z. Ren, A. Zhao, and S. Wu, “MIMO antenna with compact decoupled antenna pairs for 5G mobile terminals,” IEEE Antennas Wireless Propag. Lett., vol. 18, no.7, pp. 1367–1371, May 2019.

[50] R. Li, Z. Mo, H. Sun, X. Sun, and G. Du, “A low-profile and high-isolated MIMO antenna for 5G mobile terminal,” Micromachines, vol. 11, pp. 1–12, Oct. 2018.

[51] H. Piao, Y. Jin and L. Qu, “A compact and straightforward self-decoupled MIMO antenna system for 5G applications,” IEEE Access, vol. 8, pp. 129236–129245, Jul. 2020.

[52] W. Jiang, B. Liu, Y. Cui, and W. Hu, “High-isolation eight-element MIMO array for 5G smartphone applications,” IEEE Access, vol. 7, pp. 34104–34112, Mar. 2019.

[53] Y. Luo, L. Zhu, Y. Liu, N. -W. Liu and S. Gong, "Multiband Monopole Smartphone Antenna With Bandwidth Enhancement Under Radiation of Multiple Same-Order Modes," in *IEEE Transactions on Antennas and Propagation*, vol. 70, no. 4, pp. 2580-2592, April 2022, doi: 10.1109/TAP.2021.3125364.

[54] S.W Dong and J. Mo, "Design of a Twelve-Port MIMO Antenna System for Multi-Mode 4G/5G Smartphone Applications Based on Characteristic Mode Analysis," in *IEEE Access*, vol. 8, pp. 90751-90759, 2020, doi: 10.1109/ACCESS.2020.2994068.

[55] W. Hu *et al.*, "Dual-Band Eight-Element MIMO Array Using Multi-Slot Decoupling Technique for 5G Terminals," in *IEEE Access*, vol. 7, pp. 153910-153920, 2019, doi: 10.1109/ACCESS.2019.2948639.

[56] H. Zou *et al.*, "Dual-Functional MIMO Antenna Array With High Isolation for 5G/WLAN Applications in Smartphones," in *IEEE Access*, vol. 7, pp. 167470-167480, 2019, doi: 10.1109/ACCESS.2019.2953311

[57] Z. Ren, and A. Zhao, “Dual-band MIMO antenna with compact self-decoupled antenna pairs for 5G mobile applications,” IEEE Access, vol. 7, pp. 82288–82296, Jun. 2019

[58] A. Zhao and Z. Ren, “Wideband MIMO antenna systems based on coupled-loop antenna for 5G n77/n78/n79 applications in mobile terminals,” IEEE Access, vol. 7, pp. 93761–93771, May 2019.

[59] Z. Ren, A. Zhao, and S. Wu, “MIMO antenna with compact decoupled antenna pairs for 5G mobile terminals,” IEEE Antennas Wireless Propag. Lett., vol. 18, no. 7, pp. 1367–1371, May 2019.

[60] D. Serghiou, M. Khalily, V. Singh, A. Araghi, and R. Tafazolli, “Sub-6 GHz dual-band 8 × 8 MIMO antenna for 5G smartphones,” IEEE Antennas Wireless Propag. Lett., vol. 19, no. 9, pp. 1546–1550, Sept. 2020.

[61] L. Cui, J. Guo, Y. Liu, and C. Y. D. Sim, “An 8-element dual-band MIMO antenna with decoupling stub for 5G smartphone applications,” IEEE Antennas Wireless Propag. Lett., vol. 18, no. 10, pp. 2095–2099, Oct. 2019.

[62] Y. Li, C.Y.D. Sim, Y. Luo, and G. Yang, “Multiband 10-antenna array for sub-6 GHz MIMO applications in 5-G smartphones,” IEEE Access, vol. 6, pp. 28041–28253, Jun. 2018.

[63] L. Sun, Y. Li, and Z. Zhang, “Wideband decoupling of integrated slot antenna pairs for 5G smartphones,” IEEE Trans. Antennas Propag., vol. 69, no. 4, pp. 2386–2391, Apr. 2021.

[64] X. Zhao, S. P. Yeo, and L. C. Ong, “Decoupling of inverted-F antennas with high-order modes of ground plane for 5G mobile MIMO platform,” IEEE Trans. Antennas Propag., vol. 66, no. 9, pp. 4485–4495, Jun. 2018.

[65] Z. Qin, W. Geyi, M. Zhang, and J. Wang, “Printed eight-element MIMO system for compact and thin 5G mobile handest,” Electron. Lett., vol. 52, no. 6, pp. 416–418, Mar. 2016.

[66] Z. Tian, R. Chen, and C. Li, “Dual-band inverted F-shaped antenna array for Sub-6 GHz smartphones,” in 2019 IEEE 89th Vehicular Technology Conference (VTC2019-Spring), Kuala Lumpur, Malaysia, 2019.

[67] Y. J. Deng, J. Yao, D. Q. Sun, and L. X. Guo, “Ten-element MIMO antenna for 5G terminals,” Microwave Opt. Technol. Lett., vol. 60, no. 12, pp. 3045–3049, Dec. 2018.

[68] X. Shi, M. Zhang, S. Xu, D. Liu, H. Wen, and J. Wang, “Dual-band 8-element MIMO antenna with short neutral line for 5G mobile handset,” in Proc. 11th Eur. Conf. Antennas Propag. (EUCAP), pp. 3140–3142, Paris, France, Mar. 2017.

[69] W. J. Zhang, Z. B. Weng, and L. Wang, “Design of a dual-band MIMO antenna for 5G smartphone application,” in 2018 Int. Workshop Antenna Technol. (iWAT), Nanjing, China, Jun. 2018.

[70] L. Sun, Y. Li, Z. Zhang, and Z. Feng, “Wideband 5G MIMO antenna with integrated orthogonal-mode dual-antenna pairs for metal-rimmed smartphones,” IEEE Trans. Antennas Propag., vol. 68, no. 4, pp. 2494–2503, Apr. 2020.

[71] X. T. Yuan, W. He, K. D. Hong, C. Z. Han, Z. Chen, and T. Yuan, “Ultra-wideband MIMO antenna system with high element-isolation for 5G smartphone application,” IEEE Access, vol. 8, pp. 56281–56289, Mar. 2020.

[72] Q. Cai, Y. Li, X. Zhang, and W. Shen, “Wideband MIMO antenna array covering 3.3–7.1 GHz for 5G metal-rimmed smartphone applications,” IEEE Access, vol. 7, pp. 142070–142084, Sept. 2019.

[73] A. Singh and C. E. Saavedra, “Wide-bandwidth inverted-F stub fed hybrid loop antenna for 5G sub-6 GHz massive MIMO enabled handsets,” IET Microwave Antennas Propag., vol. 14, no. 7, pp. 677–683, Jun. 2020.

[74] W. Jiang,, Y. Cui, B. Liu, W. Hu, and Y. Xi, “A Dual-Band MIMO Antenna With Enhanced Isolation for 5G Smartphone Applications,” *IEEE Access*, Vol. 7, pp.112554-112563, 2019 doi: 10.1109/access.2019.2934892.

[75] S. Islam, M. Zada and H. Yoo, "Low-Profile P-I-N-Diode-Controlled Bezel Fit Radiation-Pattern Reconfigurable Antenna Arrays for 5G Smartphones," in IEEE Transactions on Antennas and Propagation, vol. 71, no. 8, pp. 6470-6480, Aug. 2023, doi: 10.1109/TAP.2023.3285109.

[76] L. Sun, H. Feng, Y. Li, and Z. Zhang, “Compact 5G MIMO mobile phone antennas with tightly arranged Orthogonal-Mode pairs,” *IEEE Transactions on*

Antennas and Propagation, vol. 66, no. 11, pp. 6364–6369, Nov. 2018, doi: 10.1109/tap.2018.2864674.

[77] A. A. Al-Hadi, J. Ilvonen, R. Valkonen, and V. Viikari, "Eight-element antenna array for diversity and mimo mobile terminal in LTE 3500 MHz band," *Microwave and Optical Technology Letters*, vol. 56, no. 6, pp. 1323–1327, Mar. 2014, doi: 10.1002/mop.28316.

[78] H. Zou, Y. Li, C. Y. D. Sim, and G. Yang, "Design of 8×8 dual-band MIMO antenna array for 5G smartphone applications," *International Journal of RF and Microwave Computer aided Engineering*,pp. 1-12, May 2018.

[79] Y. Li, C.-Y.-D. Sim, Y. Luo, and G. Yang, "12-Port 5G massive MIMO antenna array in sub-6 GHz mobile handset for LTE bands 42/43/46 applications," *IEEE Access*, vol. 6, pp. 344–354, Jan. 2018, doi: 10.1109/access.2017.2763161.

[80] M.-Y. Li *et al.*, "Eight-Port orthogonally Dual-Polarized antenna array for 5G smartphone applications," *IEEE Transactions on Antennas and Propagation*, vol. 64, no. 9, pp. 3820–3830, Sep. 2016, doi: 10.1109/tap.2016.2583501.

[81] N.O. Parchin,, Y. I. A. Al-Yasir, A. H. Ali, I. Elfergani, J. M. Noras, and R. A. Abd-Alhameed, " Eight- element dual-polarised MIMO slot antenna system for 5G smartphone applications," *IEEE Access*,pp.15612-15622, 2019.

[82] L. Yixin, S.D.Y. Chow, L. Yong, and Y. Guangli, "High isolation 3.5GHz eight antenna MIMO array using balanced open-slot antenna element for 5G smartphones," *IEEE Transactions on Antenna and Propagation*, Vol.67, No.6, pp.3820-3830, 2019.

[83] W. Jiang, B. Liu, Y. Cui, and W. Hu, "High-Isolation Eight-Element MIMO array for 5G smartphone applications," *IEEE Access*, vol. 7, pp. 34104–34112, Jan. 2019, doi: 10.1109/access.2019.2904647.

[84] Z. Yu, Y. Chen, Y. Xie, and N. Guo, "Eight-Element With H-Shaped Slot Mimo Antenna For 5g Applications," *Progress in Electromagnetics Research*, vol. 90, pp. 7–13, Jan. 2020, doi: 10.2528/pierl19110703.

[85] Z. Ren and A. Zhao, "Dual-Band MIMO antenna with compact Self-Decoupled antenna pairs for 5G mobile applications," *IEEE Access*, vol. 7, pp. 82288–82296, Jan. 2019, doi: 10.1109/access.2019.2923666.

[86] W. Hu *et al.*, "Dual-Band Ten-Element MIMO array based on Dual-Mode IFAs for 5G terminal applications," *IEEE Access*, vol. 7, pp. 178476–178485, Jan. 2019, doi: 10.1109/access.2019.2958745.

[87] H. Zou, Y. Li, B. Xu, et al, " Dual-Function MIMO Antenna Array with High isolation for 5G/WLAN Applications in smartphones," *IEEE Access*, vol.7, pp.167470-167480,2019.

[88] X. Zhang, Y. Li, W. Wang, and W. Shen, "Ultra-Wideband 8-Port MIMO antenna array for 5G Metal-Frame smartphones," *IEEE Access*, vol. 7, pp. 72273–72282, Jan. 2019, doi: 10.1109/access.2019.2919622.

[89] H. Wang, R. Zhang, Y. Luo, and G. Yang, "Compact Eight-Element antenna array for Triple-Band MIMO operation in 5G mobile terminals," *IEEE Access*, vol. 8, pp. 19433–19449, Jan. 2020, doi: 10.1109/access.2020.2967651.

[90] W. Hu *et al.*, "Dual-Band Ten-Element MIMO array based on Dual-Mode IFAs for 5G terminal applications," *IEEE Access*, vol. 7, pp. 178476–178485, Jan. 2019, doi: 10.1109/access.2019.2958745.

[91] Li, J., Zhang, X., Wang, Z., Chen, X., Chen, J., Li, Y., & Zhang, A. (2019). Dual-band eight-antenna array design for MIMO applications in 5G mobile terminals. IEEE Access, 7, 71636–71644. J. Li *et al.*, "Dual-Band Eight-Antenna array design for MIMO applications in 5G mobile terminals," *IEEE Access*, vol. 7, pp. 71636–71644, Jan. 2019, doi: 10.1109/access.2019.2908969.

[92] H., Zou, Li, Y., Sim, C.-Y.-D., & Yang, G. (2018). Design of 8x8 dual-band MIMO antenna array for 5G smartphone applications. International Journal of RF and Microwave Computer Aided Engineering, 28(9), e21420.

[93] K.-L. Wong, C.-Y. Tsai, and J.-Y. Lu, "Two asymmetrically mirrored GaP-Coupled loop antennas as a compact building block for Eight-Antenna MIMO array in the future smartphone," *IEEE Transactions on Antennas and Propagation*, vol. 65, no. 4, pp. 1765–1778, Apr. 2017, doi: 10.1109/tap.2017.2670534.

[94] Q. Cai, Y. Li, X. Zhang, and W. Shen, "Wideband MIMO antenna array covering 3.3–7.1 GHz for 5G Metal-Rimmed smartphone applications," *IEEE Access*, vol. 7, pp. 142070–142084, Jan. 2019, doi: 10.1109/access.2019.2944681.

[95] Yuan, X.-T., He, W., Hong, K.-D., Han, C.-Z., Chen, Z., & Yuan, T. (2020). Ultra-wideband MIMO antenna system with high element-isolation for 5G smartphone application. IEEE Access, 8, 56281–56289.

[96] X.-T. Yuan, W. He, K.-D. Hong, C.-Z. Han, Z. Chen, and T. Yuan, "Ultra-Wideband MIMO antenna system with High Element-Isolation for 5G smartphone application," *IEEE Access*, vol. 8, pp. 56281–56289, Jan. 2020, doi: 10.1109/access.2020.2982036.

[97] Y. Hei, J. He, and W. Li, "Wideband decoupled 8-Element MIMO antenna for 5G mobile terminal applications," *IEEE Antennas and Wireless Propagation Letters/Antennas and Wireless Propagation Letters*, vol. 20, no. 8, pp. 1448–1452, Aug. 2021, doi: 10.1109/lawp.2021.3086261.

[98] Z. Ren and A. Zhao, "Dual-Band MIMO antenna with compact Self-Decoupled antenna pairs for 5G mobile applications," *IEEE Access*, vol. 7, pp. 82288–82296, Jan. 2019, doi: 10.1109/access.2019.2923666

[99] C.-Y.-D. Sim, H.-Y. Liu, and C.-J. Huang, "Wideband MIMO Antenna Array Design for Future Mobile Devices Operating in the 5G NR Frequency Bands n77/n78/n79 and LTE Band 46," *IEEE Antennas and Wireless Propagation Letters/Antennas and Wireless Propagation Letters*, vol. 19, no. 1, pp. 74–78, Jan. 2020, doi: 10.1109/lawp.2019.2953334.

[100] H. Zhou, D. Wu, M. Zhu, Y. Qiu, G. Yu, and H.-M. Zhou, "Wideband Low-Profile 8 × 8 MIMO antenna based IFA pair for ultrathin 5G smartphones," *International Journal of Antennas and Propagation*, vol. 2022, pp. 1–10, May 2022, doi: 10.1155/2022/5281470.

[101] R. S. Aziz, A. K. Arya, and S.-O. Park, "Multiband Full-Metal-Rimmed antenna design for smartphones," *IEEE Antennas and Wireless Propagation Letters/Antennas and Wireless Propagation Letters*, vol. 15, pp. 1987–1990, Jan. 2016, doi: 10.1109/lawp.2016.2548018.

[102] Q. Chen, H. Lin, J. Wang, J. Ge, Y. Li and T. Pei, " Single ring slotbased antennas for metal-rimmed 4G/5G smartphones," *IEEE Transactions on Antennas and Propagation, vol.* 67, no.3, pp.1476–1487,2019.

[103] J.-W. Lian, Y.-L. Ban, Y.-L. Yang, L.-W. Zhang, C.-Y.-D. Sim, and K. Kang, "Hybrid Multi-Mode Narrow-Frame antenna for WWAN/LTE Metal-Rimmed smartphone applications," *IEEE Access*, vol. 4, pp. 3991–3998, Jan. 2016, doi: 10.1109/access.2016.2593538.

[104] Y.-L. Ban, Y.-F. Qiang, Z. Chen, K. Kang, and J.-H. Guo, "A Dual-Loop antenna design for Hepta-Band WWAN/LTE Metal-Rimmed smartphone applications," *IEEE Transactions on Antennas and Propagation*, vol. 63, no. 1, pp. 48–58, Jan. 2015, doi: 10.1109/tap.2014.2368573.

[105] C. Deng, Z. Feng, and S. V. Hum, "MIMO mobile handset antenna merging characteristic modes for increased bandwidth," *IEEE Transactions on Antennas and Propagation*, vol. 64, no. 7, pp. 2660–2667, Jul. 2016, doi: 10.1109/tap.2016.2537358.

[106] C. Deng, Z. Xu, A. Ren, and S. V. Hum, "TCM-Based bezel antenna design with small ground clearance for mobile terminals," *IEEE Transactions on Antennas and Propagation*, vol. 67, no. 2, pp. 745–754, Feb. 2019, doi: 10.1109/tap.2018.2880045.

[107] Y. Wang and Z. Du ,"Wideband monopole antenna with less non ground portion for octa-band WWAN/LTE mobile phones," *IEEE Transactions on Antennas and Propagation , vol.*64, no.1,pp. 383–388,2016.

[108] L.-W. Zhang, Y.-L. Ban, C.-Y.-D. Sim, J. Guo, and Z.-F. Yu, "Parallel Dual-Loop antenna for WWAN/LTE Metal-Rimmed smartphone," *IEEE Transactions on Antennas and Propagation*, vol. 66, no. 3, pp. 1217–1226, Mar. 2018, doi: 10.1109/tap.2018.2796724.

[109] Liu Y, Zhang J, Ren A, Wang H and Sim CYD (2019). *IEEE Antennas and Wireless Propagation Letters* 18(4), 717–721. TCM-based hepta-band antenna with small clearance for metal-rimmed mobile phone applications Y. Liu, J. Zhang, A. Ren, H. Wang, and C.-Y.-D. Sim, "TCM-Based Hepta-Band antenna with small clearance for Metal-Rimmed mobile phone applications," *IEEE Antennas and Wireless Propagation Letters/Antennas and Wireless Propagation Letters*, vol. 18, no. 4, pp. 717–721, Apr. 2019, doi: 10.1109/lawp.2019.2901808.

[110] Choi J, Hwang W, You C, Jung B and Hong W (2019) Four-element recongurable coupled loop MIMO antenna featuring LTE full-band operation for metallic-rimmed smartphone. *IEEE Transactions on Antennas and Propagation* 67(1), 99–107.

[111] Y. Liu, W. Cui, Y. Jia, and A. Ren, "Hepta-Band Metal-Frame antenna for LTE/WWAN Full-Screen smartphone," *IEEE Antennas and Wireless Propagation Letters/Antennas and Wireless Propagation Letters*, vol. 19, no. 7, pp. 1241–1245, Jul. 2020, doi: 10.1109/lawp.2020.2996712.

[112] Z.-Q. Xu, Q.-Q. Zhou, Y.-L. Ban, and S. S. Ang, "Hepta-Band Coupled-Fed Loop antenna for LTE/WWAN unbroken Metal-Rimmed smartphone applications," *IEEE Antennas and Wireless Propagation Letters/Antennas and Wireless Propagation Letters*, vol. 17, no. 2, pp. 311–314, Feb. 2018, doi: 10.1109/lawp.2017.2787863.

[113] Yang Y, Zhao Z, Yang W, Nie Z and Liu QH (2017) Compact multimode monopole antenna for metal-rimmed mobile phones. *IEEE Transactions on Antennas and Propagation* 65(5), 2297–2304. Y. Yang, Z. Zhao, W. Yang, Z. Nie, and Q.-H. Liu, "Compact Multimode Monopole antenna for Metal-Rimmed mobile phones," *IEEE Transactions on Antennas and Propagation*, vol. 65, no. 5, pp. 2297–2304, May 2017, doi: 10.1109/tap.2017.2679059.

[114] Y. Liu, Y.-M. Zhou, G.-F. Liu, and S.-X. Gong, "Heptaband Inverted-F antenna for Metal-Rimmed mobile phone applications," *IEEE Antennas and Wireless Propagation Letters/Antennas and Wireless Propagation Letters*, vol. 15, pp. 996–999, Jan. 2016, doi: 10.1109/lawp.2015.2489763.

[115] M.H.Alshamaileh, S.S. Alja'afreh and E. Almajali, " Nona-band, hybrid antenna for metal-rimmed smartphone applications," *IET Microwaves, Antennas & Propagation , vol.*13, pp.2439–2448,2019

[116] Z.-Q. Xu, Y.-T. Sun, Q.-Q. Zhou, Y.-L. Ban, Y.-X. Li, and S. S. Ang, "Reconfigurable MIMO antenna for Integrated-Metal-Rimmed smartphone applications," *IEEE Access*, vol. 5, pp. 21223–21228, Jan. 2017, doi: 10.1109/access.2017.2757949.

[117] H.B. Zhang, Y.L. Ban, Y.F. Qiang, J. Guo and Z.F. Yu ," Reconfigurable loop antenna with two parasitic grounded strips for WWAN/LTE unbroken-metal-rimmed smartphones," *IEEE Access , vol.*5, pp.4853–4858,2017.

[118] Y. Ye, X. Zhao, and J. Wang, "Compact High-Isolated MIMO antenna module with chip capacitive decoupler for 5G mobile terminals," *IEEE Antennas and Wireless Propagation Letters/Antennas and Wireless Propagation Letters*, vol. 21, no. 5, pp. 928–932, May 2022, doi: 10.1109/lawp.2022.3152236.

[119] A. M. Elshirkasi *et al.*, "Numerical analysis of users' body effects on a Fourteen-Element Dual-Band 5G MIMO mobile terminal antenna," *IEEE Access*, vol. 10, pp. 2083–2096, Jan. 2022, doi: 10.1109/access.2021.3139451.

[120] S. H. Kiani, A. Iqbal, S. W. Wong, H. S. Savci, M. Alibakhshikenari, and M. Dalarsson, "Multiple elements MIMO antenna system with broadband operation

for 5th generation smart phones," *IEEE Access*, vol. 10, pp. 38446–38457, Jan. 2022, doi: 10.1109/access.2022.3165049.

[121] W. Hu *et al.*, "Wideband Back-Cover antenna design using dual characteristic modes with high isolation for 5G MIMO smartphone," *IEEE Transactions on Antennas and Propagation*, vol. 70, no. 7, pp. 5254–5265, Jul. 2022, doi: 10.1109/tap.2022.3145456.

[122] L. Chen, Y. Huang, H. Wang, H. Zhou, and K. Liu, "A reconfigurable metal rim antenna with smallest clearance for smartphone applications," *IEEE Access*, vol. 10, pp. 112250–112260, Jan. 2022, doi: 10.1109/access.2022.3216237.

[123] L. Zhao, F. Liu, X. Shen, G. Jing, Y.-M. Cai, and Y. Li, "A High-Pass antenna interference cancellation chip for mutual coupling reduction of antennas in contiguous frequency bands," *IEEE Access*, vol. 6, pp. 38097–38105, Jan. 2018, doi: 10.1109/access.2018.2853709.

[124] F. Liu, J. Guo, L. Zhao, G.-L. Huang, Y. Li, and Y. Yin, "Ceramic Superstrate-Based decoupling method for two closely packed antennas with Cross-Polarization suppression," *IEEE Transactions on Antennas and Propagation*, vol. 69, no. 3, pp. 1751–1756, Mar. 2021, doi: 10.1109/tap.2020.3016388.

[125] F. Liu, J. Guo, L. Zhao, G.-L. Huang, Y. Li, and Y. Yin, "Dual-Band Metasurface-Based decoupling method for two closely packed Dual-Band antennas," *IEEE Transactions on Antennas and Propagation*, vol. 68, no. 1, pp. 552–557, Jan. 2020, doi: 10.1109/tap.2019.2940316.

[126] W. Zhou, J. Qi and Y. Li ,"Self-decoupling 5G MIMO antenna via grounding for mobile phones," *2022 IEEE 10th Asia-Pacific Conference on Antennas and Propagation (APCAP*), Xiamen, China,pp. 1–2,2022.

[127] M. Stanley, Y. Huang, H. Wang, H. Zhou, Z. Tian, and Q. Xu, "A novel reconfigurable metal rim integrated open slot antenna for Octa-Band smartphone applications," *IEEE Transactions on Antennas and Propagation*, vol. 65, no. 7, pp. 3352–3363, Jul. 2017, doi: 10.1109/tap.2017.2700084.

[128] R. Tang and Z. Du, "Wideband monopole without lumped elements for Octa-Band Narrow-Frame LTE smartphone," *IEEE Antennas and Wireless Propagation Letters/Antennas and Wireless Propagation Letters*, vol. 16, pp. 720–723, Jan. 2017, doi: 10.1109/lawp.2016.2600761.

[129] M. Abdullah, S. H. Kiani, and A. Iqbal, "Eight element Multiple-Input Multiple-Output (MIMO) antenna for 5G mobile applications," *IEEE Access*, vol. 7, pp. 134488–134495, Jan. 2019, doi: 10.1109/access.2019.2941908.

[130] Y. Li, C.-Y.-D. Sim, Y. Luo, and G. Yang, "High-Isolation 3.5 GHz Eight-Antenna MIMO array using balanced Open-Slot antenna element for 5G smartphones," *IEEE Transactions on Antennas and Propagation*, vol. 67, no. 6, pp. 3820–3830, Jun. 2019, doi: 10.1109/tap.2019.2902751.

[131] L. Sun, H. Feng, Y. Li, and Z. Zhang, "Compact 5G MIMO mobile phone antennas with tightly arranged Orthogonal-Mode pairs," *IEEE Transactions on*

Antennas and Propagation, vol. 66, no. 11, pp. 6364–6369, Nov. 2018, doi: 10.1109/tap.2018.2864674.

[132] K.-L. Wong, J.-Y. Lu, L.-Y. Chen, W.-Y. Li, and Y.-L. Ban, "8-antenna and 16-antenna arrays using the quad-antenna linear array as a building block for the 3.5-GHz LTE MIMO operation in the smartphone," *Microwave and Optical Technology Letters*, vol. 58, no. 1, pp. 174–181, Nov. 2015, doi: 10.1002/mop.29527.

[133] M.-Y. Li, Y.-L. Ban, Z.-Q. Xu, J. Guo, and Z.-F. Yu, "Tri-Polarized 12-Antenna MIMO array for future 5G smartphone applications," *IEEE Access*, vol. 6, pp. 6160–6170, Jan. 2018, doi: 10.1109/access.2017.2781705.

[134] A. Zhao and Z. Ren, "Size reduction of Self-Isolated MIMO antenna system for 5G mobile phone applications," *IEEE Antennas and Wireless Propagation Letters/Antennas and Wireless Propagation Letters*, vol. 18, no. 1, pp. 152–156, Jan. 2019, doi: 10.1109/lawp.2018.2883428.

[135] H. Xu, H. Zhou, S. Gao, H. Wang, and Y. Cheng, "Multimode decoupling technique with independent tuning characteristic for mobile terminals," *IEEE Transactions on Antennas and Propagation*, vol. 65, no. 12, pp. 6739–6751, Dec. 2017, doi: 10.1109/tap.2017.2754445.

[136] Z. Yu, Y. Chen, Y. Xie, and N. Guo, "Eight-Element With H-Shaped Slot Mimo Antenna For 5g Applications," *Progress in Electromagnetics Research*, vol. 90, pp. 7–13, Jan. 2020, doi: 10.2528/pierl19110703.

[137] Y. Li, CYD. Sim, Y. Luo, et al. ,"Metal-frame-integrated eight-element multiple-input multiple output antenna array in the long term evolution bands 41/42/43 for 5th generation smart phones," *Int J RF Microw Comput-Aided Eng*. ;vol.29 , no.1:1–12,2019

[138] D. Huang, Z. Du, and Y. Wang, "Slot antenna array for fifth generation metal frame mobile phone applications," *International Journal of RF and Microwave Computer-aided Engineering*, vol. 29, no. 9, May 2019, doi: 10.1002/mmce.21841.

[139] V. Thakur, N. Jaglan, and S. D. Gupta, "Side edge printed eight-element compact MIMO antenna array for 5G smartphone applications," *Journal of Electromagnetic Waves and Applications*, vol. 36, no. 12, pp. 1685–1701, Feb. 2022, doi: 10.1080/09205071.2022.2040057.

[140] Q. Guo, R. Mittra, F. Lei, Z. Li, J. Ju, and J. Byun, "Interaction between internal antenna and external antenna of mobile phone and hand effect," *IEEE Transactions on Antennas and Propagation*, vol. 61, no. 2, pp. 862–870, Feb. 2013, doi: 10.1109/tap.2012.2220323.

[141] L. Sun, Y. Li, Z. Zhang, and Z. Feng, "Wideband 5G MIMO antenna with integrated Orthogonal-Mode Dual-Antenna pairs for Metal-Rimmed smartphones," *IEEE Transactions on Antennas and Propagation*, vol. 68, no. 4, pp. 2494–2503, Apr. 2020, doi: 10.1109/tap.2019.2948707.

[142] L. Chang, Y. Yu, K. Wei, and H. Wang, “Polarization-Orthogonal co-frequency dual antenna pair suitable for 5G MIMO smartphone with metallic bezels,” *IEEE Transactions on Antennas and Propagation*, vol. 67, no. 8, pp. 5212–5220, Aug. 2019, doi: 10.1109/tap.2019.2913738.

[143] P. Ramanujam, V. Prasad and K. Arunachalam, "Design of reflector based dipole antenna for sub-6 GHz 5G applications,"*2022 IEEE Microwaves, Antennas, and Propagation Conference (MAPCON)*, Bangalore, India, 2022, pp. 1661-1665, doi: 10.1109/MAPCON56011.2022.10047069.

[144] A. Ranjha, G. Kaddoum and K. Dev, "Facilitating URLLC in UAV-Assisted Relay Systems With Multiple-Mobile Robots for 6G Networks: A Prospective of Agriculture 4.0," in *IEEE Transactions on Industrial Informatics*, vol. 18, no. 7, pp. 4954-4965, July 2022, doi: 10.1109/TII.2021.3131608

[145] Hallbjorner, P., “ The significance of radiation efficiencies when using S-parameters to calculate the received signal correlation from two antennas,” IEEE Antennas Wireless Propag. Lett., vol.4 , 97–99, 2005.

[146] K. Zhang, J. Chen, P. J. Soh, M. Wang, and S. Yan, "Design of a Multiband Antenna with Polarization Diversity for Smartwatch Applications," IEEE Trans. Antennas Propag., doi: 10.1109/TAP.2025.3545591.

[147] Y. Feng, L.-K. Zhang, J.-Y. Li, Y.-H. Yang, S.-G. Zhou, and X.-J. Yu, "A Compact Share-Aperture Antenna With Pattern/Polarization Diversity for 5G Sub-6G Applications," IEEE Trans. Circuits Syst. II, Exp. Briefs, vol. 70, no. 3, pp. 954–958, Mar. 2023, doi: 10.1109/TCSII.2022.3216737.

[148] W. Hu et al., "Wideband Back-Cover Antenna Design Using Dual Characteristic Modes With High Isolation for 5G MIMO Smartphone," IEEE Trans. Antennas Propag., vol. 70, no. 7, pp. 5254–5265, Jul. 2022.

[149] M. Hu and Y. Li, "Wideband Back Cover Microstrip Antenna With Multiple Shorting Vias for Mobile 5G MIMO Applications," IEEE Trans. Antennas Propag., vol. 71, no. 10, pp. 8290–8295, Oct. 2023, doi: 10.1109/TAP.2023.3291802.

[150] W.-F. Zeng, F.-C. Chen, and Q.-X. Chu, "Bandwidth-Enhanced 5G Mobile Phone Antenna Pair With Tunable Electric Field Null," IEEE Trans. Antennas Propag., vol. 71, no. 2, pp. 1960–1964, Feb. 2023, doi: 10.1109/TAP.2022.3232748.

[151] A. K. Saurabh and M. K. Meshram, "Integration of Sub-6 GHz and mm-Wave Antenna for Higher-Order 5G-MIMO System," *IEEE Trans. Circuits Syst. II, Exp. Briefs*, vol. 69, no. 12, pp. 4834–4838, Dec. 2022, doi: 10.1109/TCSII.2022.3197598.

[152] S. H. Kiani *et al.*, "Dual-Polarized Wideband 5G N77 Band Slotted MIMO Antenna System for Next-Generation Smartphones," in *IEEE Access*, vol. 12, pp. 34467-34476, 2024, doi: 10.1109/ACCESS.2024.3370860.

[153] CTIA Certification, CTIA 01.72 NEAR-FIELD PHANTOMS**,** PDF document, [Online]. Available: https://ctiacertification.org

[154] K. Sultan, M. Ikram and N. Nguyen-Trong, "A multiband multibeam antenna for sub-6 GHz and mm-wave 5G applications", *IEEE Antennas Wireless Propag. Lett.*, vol. 21, no. 6, pp. 1278-1282, Jun. 2022.

[155] X. Meng *et al.*, "Sub-6 GHz and mm-Wave Dual-Band Aperture-Shared Phone MIMO Antenna for 5G/6G Applications," *IEEE Antennas Wireless Propag. Lett.*, vol. 23, no. 11, pp. 3639–3643, Nov. 2024, doi: 10.1109/LAWP.2024.3423017.

[156] M.-A. Chung, M.-C. Lee, C.-C. Hsu, and C.-W. Lin, "Multi-Band Coupled-Fed Antenna for 4G LTE, Sub-6G, and WLAN Frequency Bands in Various Electronic Devices," *IEEE Access*, vol. 12, pp. 45398–45422, 2024, doi: 10.1109/ACCESS.2024.3380620.

[157] S. H. Kiani, H. S. Savci, H. S. Abubakar, N. O. Parchin, H. Rimli and B. Hakim, "Eight element MIMO antenna array with tri-band response for modern smartphones", *IEEE Access*, vol. 11, pp. 44244-44253, 2023.

[158] Y. Yang, J. Ren, B. Zhang, J. Liu, H. Wang, D. Song, et al., "Wideband tripolarized MIMO antenna with pattern diversity for 5G application", *IEEE Antennas Wireless Propag. Lett.*, vol. 23, no. 1, pp. 349-353, Jan. 2024.

[159] J. Ahn, Y. Youn, B. Kim, J. Lee, N. Choi, Y. Lee, et al., "Wideband 5G N77/N79 4 × 4 MIMO antenna featuring open and closed stubs for metal-rimmed smartphones with four slits", *IEEE Antennas Wireless Propag. Lett.*, vol. 22, no. 12, pp. 2798-2802, Dec. 2023.